

Community-Centric Microgrid Feasibility Analysis Framework to Accelerate Resilience of Island Communities

A Case Study for Pribilof Islands

JANUARY 2025

Bikash Poudel, Mahesh Acharya, and S M Shafiul Alam

Idaho National Laboratory

Katherine Reedy

Idaho State University

Andrew Miles

Alaska Center for Energy and Power

Nishaant Sinha, Kelsey Fahy, and Michael Stadler

Xendee Corporation

[INL/RPT-25-84046]
[Revision 0]

Marine Energy Program Water
Power Technologies Office



DISCLAIMER

This information was prepared as an account of work sponsored by an agency of the U.S. Government. Neither the U.S. Government nor any agency thereof, nor any of their employees, makes any warranty, expressed or implied, or assumes any legal liability or responsibility for the accuracy, completeness, or usefulness, of any information, apparatus, product, or process disclosed, or represents that its use would not infringe privately owned rights. References herein to any specific commercial product, process, or service by trade name, trade mark, manufacturer, or otherwise, does not necessarily constitute or imply its endorsement, recommendation, or favoring by the U.S. Government or any agency thereof. The views and opinions of authors expressed herein do not necessarily state or reflect those of the U.S. Government or any agency thereof.

Community-Centric Microgrid Feasibility Analysis Framework to Accelerate Resilience of Island Communities

A Case Study for Pribilof Islands

Bikash Poudel, Mahesh Acharya, and S M Shafiul Alam
Idaho National Laboratory
Katherine Reedy
Idaho State University
Andrew Miles
Alaska Center for Energy and Power
Nishaant Sinha, Kelsey Fahy, and Michael Stadler
Xendee Corporation

January 2025

Idaho National Laboratory
Marine Energy Program Water Power Technologies Office
Idaho Falls, Idaho 83415

<http://www.inl.gov>

Prepared for the
U.S. Department of Energy
Office of Energy Efficiency & Renewable Energy
Under DOE Idaho Operations Office
Contract DE-AC07-05ID14517

Page intentionally left blank

SUMMARY

Marine energy offers a reliable energy solution for coastal and island communities, which often lack local renewable generation, to support their transition to energy independence and reduce reliance on externally imported fuels. Successful deployment of new technologies in these isolated locations requires community acceptance and approval from the outset, as these communities typically lack the financial and technical resources to operate and maintain new systems. This report presents a community-centric microgrid planning framework for remote coastal and island communities. Community engagement is integrated as the first step in the planning process, incorporating community profiles and visions into energy development scenarios.



Figure S-1. Community-informed pre-deployment feasibility analysis framework proposed in this work.

A case study was conducted in St. George, Pribilof Islands, Alaska, which relies entirely on diesel yet has significant wind and wave energy potential. Community engagement revealed a unique history and current economic status, with an interest in adopting advanced energy technologies despite past failures. Various microgrid configurations were optimized, considering different technologies to meet current and future energy needs while balancing cost and energy resilience. Wave energy converters (WECs) were a key component, integrated with other energy sources using the Xendee optimization tool.

Results indicated that adding local generation and energy storage economically reduces diesel imports. However, aggressive fuel import reduction targets introduce challenges, such as increased costs, oversized systems, and higher generation curtailment, particularly when both heat and electricity demands are considered. Replacing diesel heating through electrification is uneconomic and risky, especially during extreme weather. Producing and utilizing hydrogen locally could resolve operational issues with intermittent generation resources. Given the community's skepticism about wind energy, influenced by past unsuccessful attempts to install wind turbines, the team explored a scenario that excluded wind energy. The results show higher levelized cost of energy (LCOE) and capital costs for scenarios without

wind, and no significant improvements are seen in generation curtailment. The superior wind resource potential is challenged by the lack of appropriate technology to reliably harness high-speed winds at the given scale.

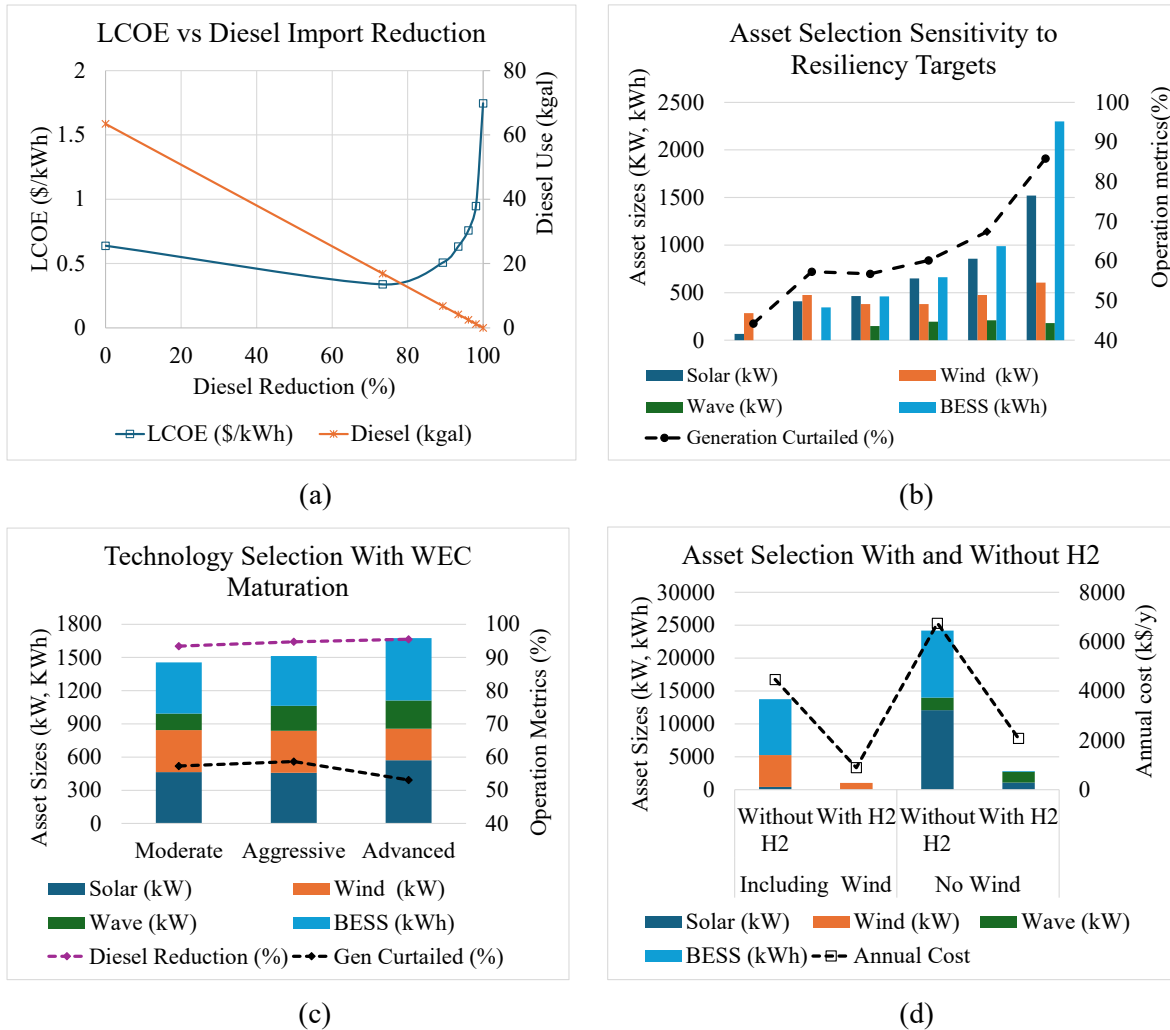


Figure S-2. Technoeconomic analysis and sensitivity analysis results: (a) LCOE versus resiliency goal, (b) asset selection sensitivity to resiliency goal, (c) asset selection with aggressive technology maturation of WEC to reduce operation and maintenance, and (d) improvement in economics through efficient use of generation resources considering hydrogen in the optimization. WECs currently have a lower technology readiness level compared to wind and solar technologies and are not yet cost-competitive. WECs also have significantly higher operation and maintenance (O&M) costs, leading to their exclusion from most optimization scenarios. However, when a more aggressive maturation scenario is considered, the optimizer selects more WECs for the system. The optimization results indicate that WECs have good hybridization potential with photovoltaic and wind, showing a significant reduction in generation curtailment when they are included in the solution.

The infrastructure and operations evaluation, using PowerFactory’s quasi-dynamic, root mean square (RMS), and electromagnetic transient (EMT) simulations, assessed whether the existing infrastructure can accommodate new resources without operational challenges. Power flow analysis revealed significant differences between scenarios with and without wind. Scenarios with wind experienced substantial increases in transmission losses, voltage violations, and transformer overloads due to the siting of wind turbines far from the load center. These issues could be mitigated by strategically placing energy storage

closer to wind turbines or upgrading power lines. Scenarios without wind showed reduced transmission losses and no additional violations but were economically less viable. Optimizing the siting of wind turbines and enhancing infrastructure could improve its efficiency and feasibility.

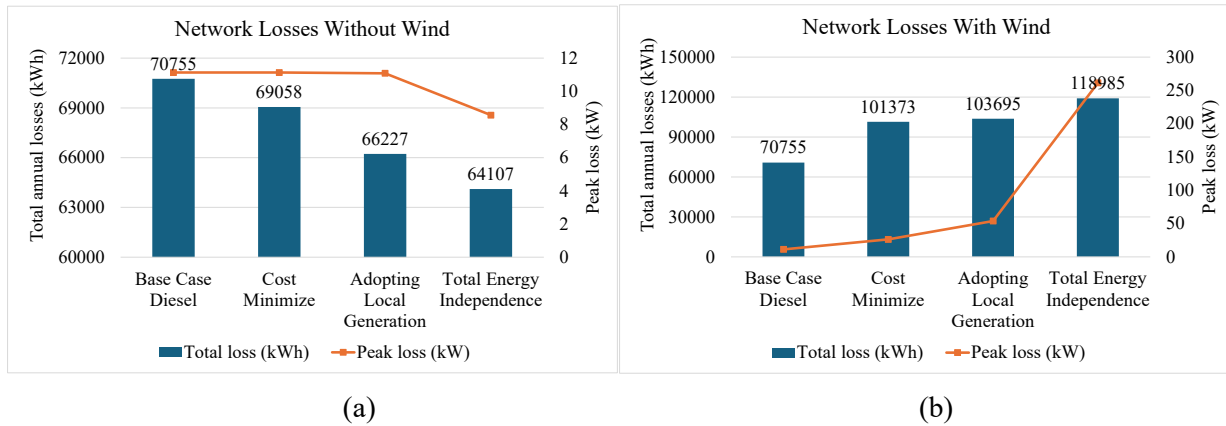


Figure S-3. Network losses (a) without wind and (b) with wind for various optimization objectives.

RMS and EMT simulations analyzed the dynamic behavior of the microgrid under various conditions, highlighting the critical role of battery energy storage systems (BESS) in maintaining stability alongside diesel generators. Balancing loads improved stability and reduced power and frequency fluctuations. The simulations emphasized the need for coordinated control between BESS and diesel generators to manage power imbalances effectively and enhance the microgrid’s dynamic response.

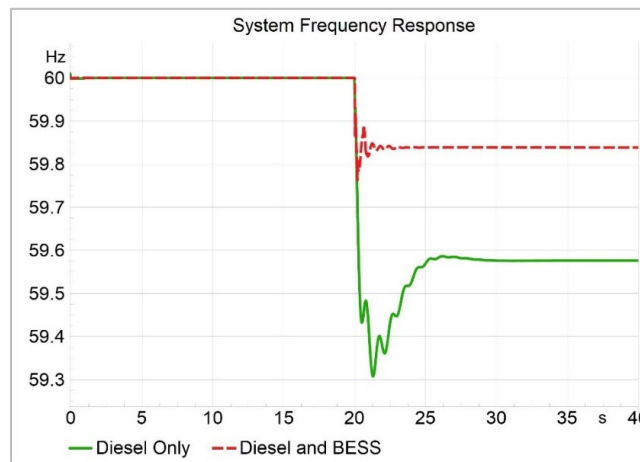


Figure S-4. RMS simulation shows the frequency response against loss of Zapadni Bay feeder during peak load condition with and without BESS participating in frequency control.

The Marine Energy Microgrid Toolkit, developed as part of this work, uses Xendee and PowerFactory tools to optimize and analyze microgrid scenarios. Xendee provides sizing and dispatch solutions, while PowerFactory evaluates power flow, identifies network violations, and predicts operational performance during normal operations and disruptions, offering insights into control performance. This toolkit can be applied to island and coastal communities to enhance resilience and support microgrid deployments. Future enhancements will include incorporating new marine resources, developing dynamic models, and automating the integration of Xendee and PowerFactory simulations.

Page intentionally left blank

CONTENTS

SUMMARY	v
ACRONYMS.....	xvi
1. BACKGROUND.....	1
2. METHODOLOGY.....	3
2.1. Overall Framework	3
2.2. Community Selection.....	4
2.3. Community Engagement.....	4
3. QUALITATIVE OUTCOMES OF COMMUNITY ENGAGEMENT	5
3.1. Community Profile.....	5
3.2. Community History.....	7
3.3. Community Vision.....	7
4. DATA COLLECTED FROM FIELD TRIP FROM ST. GEORGE	8
4.1. Overview of St. George Power System.....	8
4.2. Existing Wind Turbines	10
4.3. Heating and Electricity Demand.....	10
4.4. Resource Assessment: Solar, Wind, and Wave.....	10
4.5. Power Distribution Network	11
4.6. Power Cost Equalization Incentives.....	11
5. MICROGRID MODEL.....	12
5.1. Wave Energy Converter.....	12
5.2. Other Microgrid Technologies.....	14
5.3. Xendee Optimization Model	15
5.4. St. George Infrastructure Model	17
5.4.1. Xendee Multi-Node Model	18
5.4.2. PowerFactory Dynamic Model	20
5.5. Resource and Demand Data	22
6. TECHNOECONOMIC ANALYSIS.....	23
6.1. Scenario Development	23
6.2. Base Case Scenario	24
6.3. Adopting Local Generation.....	24
6.4. Cost-Resilience Tradeoffs.....	26
6.5. Sensitivity to Uncertainties	27
6.5.1. Cost of Technologies	27

6.5.2.	Wave Energy Converter Technology Maturation	28
6.6.	Integrating Community Perspective.....	29
6.6.1.	Future Growth.....	29
6.6.2.	Without Wind.....	30
6.7.	Electrification of Heating Demand	31
6.8.	Exploring the Role of Hydrogen.....	33
7.	INFRASTRUCTURE EVALUATION.....	36
7.1.	Network Power Flow	36
7.1.1.	Base Case Diesel.....	36
7.1.2.	Optimized Electricity with Wind.....	38
7.1.3.	Optimized Electricity Without Wind.....	42
7.1.4.	Optimized Heat and Electricity.....	44
7.2.	Operations Evaluation.....	46
7.2.1.	Root Mean Square Simulation	47
7.2.2.	Electromagnetic Transients Simulation	55
8.	MARINE ENERGY MICROGRID TOOLKIT.....	59
9.	CONCLUSIONS.....	60
10.	ACKNOWLEDGEMENTS	62
11.	REFERENCES.....	62

FIGURES

Figure S-1.	Community-informed pre-deployment feasibility analysis framework proposed in this project.	v
Figure S-2.	Technoeconomic analysis and sensitivity analysis results: (a) LCOE versus resiliency goal, (b) asset selection sensitivity to resiliency goal, (c) asset selection with aggressive technology maturation of WEC to reduce operation and maintenance, and (d) improvement in economics through efficient use of generation resources considering hydrogen in the optimization.	vi
Figure S-3.	Network losses (a) without wind and (b) with wind for various optimization objectives.	vii
Figure S-4.	RMS simulation shows the frequency response against loss of Zapadni Bay feeder during peak load condition with and without BESS participating in frequency control.	vii
Figure 1.	Community-conscious ME microgrid planning.	3
Figure 2.	Community engagement stages.	4
Figure 3.	Population trend of St. George, AK (U. S. Census Bureau 2020).	5
Figure 4.	St. George Island, Pribilof Islands, AK (a) commercial fur sealing “Blubbering” (Jeanette and Klauk 2007).	6
Figure 5.	St. George power system: (a) Diesel generators and (b) heat recovery system.	9

Figure 6. Power System Upgrades in St. George: (a) Wind turbine and (b) rebuilt distribution system.	9
Figure 7. WEC cable configuration layout.	12
Figure 8. Wave performance matrix for WEC devices (a) 15-kW BREF-HB and (b) 260-kW BREF-SHB.	14
Figure 9. Key constraints for optimization.	16
Figure 10. Google Earth location map.	17
Figure 11. Google Earth location map of the town view.	18
Figure 12. Infrastructure model in Xendee considering multi-node capability.	20
Figure 13. Geographic diagram of PowerFactory model of St. George.	21
Figure 14. Scenario development for technoeconomic analysis.	23
Figure 15. Sensitivity of LCOE and generation curtailment with respect to resiliency and energy independence.	26
Figure 16. Asset selection and sizing, and generation curtailment with respect to resiliency targets.	27
Figure 17. Comparing LCOE sensitivity to diesel use reduction for various cost adjustment factors.	28
Figure 18. Comparing sensitivity of generation curtailment to diesel use reduction for various cost adjustment factors.	28
Figure 19. Sensitivity of asset selection and sizing and generation curtailment with respect to local generation adoption target (PCF=1).	29
Figure 20. Comparing LCOE and generation curtailment for diesel use reduction targets.	31
Figure 21. Comparing operational metrics for electricity and heat (E&H) cases with electricity only (EO) cases for diesel use reduction targets.	32
Figure 22. Sensitivity of technology selection and generation curtailment with respect to diesel import reduction targets.	33
Figure 23. Comparing asset selection and annual cost for energy independence cases with and without hydrogen.	35
Figure 24. Comparing generation curtailment for energy independence cases with and without hydrogen.	35
Figure 25. Power flow results for base case diesel scenario.	37
Figure 26. Voltage and transmission line loadings in the town facility for base case scenario. The only overload seen is in the transformer connecting diesel generator substation to the St. George residential area.	38
Figure 27. Voltage and transmission line loadings in Zapadni Bay feeder for base case scenario. No overload or voltage violation seen for diesel base case.	38
Figure 28. Power flow results for the case with wind for local generation adoption objective (PCF=1).	39

Figure 29. Voltages and transmission line loadings in the town facility for cost minimization with wind. Both the transformers connecting the central substation to the St. George residential area and Zapadni Bay feeder are overloaded.	39
Figure 30. Power flow results for the case with wind for local generation adoption objective. Network losses increase when more power comes from wind turbines.	40
Figure 31. Voltages and distribution line loadings for the energy independence case with wind. The entire network face overvoltage issue during peak wind generation.....	41
Figure 32. Transmission losses compared for optimized scenarios, including wind with different objectives.	42
Figure 33. Power flow results for local generation adoption objective without wind. Network losses show a decreasing trend with new generation resources.....	43
Figure 34. Transmission losses compared for optimized scenarios without wind with different objectives.	43
Figure 35. Voltages and transmission line loadings for heat and electricity optimization with cost minimization objective, including wind. Numerous load transformers across the network are overloaded due to the increase in demand from electrical heating.	44
Figure 36. Power flow results for heat and electricity optimization with cost minimization objective with wind. Network losses increase more when heating loads are electrified.	45
Figure 37. Transmission losses compared for heat and electricity optimization with and without wind for cost minimization objective.	46
Figure 38. Dynamic performance of the system for the peak load scenario based on RMS simulation. BESS frequency control is deactivated, and only the diesel generator provides dynamic response.....	48
Figure 39. Dynamic performance of the system for the peak load scenario based on RMS simulation. BESS frequency control is activated, and both diesel generator and BESS contribute to stabilizing system frequency.	49
Figure 40. Comparing frequency responses for cases when only diesel provides frequency response vs. both diesel and BESS provide frequency response.....	49
Figure 41. Dynamic performance of the system for the peak diesel generation scenario with both BESS and diesel providing frequency response.	50
Figure 42. Dynamic performance of the system for the peak PV generation scenario with BESS tripped alongside PV. Only diesel generator provides the frequency response.....	51
Figure 43. Dynamic performance of the system for the peak PV generation scenario with both BESS and diesel providing frequency response.	52
Figure 44. Dynamic performance of the system for the peak wind generation scenario with both BESS and diesel providing frequency response.	53
Figure 45. Dynamic performance of the system for the peak wave generation scenario with both BESS and diesel providing frequency response. WEC is tripped off at t=20 s.	54
Figure 46. Dynamic performance of the system for the peak BESS generation scenario with BESS tripped off at t=20 s.	55
Figure 47. System measurements for the peak wave generation scenario with Zapadni Bay feeder tripped off at t=5 s (unbalanced case).....	56

Figure 48. Current measurements in different phases of diesel generator output terminal (unbalanced case).	57
Figure 49. System measurements for the peak wave generation scenario with Zapadni Bay feeder tripped off at t=5 s (balanced case).....	58
Figure 50. Current measurements in different phases of diesel generator output terminal (balanced case).....	58
Figure 51. The proposed Marine Energy Microgrid Toolkit. The analysis kicks off with the community engagement followed by technoeconomic analysis and infrastructure evaluation using the capabilities of Xendee and PowerFactory capabilities.	60
Figure A-1. Eight communities considered from Aleutian and Pribilof Islands.....	65
Figure A-2. NOAA meteorological stations in St. George, St. Paul, and Bering Sea. The St. George and St. Paul stations do not report wave meteorological data, whereas the Bering Sea station does.....	69
Figure A-3. A snapshot of wave meteorological data reported by the Bering Sea station. Significant wave height and dominant wave periods are extracted for this analysis.....	69
Figure A-4. Average wave energy contours from NREL’s Marine Energy Atlas.....	70
Figure A-5. Significant wave height distribution at Bering Sea station #46073.....	71
Figure A-6. Dominant wave period distribution at Bering Sea station #46073.....	71
Figure A-7. A sample wave performance matrix for a WEC device.....	72
Figure A-8. Bilinear interpolation of wave height and energy period to calculate maximum wave generation for each interval.	73
Figure A-9. Wind power potential for St. George Island, AK.....	74
Figure A-10. Solar power potential for St. George Island, AK.	74
Figure A-11. Wave energy period performance data for St. George, AK.	75
Figure A-12. Wave height performance data for St. George, AK.	75
Figure A-13. Electricity demand for St. George Island, AK.	76
Figure A-14. Space heating demand for St. George Island, AK.....	76
Figure A-15. Water heating demand for St. George Island, AK.....	77
Figure A-16. Load demand profile considered for the proposed fish processing plant.	78
Figure A-17. Load demand profile considered for the proposed new harbor.	78
Figure B-1. NREL ATB estimates wind turbines for commercial-scale distributed wind turbines. (2023 Moderate estimates for CAPEX and fixed O&M are used for the analysis.).....	85
Figure B-2. NREL ATB estimates for residential-scale PV and battery energy storage considered for St. George. (2023 Moderate estimates for CAPEX and fixed O&M are used for the analysis.).....	85

TABLES

Table 1. Key inputs and outputs for WEC Modeling.....	13
---	----

Table 2. Comparing base case scenario results for electricity-only and electricity and heat.....	24
Table 3. Results for electricity-only scenario for different objectives enabling all generation assets, including wind.....	25
Table 4. Future scenario with demand growth supported by diesel-based electricity (electricity-only case).....	29
Table 5. Results for electricity-only scenario for different objectives considering future.....	30
Table 6. Results for electricity-only scenario for different objectives excluding wind.	30
Table 7. Prospect of using local generation resources to support both heat and electricity demand.	32
Table 8. Prospect of using hydrogen in the mix to fully replace diesel use (total energy independence) for both electricity and heat.....	34
Table 9. Operational instances analyzed for RMS simulation. The Xendee dispatch results optimize generation from hosted resources without considering network losses. The PowerFactory results show correct diesel output considering network losses.	47
Table A-1. Community profile summarized for eight selected communities during community selection process. False Pass had an existing, ongoing commercial project and, therefore, the second-ranked island, St. George, was selected for this study.	66
Table A-2. Monthly average wave energy reported by NREL Marine Energy Atlas at St. George and Bering Sea locations.	70
Table B-1. Modeling parameters and considerations for existing primary, reserve diesel generator (Alaska Energy Authority 2012).	79
Table B-2. Modeling parameters for WEC (before cost adjustment).	79
Table B-3. Modeling parameters for solar photovoltaic (before cost adjustment).	80
Table B-4. Modeling parameters for BESS (before cost adjustment).....	80
Table B-5. Modeling parameters for wind (before cost adjustment).	80
Table B-6. Modeling parameters and considerations for electric heaters.	80
Table B-7. Modeling parameters for electrolyzer (before cost adjustment).	80
Table B-8. Modeling parameters for hydrogen storage (before cost adjustment).....	81
Table B-9. Modeling parameters for fuel cells (before cost adjustment).....	81
Table B-10. Modeling parameters for hydrogen boiler (before cost adjustment).....	81
Table B-11. AEA past wind and solar projects in Aleutian and Pribilof Islands.....	82
Table B-12. Expected capital and O&M costs for energy projects in remote communities and off-grid locations.	83

Page intentionally left blank

ACRONYMS

AEA	Alaska Energy Authority
BESS	battery energy storage systems
BREF-HB	bottom-referenced heaving buoy
BREF-SHB	bottom-referenced submerged heaving buoy
CAF	cost adjustment factor
CAPEX	capital expenditure
CHP	combined heat and power
DC	direct current
DOE	U.S. Department of Energy
EMT	electromagnetic transients
EPR	ethylene propylene
GPS	Global Positioning System
HOMER	hybrid optimization model for electric renewables
IEEE	Institute of Electrical and Electronics Engineers
kVAr	kilovolt ampere reactive
LCOE	levelized cost of electricity
ME	marine energy
MT	metric ton
O&M	operation and maintenance
OPEX	operational expenditure
PCE	power cost equalization
PCF	premium cost factor
PV	photovoltaic
RMS	root mean square
WEC	wave energy converter

Page intentionally left blank

Community-Centric Microgrid Feasibility Analysis Framework to Accelerate Resilience of Island Communities

A Case Study for Pribilof Islands

1. BACKGROUND

Microgrids, often considered a foundational element of the future grid, incorporate distributed generation systems and leverages smart control technologies to establish an automated or semi-automated energy delivery network. This configuration allows for more efficient management and distribution of energy, improving reliability, resilience, and sustainability in power systems (Uddin et al. 2023). Integrating microgrids based on locally available natural energy resources into islanded communities can significantly transform local energy systems and provide multiple benefits (Elliott et al. 2022). One of the primary impacts is enhanced community resilience, achieved through diversifying energy generation sources. This diversification not only reduces dependency on any single energy source but also improves the reliability of the power supply, particularly important in areas prone to supply disruptions (Elliott et al. 2022). Additionally, by shifting away from diesel generation relying on externally imported fuels to local natural energy resources, microgrids promote community sustainability and energy independence aligning with current administration goals. Furthermore, the construction, operation, and maintenance of microgrids offer vital economic opportunities for remote communities. These activities can create jobs and stimulate local economies, fostering economic growth and development. By adopting microgrids powered by locally available generation resources, remote and island communities can achieve resilient and economical energy systems.

Introducing microgrids that use new technologies in remote areas (e.g., isolated islands in Alaska) often encounters difficulties due to various factors, including isolation, lack of standard utility services, insufficient community involvement, uncertainty in system ownership, poor maintenance practices, concerns about financial sustainability, and less-than-ideal system design. In the coastal areas of Alaska, the availability of solar energy is often insufficient, and the conditions are too extreme for effective wind energy utilization. These issues are exacerbated when implementing cutting-edge technologies like marine energy (ME) generation, which has limited practical deployment experience. Furthermore, remote coastal communities deal with extra challenges, such as harsh weather conditions, disruptions from ocean ice, and unique natural disasters like tsunamis, coastal erosion, and flooding, all of which pose threats to both inhabitants and infrastructure.

Islanded communities have traditionally depended on expensive imported fossil fuels for energy. Although wind and solar power have provided alternatives to these communities, integrating wave or tidal energy with other technologies could accelerate their energy independence in a cost-effective manner (Keiner et al. 2022; Contestabile et al. 2017). Wave energy, derived from the continual movement of ocean waves, provides a reliable and periodic source of energy. This energy can be captured and converted into electricity using a device known as a wave energy converter (WEC), which leverages wave motion to operate a generator. Unlike wind energy, wave energy is characterized by fluctuations with lower frequency but higher amplitude variations (Blavette et al. 2014; Du et al. 2020). Conversely, tidal energy results from the Earth's rotation and the gravitational pulls of the moon and sun, affecting oceanic tides (Hagerman and Polagye 2006). This energy can be converted into electrical power by using variances in water levels or the kinetic energy produced by the movement of tides and geographical factors (Thresher 2011). Tidal power generation takes advantage of the predictable energy from approximately four tides each day, with its output closely tied to the lunar cycle, including phases like the third quarter, new moon, first quarter, and full moon.

Wave and tidal energy offer significant advantages for island communities, providing a more stable source of electricity generation compared to other local generation technologies. However, there are specific challenges in some island communities, particularly those where the ocean freezes for several months each year, which can impede the operation of wave and tidal energy systems. Although wave and tidal energy are still emerging technologies and currently have higher costs compared to more established wind and PV technologies, they are receiving increased attention. This interest, combined with support from federal and state levels, is expected to drive down the levelized cost of these energies over time. As a result, integrating wave and tidal energy presents a promising alternative for enhancing energy resilience and advancing towards total energy independence in island communities (Elliott et al. 2022).

This report introduces a comprehensive framework for analyzing ME microgrids, covering a broad range of planning aspects. This includes initial strategies for community engagement, modeling of the ME microgrid, and evaluation of its technoeconomic performance and long-term viability. The toolkit will center on ME generation technologies in synergy with other local natural resources and energy storage solutions, aiming to achieve energy independence. Leveraging established power system methodologies, technoeconomic assessments, and community interaction guidelines, the framework will facilitate the co-development of ME microgrids in remote coastal communities.

The rest of the report is organized as follows. Section 2 provides the methodology of this study, including the community-conscious microgrid planning framework (e.g., community selection and community engagement approach). Section 3 describes the outcomes of community engagement, discussing the qualitative results of interviews with community members. Section 4 provides the data collected for demand, generation resources, and existing infrastructure. Section 5 presents the modeling of WEC and other technologies within the Xendee tool, along with optimization formulation for technoeconomic analysis and Xendee and PowerFactory models for infrastructure and operations evaluation. Section 6 discusses the optimization scenarios and results of the sensitivity analysis, considering cost and resilience objectives, community goals and perspectives, uncertainties related to technology costs and maturation, and the integration of heat, electricity, and hydrogen. Section 7 describes the results of infrastructure and operations evaluations, discussing network issues due to asset selection and placement as well as the frequency and voltage dynamic response of the microgrid to network disruptions and contingencies. Section 8 wraps up the overall framework into the Marine Energy Microgrid Toolkit, which can be applied to provide pre-deployment feasibility analysis of marine coastal and island communities. Section 9 concludes the report with recommendations and potential future work. The acknowledgements, recognizing the contributions and support of individuals and organizations involved in this study, are provided in Section 10. Section 11 provides references cited in this report, followed by more details of community engagement outcomes in Appendix A, Community Engagement and Data Collection, and a review of cost and modeling parameters in Appendix B, Cost and Modeling Parameters.

2. METHODOLOGY

2.1. Overall Framework

The proposed planning framework involves various stages, starting from community engagement, demand evaluation, and resource assessment to technoeconomic evaluation, as shown in Figure 1. Community engagement helps identify and prioritize various aspects, including community goals, environmental and social constraints, financial limitations, and technical restrictions, to build community development scenarios. Based on these identified scenarios, constraints, and objective functions, technoeconomic optimization is conducted to determine the energy technologies that meet adequacy and supplemental objectives by analyzing economic operation and dispatch. This evaluation involves one or more decision metrics, including cost minimization, adoption of local energy resources, and energy independence. The technoeconomic evaluation is followed by the infrastructure and operations evaluation. This subsequent stage will analyze the steady-state and transient performance of the microgrid with new resources under various operating scenarios before testing deployment.

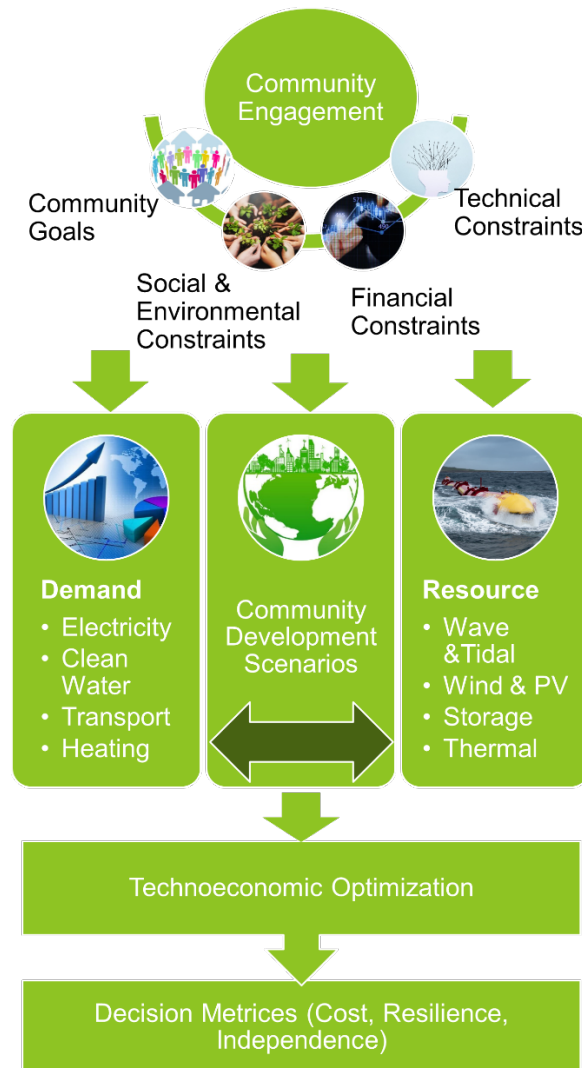


Figure 1. Community-conscious ME microgrid planning.

2.2. Community Selection

The project team evaluated rural coastal communities in Western Alaska for wave and tidal energy potential, energy resilience issues, and potential local interest in the project. Building on the regional experience of the anthropologist on the team, and the community features needed for an ME project, the team concentrated its efforts on Aleutian and Pribilof Islands communities. These coastal communities share similar environmental conditions, transportation and shipping challenges, and utility service challenges. These communities are also free of sea ice year-round.

The project team consulted with the Aleutian Pribilof Islands Association’s Tribal Services Energy department to discuss potential communities to approach. Eight candidate communities were ranked based upon features, including population size, commercial activities, primary and identified energy sources, infrastructure needs, and stakeholders involved. The first community selected already had a project in progress. The second-ranked community was St. George, and was selected for its wave energy potential, diesel dependence, data availability, population, and engagement in commercial fishing. More details on the community selection process are provided in Appendix A-1.

2.3. Community Engagement

Following the community selection, the team prepared for the community engagement. Relevant gatekeepers at the native corporation, tribal, and municipal levels governing the community were contacted by telephone and email and provided project descriptions. In this case, the City of St. George, St. George Tanaq Corporation, and the Aleut Community of St. George Island, were each contacted about the project. The entity in charge of the energy utility, the City of St. George, became the primary contact, and they provided a letter of support to include in the Institutional Review Board human subjects’ research application. The Institutional Review Board approval included an informed consent form as well as a questionnaire and interview guide containing a set of questions on energy uses and needs for households, businesses, and government entities. The mayor was identified as the primary point of contact. Members of the project team also studied information about the community’s history and development to better understand the local context before engaging in fieldwork.

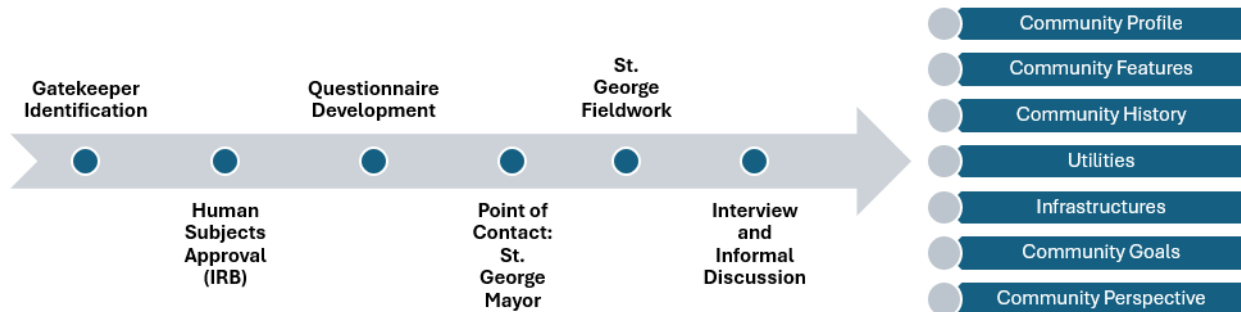


Figure 2. Community engagement stages.

A timeframe for fieldwork was selected in consultation with the community. Fieldwork in St. George took place in July 2023, which consisted of interviews and informal discussions with community leaders and members and of an evaluation of the community’s utilities and infrastructure. It is important to be responsive to local circumstances and maintain flexibility in field methods and engagement. Constraints to fieldwork in this case included a COVID-19 outbreak in the neighboring community of St. Paul with several St. George community members in quarantine as well as the recent death of an elder and his funeral on the day of team’s arrival. The project team carefully navigated the community to respect both situations. Community engagement yielded a comprehensive profile, including a description of St. George’s unique history, community features, status of the utility services, community goals and priorities, and attitudes towards locally available energy resources.

3. QUALITATIVE OUTCOMES OF COMMUNITY ENGAGEMENT

3.1. Community Profile

Community engagement methods yielded a 2023 community profile. St. George is located on the northeast bay on St. George Island. The island is 47 miles from St. Paul Island, 750 air miles from Anchorage, and 250 air miles from Dutch Harbor. There are only three low spots on the island available for development. One of these low spots serves as the community site, and a second spot contains the harbor and airport. Fur seals and Steller sea lions also haul out on the beaches. The rest of the shoreline is marked by high cliffs filled with nesting seabirds. St. George is remotely accessed via airplanes through Dutch Harbor. St. George residents described “two seasons: fog and wind,” which determine all air travel and fishing access.

St. George is primarily administered by the City of St. George, with a mayor and city council form of government. The city coordinates with the tribal council and the village corporation on major projects affecting the community. The city’s revenue derives from various taxes, grants, fuel sales, and the electric utility. Waste heat from the power plant is used to heat their building.

St. George is statistically an older community, with 60% of the population over the age of 60, and a shrinking community. The population when the team visited the community in 2023 was 39, which is a reduction from 67 residents in the 2020 U.S. Census (U. S. Census Bureau 2020) as shown in Figure 3. There are many unoccupied homes that are degrading from the elements and that cannot be re-occupied without extensive work. The school closed in 2017 due to falling below the enrollment threshold for state-level support, and the few community children attend an online school. Many residents identify as Russian Orthodox and maintain a church in the center of the village.

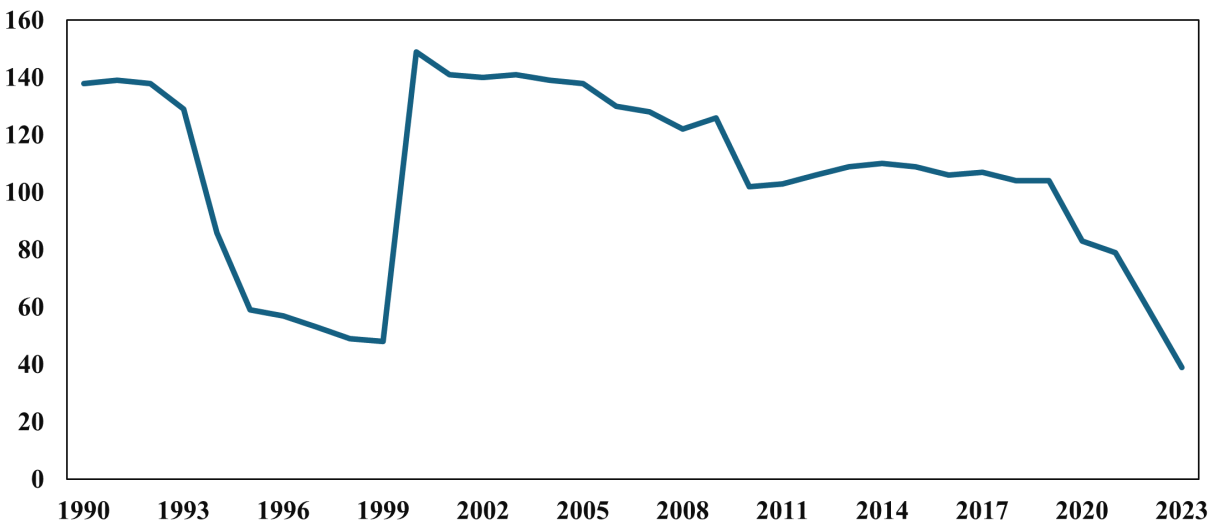


Figure 3. Population trend of St. George, AK (U. S. Census Bureau 2020). Commercial fishing is the main industry with five vessels participating in the halibut fishery. Each vessel employs approximately two crews and often attracts those who have moved away to return for the season. June and July are the peak fishing times, but they can fish into September or October “if lucky” with less stormy weather. Fishing in 2023 did not occur for logistical reasons; they were unable to coordinate with St. Paul effectively to get an ice machine working for the fishing vessels and tenders.

The community engages in subsistence harvesting of numerous species, primarily fur seals (Figure 4 [a]), introduced reindeer, shellfish, halibut (Figure 4 [b]), cod, and berries. They have a community greenhouse. While there is a grocery store, food insecurity is present due to intermittent airplanes from Anchorage and Dutch Harbor, freight costs, and quality issues.



(a)

(b)

Figure 4. St. George Island, Pribilof Islands, AK (a) commercial fur sealing “Blubbering” (Jeanette and Klauk 2007). Community infrastructure includes a hotel owned by the village corporation, a school building that is being converted into a community center, health clinic, post office, and store with adjacent liquor store. The city administers the utilities of electricity, water, and heat. Electricity is sold by the city to households and businesses and monitored on Marshall Creek AMPY meters. These are pay-as-you-go smart card readers with displays that allow users to monitor costs, usages, history of costs and usage, and monthly totals. Households and businesses keep portable generators on hand for backup. The city employs a power plant engineer who coordinates bulk fuel purchases that come by charter vessel from Dutch Harbor and maintains the plant. Diesel deliveries to the community are only possible in a good weather window. Residential customers pay \$0.23/kWh and commercial customers pay \$1.25/kWh. The utility cost is offset by a state Power Cost Equalization (PCE) program or else residents would pay \$16-20/kwh. The city sets household use limits, and they pay the non-subsidized cost if they go over the limit.

Homes are heated with diesel boilers (diesel was \$8.10/gallon and #2 heating fuel was \$7.93/gallon), and households average 70 gallons each month. Freshwater is plentiful and is pumped from underground up to a holding tank that is then piped to homes and businesses. Most homes have standard electric appliances such as stoves, refrigerators, microwaves, coffee pots, and televisions. People employ conservation tricks, such as using light emitting diode lightbulbs, zone valves, short showers, cooking less, and laundering in cold water, to keep from going over the electricity residential limits. They also use portable generators to run power tools or charge devices. They also try to conserve as a community to “keep the fuel for the elders.” The mayor described conserving fuel as having “a pretty good algorithm” to keep their microgrid running. They manage month to month, but they need to be planning and coordinating all the time. Their systems were tested in November 2022 when a series of events collided. The power plant shut down due to human error, the water line broke, the sewer lines froze, phones were down, and they had not had a grocery delivery plane in weeks. The community had one working satellite phone to call for emergency assistance. Lessons from this included replacing the power plant operator, labeling the grid correctly, increasing the number of portable generators in the community, and increased food storage.

Regarding ice conditions, St. George is largely ice-free. Shore ice occasionally drifts by but is generally loose and does not last long. The last instance of shore ice remaining around the island for more than three days occurred 4–5 years ago. North winds may push ice toward St. Paul, but since it is 40 miles north of St. George, the ice rarely reaches that far south.

3.2. Community History

Responsible community engagement begins with an understanding of the community's history and development. St. George was uninhabited until Russian fur hunters moved indigenous Unangâ (Aleut) hunters from Aleutian Islands villages to both Pribilof Islands of St. George and St. Paul in the late eighteenth century to hunt fur seals for Russian-American Company profit (Black 2004; Corbett and Swibold 2000). After the American purchase of Alaska in 1867, the U.S. government became the primary administrator of the islands and their fur seal rookeries. The government kept the fur seal harvest operation going by leasing the islands and harvests to private companies who sent the profits to the U.S. Treasury. Unangâ labor was essential to this operation and they worked in exchange for housing, food, and medical treatments (Jones 1980). St. George generated over \$7 million annually from the harvest. As one interviewee commented, "The U.S. government was essentially in the fur and fashion business." Island residents were evacuated during World War II by the U.S. government following Japanese invasion of the Western Aleutian Islands and moved to abandoned canneries in Southeast Alaska for the duration of the war, ostensibly for their protection in wartime (Kohlhoff 1995). They were allowed to return to St. George following the war to resume seal harvesting work. After statehood in 1959, the government attempted to consolidate operations by moving St. George residents to St. Paul, but that proved unworkable for social reasons, and they returned to St. George. The fur seal operation closed in St. George in 1973, and then workers traveled to St. Paul to work. Commercial seal harvesting was eventually closed after the Fur Seal Act in 1983 and the withdrawal of an annual federal allocation to the islands (Corbett and Swibold 2000). Following lobbying efforts in Washington, D.C., federal settlement funds were received by islanders for the loss of their economy. The sealing facilities are still on the islands today and have been maintained for their potential to grow tourism.

The federal government was charged with developing a new economic base, which they did with a day-boat halibut fishery in the early 1980s. Investments were made in vessel purchases, constructing a harbor, and in an icing and storage facility. Since then, community members identify as fishermen. The island is in the center of several productive fisheries, but the community has only benefited from a few of these. They were involved in crab processing with floating processors anchored near the harbor in the 1990s, but the weather was too rough, and the processors eventually left. Fishermen regularly lobby the federal regional fishery council to keep their halibut quota allocations up, and they negotiate with a community development quota entity of Aleutian Pribilof Islands Community Development Association to support fishing infrastructure.

3.3. Community Vision

The community shared several infrastructure improvement plans, such as plans to construct a harbor closer to the village, convert the school building into a community center, heat more elders' homes with waste heat, and increase tourism that attracts visitors to understand their fur sealing history and view seabirds. There are mixed opinions about the need and efficacy of these plans among community members. For example, a new harbor is controversial because of the existing harbor, the declining Bering Sea fishery stocks, and challenging weather conditions, cost and maintenance, and need. Others would like the harbor closer to the village for better access to the sea and the ability to use and monitor boats more easily.

Community perspectives on adoption of non-conventional technologies vary but primarily support it. A wind turbine was installed by the Alaska Energy Authority (AEA) about a decade ago, and two turbine engines failed shortly after installation. It never really contributed to the grid. It was described as “a million-dollar matchstick” and “a light in the fog.” Even so, community members generally displayed positive attitudes toward the introduction of advanced energy technologies. They were interested in “anything that works,” even the reintroduction of wind energy technologies, rooftop solar photovoltaics, and ME technologies. They were only interested in technologies that do not interfere with fishing. The longevity of these technologies, as well as local capacity for management and maintenance, were also of primary interest. Concerns expressed about infrastructure investments, including ME development, primarily included doubts about the longevity of the community given the average age of the population, the closed school, and the uncertain future of commercial fisheries. The City of St. George also derives revenue from the electric utility and offsetting, which could affect their revenue.

This project is attempting to understand the unique challenges of coastal communities in maintaining their microgrids through extreme weather conditions and external supply chain issues and in exploring the ways in which microgrids incorporating ME have the potential to reduce these challenges. Coastal communities share many of the same challenges presented in St. George especially extreme weather conditions or events, outmigration, failed energy projects, dependency on fisheries, volatility of fisheries, shipping issues, and community longevity. There is potential for wave energy technologies to alleviate some of these issues.

4. DATA COLLECTED FROM FIELD TRIP FROM ST. GEORGE

4.1. Overview of St. George Power System

The location of this study was selected to be in the Aleutian/Pribilof Islands. As the primary focus of this project was to investigate microgrid applications to coastal communities, it was also imperative to evaluate and incorporate the design and construction of the selected coastal community. Due to the harsh weather, many of these coastal communities face accelerated equipment degradation and excessive losses. The community that was selected is no exception. In 2012–2013, AEA met with the community to revitalize and upgrade the degrading power system (Alaska Energy Authority 2012). There was an extensive effort to rebuild the power system to enhance automation, resilience, and reduce losses. The past efforts were split into the following phases:

In the first portion of the revitalization, the generation station was replaced in the islanded community by a contemporary prefabricated generation station. This station was pre-built in Anchorage, Alaska, and shipped to the community via barge. The generation station contains four 220kW diesel generators. These generators are controlled by the operator in the control room housed within the prefabricated building. The control room provides easy access for the operator to control the Supervisory Control and Data Acquisition system, manual or auto parallel the switchgear, protective relays, and Woodward generation controllers.

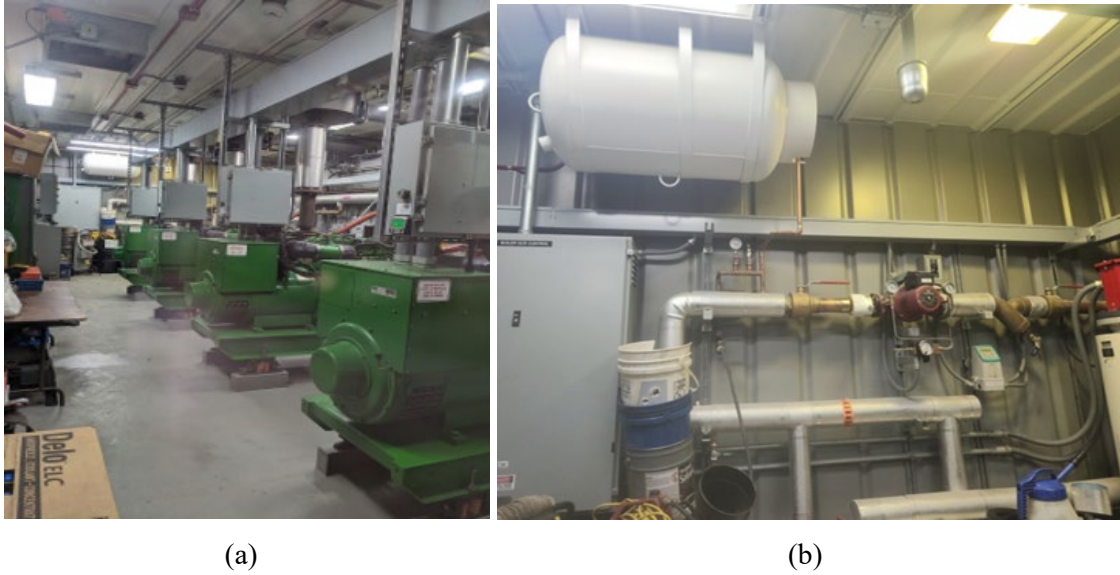


Figure 5. St. George power system: (a) Diesel generators and (b) heat recovery system.

The switchgear installed in the prefabricated unit is fully automatic by using a programmable logic controller. This controller allows the generation station to automatically match the running generator(s) to the community load and supports paralleling capability. Furthermore, the unit has a load control system that monitors the generator’s electrical demand and wind generation output to dispatch the correct amount of power and allocate the correct number of units. In this prefabricated unit, relaying is also installed for complete protection and monitoring of each generator and the feeder.

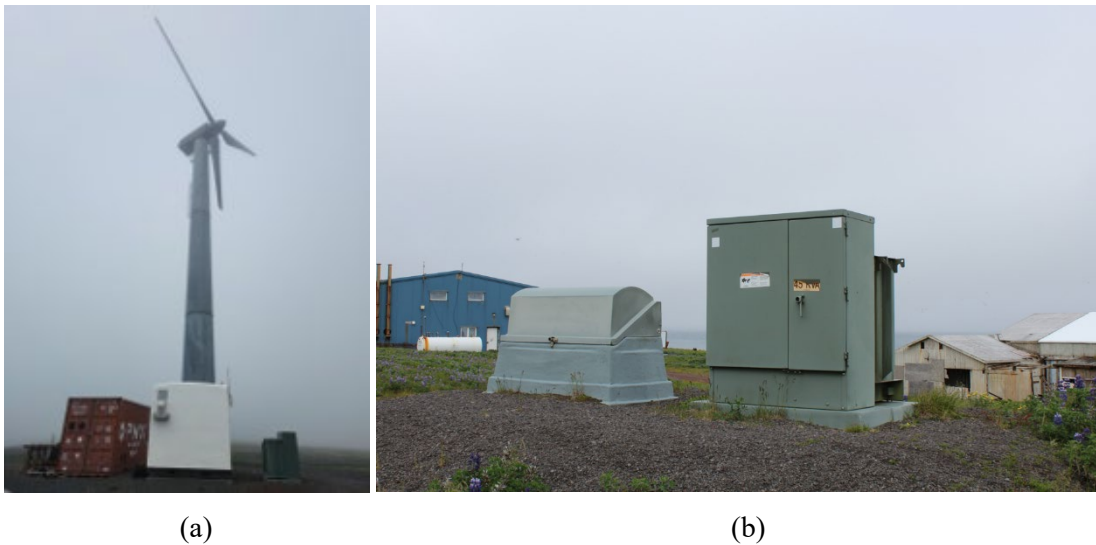


Figure 6. Power System Upgrades in St. George: (a) Wind turbine and (b) rebuilt distribution system.

With wind power integration controls, the microgrid retains a plug-and-play integration of generation technologies into the system. As surveyed, the coastal community was identified to have excellent potential for wind generation with a Class 7 wind regime. A Windmatic Model 17s Turbine with a rating of 95kW was installed. This wind turbine was installed roughly 1.5 miles north of the community. A fiber optic cable connects the generation facility to the wind turbine generator to ensure optimal efficiency. Furthermore, a boiler and heat recovery system were installed at the generation facility to assist with frequency control.

The heat recovery system captures jacket water heat from the diesel generators using a heat exchanger plus heat generated from excess wind power using an electric boiler. It will then deliver heat to the school's public safety building, city power plant building, city public works building, and future Tanaq Corporation shop. According to the AEA report, these four existing facilities and one future facility are estimated to use 15,000 gallons of diesel annually for space and water heating. Heat exchanger, pumps, and associated equipment in module-recovered heat British thermal unit (BTU) meter in module and at the school. In the field, it was indicated that the heat recovery system was supplying heat to the city public safety building and power plant. The boiler provides frequency control and a secondary dump load when the wind output exceeds the electrical demand. The boiler will be connected to the diesel heat recovery system so that excess electric power can heat buildings.

4.2. Existing Wind Turbines

The community has a Class 7 (excellent) wind regime and is an ideal location for wind energy. A single Windmatic Model 17s turbine with a capacity of 95kW was installed during the rebuilding of the power system. The modeling indicates that this turbine could have a capacity factor as high as 38%. The diesel power plant switchgear communicates via a buried fiber optic cable with the wind turbine controller. The diesel switchgear acts as the master controller to coordinate the system for optimum efficiency. Notably, this system was built under the impression that it would always require diesel generation to maintain frequency (Alaska Energy Authority 2012). The controls will be designed to use the maximum wind power available to offset diesel generation. Ideally, the excess wind power would be used for heat and stored in a battery if there is excess. However, it was noted extensively by the community that a more robust wind turbine would need to be installed. A wind turbine has been installed twice, failing mechanically both times. The brakes failed on the first wind turbine, causing it to catch fire. The second wind turbine sheared its cabling due to winding itself in one direction.

4.3. Heating and Electricity Demand

The average load in the community has been estimated and verified by in-situ data gathering to range from 90–100 kW. AEA conducted its analysis from 2011 to 2012 during the authorities' first cursory data analysis (Alaska Energy Authority 2012). The numbers in the AEA report were collected from the PCE program, from meter readings at the power plant, and estimates made by Marsh Creek in the 2011 design report (Alaska Energy Authority 2012). AEA also verified their studies by using hybrid optimization model for electric renewables (HOMER), a techno-economic analysis tool. This load calculator estimated the average load in the community to be 98 kW. After the hourly load data was imported into HOMER, projections were made by scaling the data to 90 kW and 100 kW average loads. Projections varied by less than 10% using the different techniques. For the production and economic estimates, the Alaska Village Electric Load Calculator version was used and scaled to 90kW-averaged load. The population declined from 152 in 2000 to approximately 97 in 2011 and was 39 when the team visited in 2023.

4.4. Resource Assessment: Solar, Wind, and Wave

It was determined that the community has many energy resources available to incorporate into its generation technology profile. Most notably, it has a Class 7 wind regime that contains massive wind potential. AEA has already evaluated and incorporated this wind resource into the community. However, it is essential to note that the level of interest in wind energy is low due to two unsuccessful attempts at long-term wind turbine operation. Hopefully, a more robust wind turbine would provide a longer-term solution similar to the wind turbines installed in St. Paul.

The community under consideration is on an island surrounded by the open ocean, and it retains a sizeable ME potential. During the site visit, it was discovered that the island has become relatively ocean-ice-free in the winter, solidifying the community’s interest in ME. This energy is primarily in the realm of wave energy potential, as the tide movement around the island is low compared to other regions of Alaska. The waves surrounding this island are notoriously large, as they are open ocean waves. The north and west sides of the island were suggested as locations for the ME device, primarily at the locations of the new and old harbors. It is important to note that this island’s latitude is below the Arctic Circle, and it has the potential to generate solar energy. However, this island is notorious for its cloud and fog cover. Therefore, while solar energy would positively impact the island, its daily impact may be low during months of fog and clouds.

4.5. Power Distribution Network

As an overview of the power system, power is currently generated at 480 volts, 3-phase, 4-wire, and distributed at 12.47/7.2 kV 3-phase. This community has two feeders: one 150kVA (kilovolt ampere) transformer feeding the residential village loop and another 150kVA transformer feeding the cross-island industrial radial to the airport/harbor. The fully underground distribution system consists of underground residential distribution, #1 American wire gauge, aluminum, and jacketed concentric neutral conductors. New transformers were installed in the 2012 rebuild and are made of stainless-steel construction. It is important to note that three single-phase reactors were installed at 6876mH at the beginning of the cross-island feeder to support the power flow to the harbor and airport.

The new distribution system was noted to be constructed following Rural Utility Service Bulletin 1728F-806, “Specifications and Drawings for Underground Electric Distribution.” Therefore, all new primary and secondary units were noted to be installed in a 2-in. high-density polyethylene (HDPE) conduit. All new primary cables are polyethylene-jacketed concentric neutral with ethylene propylene (EPR) insulation, 133% MV105. All connections will be above grade in junction boxes, verified along Zapandi Road by visual inspection of the junction boxes.

4.6. Power Cost Equalization Incentives

In Alaska, AEA uses the PCE price for diesel plus fifty cents as a baseline for the diesel price for heat. A price of \$6.35/gal is assumed in this case. In computations and from the AEA report, it was also noted that the industry standard of \$.04/kWh was used to estimate operations and maintenance (O&M) costs. As a group, community facilities are eligible to receive PCE credit for up to 70 kWh per month multiplied by the number of residents in a community. Customer eligibility is based on actual power purchased; therefore, the logs of purchased power must be retained. Residential customers are eligible for PCE credit up to 500 kWh per month. If residential customers purchase more than 500 kWh per month, then the remaining cost is the regular rate of the utility. State and federal offices/facilities, commercial customers, and public schools are excluded from PCE. Of the eligible cost per kWh, 95% is found in Equation (1) and Equation (2) to calculate the PCE cost.

$$19.02\text{¢}/kWh \leq \text{Eligible cost} \leq \$1.00 \tag{1}$$

$$\text{Eligiblecost} = [19.02\text{¢}/kWh, 1.00\$/kWh] \tag{2}$$

Costs below 19.02 cents/kWh and above \$1.00/kWh are not eligible for the PCE program. Once the maximum cost of \$1.00 has been reached, the maximum PCE level is 76.93 cents/kWh. This is determined from the equation (1), where $\$1.00 - 19.02 \text{ cents} = 80.98 \text{ cents} \times 95\% = 76.93 \text{ cents}$.

5. MICROGRID MODEL

Component models and optimization problem formulation for proposed island microgrid integrate various conventional and advanced energy sources and storage technologies. Key components of ME microgrid modeling and optimization formulation include the modeling of WECs, as well as the integration of other energy sources such as diesel genset, wind, solar, electrolyzer, and storage technologies like thermal storage, battery energy storage systems (BESS), and hydrogen storage. Xendee tool is used to model the components and formulate the problem scenarios for optimization (Stadler and Naslé 2019).

5.1. Wave Energy Converter

The WEC is modeled as a discrete unit, with the user having the flexibility to set the cable length based on the intended location of each WEC. This customization allows for efficient placement and configuration of WECs in the coastline. The objective is to determine the number of units needed for optimal energy generation. The cost of each WEC installation is calculated using Equation (3):

$$CAPEX = CAPEX = n \times \text{Fixed Cost} + \text{Cable Length} \times \text{Fixed Cable Cost} \times (n \times \text{conf} + (1 - \text{conf})) \quad (3)$$

where

n = number of WEC units

conf = cable configuration factor for multiple WEC units, indicating whether the cable cost scales with the number of units.

While the algorithm determines the optimal number and configuration of WEC units, the cable length is not sized by the algorithm and is set by the user based on the specific requirements of the installation site. This approach allows for greater flexibility and customization in designing ME-based microgrid systems. As shown in Figure 7, $\text{conf} = 1$ denotes the configuration model has an individual export cable designated for each WEC unit, stretching directly from each unit to the onshore substation. This setup ensures that each WEC unit has its own dedicated connection, providing a direct and streamlined pathway for energy transmission to the onshore facility. Whereas, for the cable configuration, $\text{conf} = 0$ involves connecting the units to an offshore hub using smaller export cables. From this hub, a single high-capacity export cable is deployed, linking the hub to the onshore substation. This configuration centralizes the connections offshore, reducing the number of cables running from the units to the onshore infrastructure. Furthermore, this approach optimizes efficiency by consolidating energy transmission through a single main cable while allowing for multiple WEC units to contribute to the offshore hub.

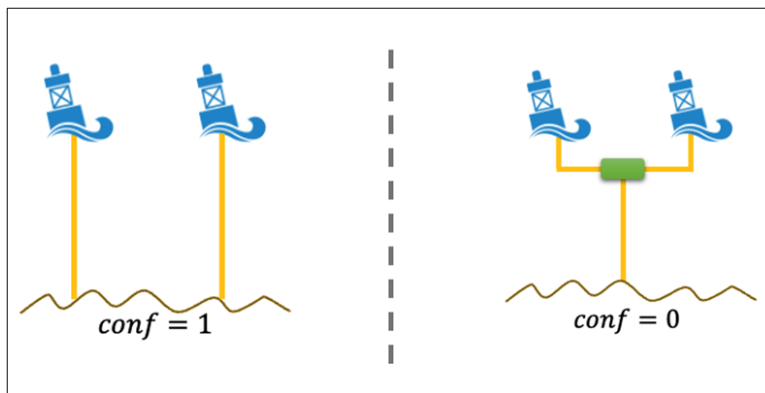


Figure 7. WEC cable configuration layout.

In the context of modeling wave energy conversion for optimization, the first step involves generating potential power data based on significant wave height and dominant wave energy period data specific to a location. This data, obtained from time-series data, captures the fluctuations in wave conditions over time. Concurrently, a critical input is the WEC performance matrix, representing its power output under varying wave height and energy period combinations. Multiplying the potential power data by the number of WEC units provides an estimate of the total potential power output of the WEC array at each timestep. However, not all potential power can be harnessed due to constraints such as WEC design limits or environmental factors. Thus, the actual power output of the WEC array is adjusted by subtracting any curtailed power with an optimal number of units n and providing balance between potential power generation and curtailment. WEC power at time t is given by Equation (4):

$$Power_t = n \times Performance_t - Curtailed_t \quad (4)$$

The optimal number of WEC units are determined in addition to ensuring efficient power generation by analyzing potential power data and considering various operational constraints. To model the WEC's behavior accurately, the cut-in and cut-out behavior of the WEC is accounted by assigning *null* power values for wave conditions outside of the WEC's operational range. This prevents the WEC from attempting to generate power under unfavorable conditions, aligning the optimization process with the realistic behavior of the WEC. Overall, this approach enables the optimization of the WEC array configuration, maximizing power generation efficiency while accounting for real-world constraints and operational behavior.

Table 1. Key inputs and outputs for WEC Modeling.

Key Inputs	Notes
Technology Decision	Specify whether tech is existing or new; specify whether unit(s) are selected or forced into solution
Rated Capacity	For reporting purposes
Lifetime and Age	Expected lifetime of WEC unit(s); age of existing unit(s)
Wave Time-Series Data	Hourly time-series data with significant wave height and energy period
WEC Performance Matrix	Specifies power generated based on the significant wave height and energy period
Cable Length	Length of export cable from WEC unit to shore
Cable Configuration	1: Individual export cable from each WEC unit all the way to onshore substation; 0: Units connected to offshore hub via small export cables; single high-capacity export cable from hub to onshore substation
CAPEX	CAPEX per WEC unit and CAPEX per meter length of cable
OPEX	Fixed O&M (\$/unit/year); Variable O&M (\$/kWh generated/year)
Incentives and Exports	Specify eligibility for state/federal Investment Tax Credit (ITC) and Modified Accelerated Cost Recovery System (MACRS) programs; option to allow exports
Key Outputs	Notes
Selection and Sizing	Identification of optimal number of WEC units (if any); report on number of existing units
Operation	Hourly dispatch of generated and curtailed power
Costs and Revenue	CAPEX and OPEX; revenue from exports; cable cost per unit; incentives

For WEC modeling, bottom-referenced heaving buoy (BREF-HB) and bottom-referenced submerged heaving buoy (BREF-SHB) systems have been used, which support the strategic choice. These two technologies are selected based on the availability of performance matrix data (Figure 8), cost analysis, and alignment with the required power output for meeting the demands of the St. George Island.

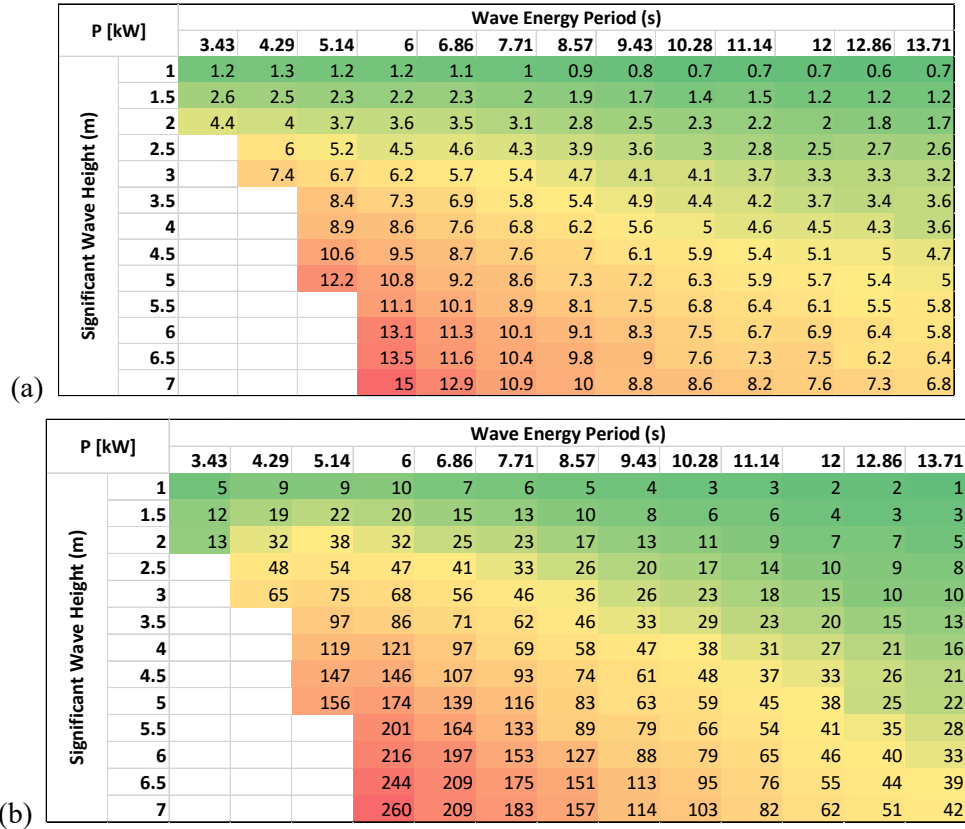


Figure 8. Wave performance matrix for WEC devices (a) 15-kW BREF-HB and (b) 260-kW BREF-SHB.

5.2. Other Microgrid Technologies

Other technologies modeled for the microgrid include diesel generator, wind turbines, solar PV, electrical heater/boilers, thermal storage, BESS, and hydrogen storage. There are currently four 210 kW diesel generators (John Deere Model: 6090 AFM75E) in use at St George. These generators have a lifespan of 10 years or 10,000 hours, and although they are rated at 244 kW at 1,800 RPM, they are currently operated at 210 kW. The fuel (diesel) storage capacity can hold up to 200 gallons. These diesel gensets have an electrical efficiency of 34.7% and a heat-to-power ratio of 1.2. These values were calculated based on electrical efficiency and a total efficiency of 67.4%. However, two other diesel gensets were not required to provide power rather they were modeled to capture the maintenance/replacement cost.

For modeling wind, a 95-kW power rating and a turbine hub height of 98 feet were selected as per the AEA studies. The Siemens model was selected, and the adjustments were made in such a way that the total potential power output of the turbine model is scaled to reflect the user-set 95 kW rating. Also, the community is likely to use Vestas V27 wind model.

To further increase the share of locally available energy, solar PV resource assessment was considered. As per the requirement, the maximum capacity of the solar PV was set to 250 kW and with a fixed ground-mounted array type.

To harvest the excess power from wind and PV, BESS was considered to further improve the resiliency standards for the community. The charging and discharging efficiencies for the modeled BESS were set to 90%, whereas the maximum and minimum state of charge were set to be 100% and 5%, respectively. The charging and discharging rate for the BESS was also modeled to be at 1C.

To meet heat demand, diesel boiler and electric heater are considered. The thermal efficiency of the boiler was set to 75%. Similarly, the electric heater was also considered to supply additional water heating loads for various facilities at the community.

The team also considered the possibility of including a hydrogen ecosystem in the mix. This includes electrolyzers, hydrogen storage, hydrogen fuel cells, and hydrogen boilers. Although the microgrid does not have a direct hydrogen demand, hydrogen can be produced using excess electricity, stored in hydrogen storage, and used to meet electricity and heat demand during low generation availability periods and emergencies.

To model the water desalination plant, a proxy water supply model was proposed using the hydrogen ecosystem in Xendee. Since water demand was not necessarily a concern for the community, it was not included in the analysis.

5.3. Xendee Optimization Model

The optimization aims to minimize the total annual cost of an energy system while ensuring energy balance and meeting a maximum payback period constraint. The objective function combines various cost components, including electricity purchases, fuel costs, investment costs, operation, and maintenance costs while accounting for revenue from selling excess electricity, shown in Equation (5). The energy balance constraint ensures that the total energy supplied by the system, from both generation and purchases, matches the total energy demand and losses. Additionally, the payback constraint limits the payback period for the total investment in the system. This approach allows for the efficient design and operation of energy systems, considering economic, environmental, and operational factors. The simplified objective function in Equation (5) is subjected to the energy balance constraint, as shown in Equation (6), and payback constraint in Equation (7).

$$minc = c_{\text{tariff}} + c_{\text{fuel}} + c_{\text{invest}} + c_{O\&M} - r_{\text{sales}} \quad (5)$$

$$D_{m,d,h} + L_{m,d,h} = \sum_t G_{t,m,d,h} + P_{m,d,h} \quad (6)$$

$$\frac{\text{Total Investment}}{\text{Annual Savings}} \leq \text{Max Payback Years} \quad (7)$$

where

- c = total annual cost
- r = revenue
- m = month (typically 12)
- d = day (typically 30)
- h = hour (typically 24)
- t = technology
- D = demand
- L = losses
- G = generation
- P = purchases.

These constraints are foundational for ensuring the optimal design and operation of microgrid systems (See Figure 9).



Figure 9. Key constraints for optimization.

The climate database is used to calculate available local generation resources, such as solar radiation and wind speed, which are crucial for estimating the microgrid’s power generation capacity. Power constraints, including losses and power quality, are integrated into optimization algorithms to ensure efficient operation and minimize energy losses. Additionally, operating constraints, such as the number of power cycles of energy storage, are accounted to ensure that assets perform within specified limits, optimizing their lifespan and efficiency. Financial constraints, such as interest rates and payback periods, are factored in helping users make economically viable decisions when designing and operating their microgrid systems. Regulatory constraints like incentives are also considered to ensure compliance with regulations and optimize the financial aspects of the microgrid project. Storage constraints, including aging and self-discharge, are incorporated to help users manage energy storage systems effectively, maximizing their performance and lifespan within the microgrid.

5.4. St. George Infrastructure Model

As an overview of the power system, power is currently generated at 480 volts, 3-phase, 4-wire, and distributed at 12.47/7.2 kV 3-phase. This community has two feeders: one 150kVA transformer feeding the residential village loop and another 150kVA transformer feeding the cross-island industrial radial to the airport/harbor. The fully underground distribution system consists of underground residential distribution, #1 American wire gauge, aluminum, and jacketed-concentric neutral conductors. New transformers were installed in the 2012 rebuild and are made of stainless-steel construction. It is important to note that three single-phase reactors were installed at 6876mH at the beginning of the cross-island feeder to support the power flow to the harbor and airport.

The new distribution system was noted to be constructed following Rural Utility Service Bulletin 1728F-806, "Specifications and Drawings for Underground Electric Distribution." Therefore, all new primary and secondary units were noted to be installed in a 2-in. HDPE conduit. All new primary cables are polyethylene-jacketed concentric neutral with EPR insulation, 133% MV105. All connections will be above grade in junction boxes, verified along Zapandi Road by visual inspection of the junction boxes.

To begin modeling the system, Alaska Center for Energy and Power used geo-tagged locations collected for all above-ground equipment. This included transformers, junction boxes, wind turbines, and wellhouse. This file of GPS (Global Positioning System) tags has been included in the folder as both a text document and Google Earth keyhole markup language, titled "StGeorgeGPS." Figure 10 is the Google Earth location file, which overviews the island and its power system, and Figure 11 overviews the town.



Figure 10. Google Earth location map.



Figure 11. Google Earth location map of the town view.

5.4.1. Xendee Multi-Node Model

While Xendee Geographic Information System (GIS) one-node model is used for technoeconomic optimization, the multi-node capability can be used for preliminary infrastructure evaluation, primarily in integrating power flow, transmission capacity, and loss constraints into the optimization problem. While Xendee multi-node also supports technology optimization and optimal operation, it can connect with Xendee one-line for a more detailed power flow evaluation.

St. George operates as an islanded microgrid with no direct import restrictions. The energy system includes diesel generators, BESS, PV, WECs, and a 95-kW wind turbine, delivering power to a mix of commercial and residential buildings. Key facilities include an airport, fish processing plant, harbor loads, and residential units, with an overall annual demand of 0.991 GWh. The Xendee multi-node model is built with an equivalent distribution system, considering the transformer and the community’s 86,364-foot cable network. The new components for the infrastructure model built in Xendee multi-node to represent the network are discussed below:

1. Voltage Levels: The voltage levels for typical commercial loads, such as those at the airport, Federal Aviation Administration, fish plant, harbor plant, Harbor 2, and school, are maintained around 480 V. In contrast, typical residential loads operate at a voltage level of 240 V. All distributed generators, including wind turbines, WECs, solar panels, and diesel generators, are configured to step down to a voltage of 480 V.
2. Cables: The cable type for all lines is “1/0 AL UG SW.TypCabsys,” indicating underground aluminum cables. The lengths of the cables range from 101.2 feet to 5,025.86 feet, while the maximum current for all cables is consistently 0.135 kA. Notable entries include Line 27 and Line 45, each with a length of 2,443.99 feet, and Line 76 and Line 77, each with the longest length of 5,025.86 feet. Other cables like ME Lines 1, 2, and 3, each have a length of 175 feet. Despite the variation in lengths, all cables are designed to handle the same maximum current of 0.135 kA. The total length of the cable networks across the St. George community is around 86,364 feet.

3. Transformers: The transformer requirements for the Xendee GIS project are based on the varying load demands at different locations, with each site needing a transformer sized according to its peak and fluctuating power usage. The step-up transformer's PM1 residential loop has a capacity of 150 kVA with a 3-phase circuit 480/277V. The commercial loop has a capacity rating of 150 kVA with a 3-phase circuit 480/277V. For the wind turbine, the transformer capacity is 113 kVA, with an impedance percent of 3.5 long with X/R ratio of 2.25. At the Federal Aviation Administration harbor and airport, the transformer capacities vary between 5 and 20 kVA, peaking at 20 kVA, indicating the need for a transformer that can efficiently manage both peak demand and the more common lower loads of 5 to 10 kVA. Similarly, Load 2 shows a consistent peak transformer rating of 20 kVA, suggesting that the transformer should be optimized for high, steady loads. The St. George community, however, presents a much more variable load profile, ranging from 5.3 to 25 kVA, with frequent fluctuations. A transformer here must accommodate both lower loads and the occasional high peaks of 25 kVA, ensuring flexibility and reliability in its operation. Finally, Load 3 requires a transformer capable of handling moderate demand, fluctuating between 5 and 15 kVA, with the highest demand reaching 15 kVA.
4. Energy System Components: The diesel generator provides essential backup power at a diesel cost of \$7.362 per gallon, ensuring reliability during periods of high demand or when local generation sources are insufficient. The BESS plays a crucial role in balancing supply and demand, significantly reducing diesel consumption and enhancing overall system reliability. Complementing the diesel generator are advanced energy sources, such as solar PV, wind turbines, and WECs, which collectively contribute to reducing fuel consumption and promoting local energy development.



Figure 12. Infrastructure model in Xendee considering multi-node capability.

5.4.2. PowerFactory Dynamic Model

The PowerFactory model is a sophisticated hybrid system that integrates three distinct types of simulations: quasi-dynamic, root mean square (RMS), and electromagnetic transient (EMT). Each simulation type is tailored to operate within specific timeframes, addressing unique aspects of power system analysis. Quasi-dynamic simulations, with timesteps ranging from minutes to years, are essential for long-term time-series power flow analysis. These simulations help identify voltage and transmission violations over extended periods, providing crucial insights for planning and ensuring the reliability of the power grid. This type of analysis is fundamental for detecting trends and potential issues that could affect the grid's stability and efficiency over time.

RMS simulations focus on the dynamic behavior of the power system over shorter periods, with timesteps in the range of seconds. By evaluating the RMS values of voltages and currents, this type of simulation helps to understand the system's response to disturbances such as faults or sudden changes in load. This is critical for assessing the short-term frequency stability and performance of the grid. On the other hand, EMT simulations provide high-resolution analysis of electromagnetic transients, operating on a sub-second timescale. These simulations capture detailed behaviors during transient events, such as switching operations, offering a granular view necessary for ensuring the power system's resilience to fast transient disturbances. By combining these three simulation types, the PowerFactory model delivers a comprehensive toolset for power system analysis, covering a wide range of temporal scales and ensuring robust, reliable, and efficient grid operation.

In the infrastructure evaluation, the St. George power system is configured for all three kinds of simulation. Each model was tested for various operations scenarios to allow the system to operate with various advanced energy sources incorporated. The objective is to identify the infrastructure adequacy to host new changes for microgrid as well as understand the stability of the microgrid system with advanced technology integration.

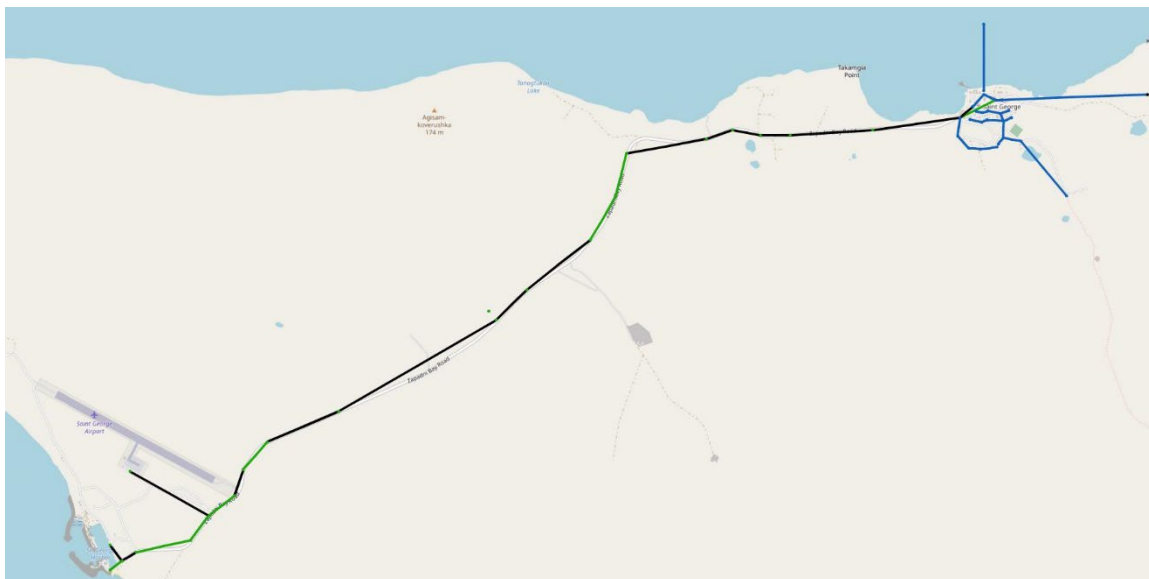


Figure 13. Geographic diagram of PowerFactory model of St. George.

To simulate the RMS and EMT responses of the system, the steady-state models of the generation technologies were extended to incorporate dynamic models. The discussion below provides a summary of the dynamic modeling of different generation resources used for infrastructure evaluation.

1. **Diesel Generator:** There are four diesel generators, but only one unit was used. One of the remaining three was the primary backup and the other two were secondary backups. The operating diesel generator is modeled using a round rotor synchronous machine model for both RMS and EMT simulations. The Institute of Electrical and Electronics Engineers (IEEE) standard EXAC1 (1981 IEEE Type AC1 Excitation System) model is used for the exciter, and the IEEE standard DEGOV1 (Woodward Diesel Governor) model is used for the governor. The backup generators are modeled as synchronous machines without governors and exciters and were out of service; therefore, they were not involved in the EMT and RMS simulations.

2. **Solar PV System:** A standard solar PV dynamic model frame represents the PV system for RMS and EMT simulations. The model includes measurement-based inputs for solar radiation and temperature, feeding into the PV array module. The module provides current and voltage measurements to the controller, which can reduce active power based on frequency deviation signals. The controller generates direct and quadrature axis current signals that are fed into the average value static generator model, which also receives sine and cosine reference signals generated by the phase-locked loop.
3. **Wind Generator:** A Type 3 model based on a doubly fed induction generator is used for the wind generator. The model includes modules for torque, pitch, aerodynamics, drivetrain, electrical components, and generator-converter. Similar to the PV system, an average value model is used for the Type 3 wind turbine generator, which receives direct and quadrature axis current signals to produce three-phase current and voltage at its terminals.
4. **Battery Energy Storage System:** The BESS is represented by a direct current (DC) voltage source connected to a standard pulse-width modulation generator model in PowerFactory. The DC voltage bus operates at 0.9 kV. A simple battery model block measures current and voltage signals from the DC side to compute the state of charge during operation based on provided ratings and initial setpoints. Simple voltage and frequency control modules are integrated, along with a charge controller that acts as a current limiter connected in series. This setup provides direct and quadrature axis reference signals to the average value pulse-width modulation converter with sinusoidal modulation.
5. **Wave Energy:** Because there is no standard dynamic modeling frame for ME devices in PowerFactory, a simplified model was created for WECs. The model produces active power based on a wave energy period and significant wave height measurement signals. Voltage and frequency bounds are provided to consider tripping the device during abnormal conditions. While a detailed dynamic model, such as WEC-Sim(National Renewable Energy Laboratory 2024b), would provide the dynamics of the wave energy device, the objective of this project was to understand infrastructure adequacy when new technologies are included in the system. For infrastructure-based analysis, this simplified model is sufficient.

5.5. Resource and Demand Data

Cost and operational parameter values used for optimization are presented in Appendix B-1. Table B-1 through Table B-10 show the modeling parameters for different technologies including diesel generator, WECs, Solar PV, BESS, wind, electrolyzer, hydrogen storage, and electric heater. The resource and demand profiles used are provided in Appendix A-2.

Figure A-9 and Figure A-10 show the wind power potential and solar PV performance for the St. George community respectively. It is important to note that, a new fish processing plant was recently completed but was not operational when the team visited the community (i.e., St. George). The ice machines used during the fishing season were broken, so many fishermen were fishing out of St. Paul. The plant has the potential to increase peak demand by as much as 100 kW if utilized in the future, and the new line across the island represents this. The community indicated that a new deep-water harbor is currently being designed with the United States Army Corps of Engineers. If constructed, it would allow larger fishing vessels to deliver products and possibly utilize them as their home port in the community. This also can potentially increase peak demand by an additional estimated 100kW. With both projects, peak loads are expected to reach 350 kW to 400kW. Figure A-16 and Figure A-17 in Appendix A-4 provide the load profiles considered for the new fish processing plant and harbor. Without the new deep-water harbor and a fish processing plant, peak loads for the community will not exceed 200 kW.

The present scenario is built considering the data available from 2011 (Alaska Energy Authority 2012). Annual power generation for the island was recorded at 886,000 kWh, with estimated annual fuel consumption of 64,000 gallons, assuming power generation efficiency of 14 kWh per gallon.

Figure A-11 and Figure A-12 show the plots for dominant wave energy period as well as the significant wave height for wave energy potential at the St. George Island, Pribilof Islands, AK. Similarly, Figure A-13 shows the plot of the electricity demand, whereas Figure A-14 and Figure A-15 provide space heating demand water heating demand considered for the community.

6. TECHNOECONOMIC ANALYSIS

6.1. Scenario Development

The overall goal of the optimization is to maximize the onsite local generation to reduce the dependency on diesel fuels. The cost of achieving absolute energy independence is also explored in this paper. Because the system is islanded, total energy independence means 100% of energy comes from local natural energy resources. A specific scenario is analyzed considering the resilience against diesel supply interruptions as well as resilience against outage of onsite generation resource.

Optimization scenarios are developed considering objectives built around cost, local generation adoption, and total energy independence targets. New investment scenarios are considered to account for the perspectives of community members (Figure 14). Particularly, the community’s negative opinion towards wind energy and expected demand growth considering proposed new development within community, including new harbor and fish processing plants are translated into optimization problems. Several additional sensitivity cases are developed considering uncertainty around the capital and operating costs of deploying microgrid resources in remote community like St. George. Due to the low technological readiness, the cost of WECs is also uncertain. The proposed analysis considers projected costs of the wave converter technologies considering advanced, moderate, and conservative estimates. In addition, the sensitivity of the microgrid project qualifying for existing energy investment and production incentives, hydrogen production incentives and federal deployment programs were analyzed.

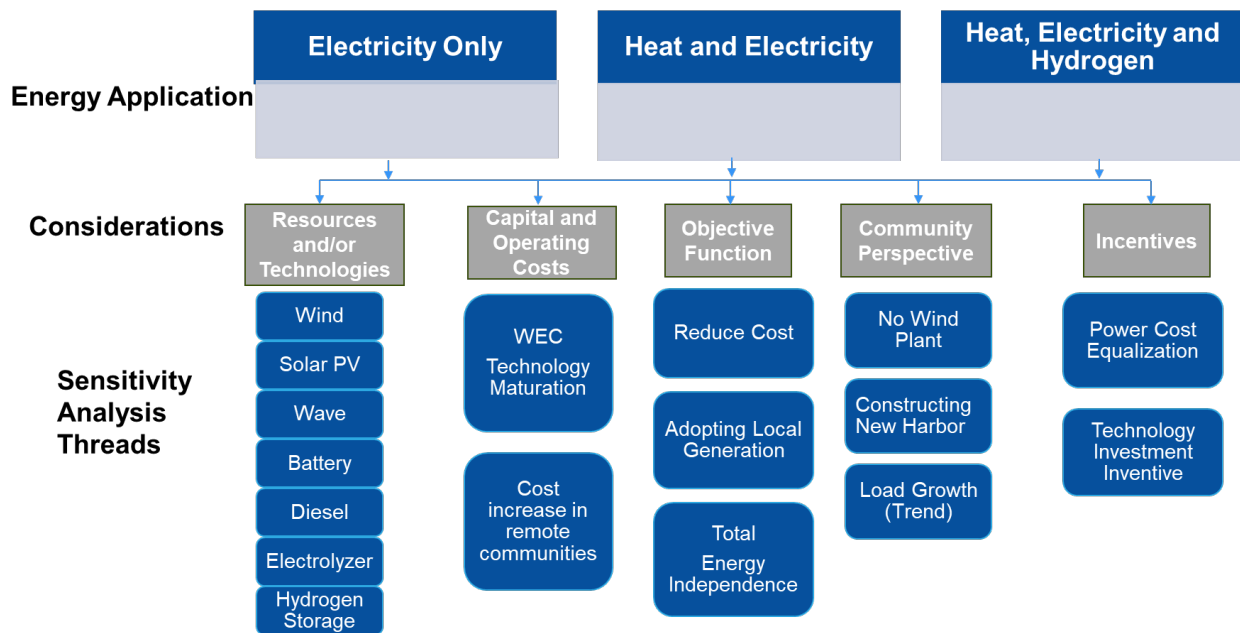


Figure 14. Scenario development for techno-economic analysis.

The overall analysis is divided into six parts: (1) base case scenario, (2) adopting local generation, (3) cost- resilience tradeoffs, (4) sensitivity to uncertainties, (5) electrification of heating demand, and (6) exploring the role of hydrogen. The base case scenario explores the optimal operation of the current state of the energy system in St. George without any investments to establish metrics for comparison with investment cases. This will be followed by an analysis of investment scenarios adopting local generation

to displace externally imported diesel fuels. The third section focuses on investigating tradeoffs between cost, adoption of local resources and resilience for electricity demand only. The fourth section will explore the financial and operation metrics with respect to uncertainties of the cost and technology maturation. The fifth part investigates the cost of displacing diesel from both heat and electricity usage. Electrical heaters/boilers are considered alongside diesel boilers and a diesel generator of combined heat and power (CHP) to meet the heating need. The final scenario explores the role of hydrogen to support the microgrid in achieving energy independence with local generation resources. The results and findings are discussed in detail in the following subsections.

6.2. Base Case Scenario

The base case considers the present state of the microgrid without new investments. During the team’s visit, they observed that the system was not operating efficiently. This analysis assumes optimized system operation without considering any new investment in technologies.

Currently, the City of St. George has four diesel generators. However, operating just one of them meets the electricity demand of the microgrid, with the other three serving as backups. Table 2 provides the optimization results for base case scenario when heat and electricity demand are met with diesel fuel. The annual diesel fuel consumption is 63.41 kgal (kilogallon). The levelized cost of electricity (LCOE) prior to incentives is calculated at \$0.6377/kWh. The actual cost of electricity to the customers is usually higher than the LCOE because the revenue from electricity is one of the primary sources of income for the island’s government. Assuming the case is similar to 2019, St. George qualifies for maximum PCE incentives of \$116,237. Due to the uncertainty in the actual electricity price set by the city for the community, the PCE incentive is not included as revenue during optimization.

Table 2. Comparing base case scenario results for electricity-only and electricity and heat.

	Electricity-only	Electricity and heat
Diesel fuel (gal)	63,410	66,382
Annualized cost (k\$/y)	564,900	590,200
Operation cost (k\$/y)	549,000	574,000
LCOE (\$/kWh)	0.638	—
PCE incentive (k\$/y)	116,237	116,237

The heat recovered from the diesel generator supports 85% of the microgrid’s space heating demand. The remaining 15% is met by operating household diesel boilers. The required total boiler capacity is 161 kWth, which is considered existing and distributed across community households. The operation of diesel boilers results in an additional consumption of 2.972 kgal of diesel fuel. The total annualized cost for heat and electricity is \$590,200 per year.

6.3. Adopting Local Generation

As shown by results in Table 2, electricity demand accounts for the majority of the energy demand of St. George. Therefore, the first part of the analysis explores the investment scenarios to add new generation technologies in microgrid considering various objectives.

Using the National Renewable Energy Laboratory’s (NREL) annual technology baseline as base cost for specific resources and escalating the cost using the cost adjustment factor (CAF), the team accounted for locational constraints. The Department of Education of the State of Alaska provides CAF for construction projects across various parts of Alaska in reference to the cost for construction project in Anchorage, AK (Department of Education and Early Development 2023). The CAF, 1.3219, for Pribilof Islands is used for St. George.

Local generation resources including wind, PV, and WEC, are considered alongside BESS. Table 3 summarizes the results for various objectives, including technology sizing, financial metrics, and operation metrics. Clearly, adopting local generation would result in a lower cost for the system. For the cost minimization objective, the system hosts new PV and wind generation. No WEC and BESS were hosted. The addition of new generation reduces the operational expenditure (OPEX) of the system by 70%, resulting in an LCOE of \$0.34/kWh, which is 47% less expensive than the base case. Diesel fuel consumption decreases by 73.4%. A significant portion of available energy from local generation technologies (i.e., PV, Wind and WEC) is curtailed.

Table 3. Results for electricity-only scenario for different objectives enabling all generation assets, including wind.

	Cases	Cost Minimize	Local Generation Adoption (PCF=1)	Total Energy Independence
Technology Sizes	New Generation (kW)	PV: 67.5, Wind: 285	PV:464, Wind:380, WEC:150	PV:606, Wind:1520, WEC:180
	BESS (kWh)	—	461	2,300
Financial Metrics	CAPEX (k\$)	2,174	6,127	17,276
	OPEX (k\$/y)	162	140	190
	Annual Cost (k\$/y)	299.1	567.7	1,568
	LCOE (\$/kWh)	0.34	0.63	1.75
Operation Metrics	Gen Curtail (%)	41.5	57.3	85.8
	Diesel (gal)	16,867.5	4,183	0

For the local generation adoption objective, a case with a premium cost factor (PCF) of 1, meaning the maximum annual cost for investment cannot exceed the investment cost, is shown in Table 3. The system hosts a mix of PV, wind, and WEC along with energy storage, indicating that a hybrid mix of resources is more effective than a single type of resource. Diesel use reduces to 4.18 kgal, which is a 93.4% reduction from the base case scenario. However, generation curtailment is worse than in the cost minimization case, resulting in the curtailment of 57% of available generation. Reducing the last 7% of diesel will be very expensive, as indicated by the results for the energy independence case. Significantly, larger capacities of generation resources and energy storage are hosted, resulting in an LCOE being almost three times more expensive than the current scenario. Due to the oversizing of energy assets, more than 85% of the hosted generation is curtailed.

6.4. Cost-Resilience Tradeoffs

Achieving energy independence without diesel will be expensive, resulting in inefficient use of resources and significant generation curtailment. A more practical scenario would include a mix of local generation resources meeting most of the demand, while diesel supporting the remaining load. Based on the results in Table 3, the team ran optimization to understand the tradeoffs between cost and resilience. In this context, resilience means reducing reliance on externally imported fuels by having onsite resources to support energy demand. Three variables are of interest in this analysis: LCOE, diesel use, and generation curtailment.

As discussed earlier, adding new local generation immediately improves the financial performance of the system while reducing diesel use. After the minimum cost point (see Table 3), LCOE starts to increase with a reduction in diesel use, as shown in Figure 15. As more aggressive resiliency targets are set, for the displacement of the last 10% of diesel use, the LCOE increases by nearly three-fold.

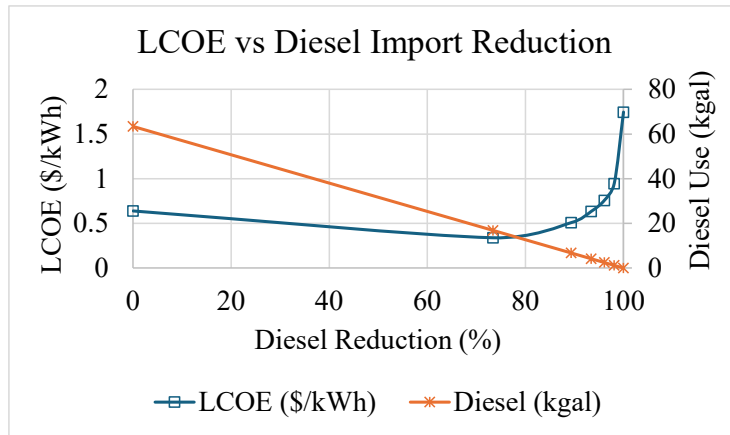


Figure 15. Sensitivity of LCOE and generation curtailment with respect to resiliency and energy independence.

The team delves deeper into the results to analyze the selection and sizes of assets and plotted the asset selection sensitivity chart in Figure 16. With the cost minimization objective alone, the system only hosts wind and PV, resulting in 44% generation curtailment. As the team enables investment up to PCF=0.8 to support the local generation adoption objective, the optimizer finds it effective to host battery energy storage alongside solar and wind generation. As more aggressive local energy adoption targets are applied, the system starts to host WEC as well. With the addition of WEC, the rate of increase in generation curtailment slows down, indicating better hybridization potential of wave energy with other resources. However, as the diesel use reduction target approaches the last 5%, generation curtailment increases sharply, even though more BESS is hosted.

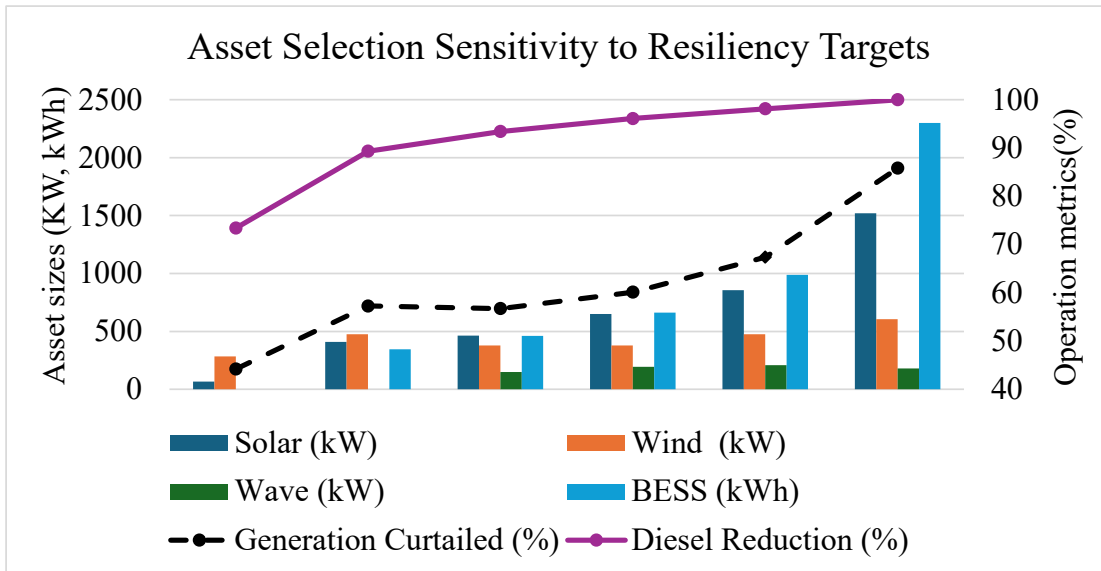


Figure 16. Asset selection and sizing, and generation curtailment with respect to resiliency targets.

Besides reducing reliance on diesel, another important form of resiliency is maintaining generation redundancy. This is particularly important when the system relies primarily on local generation depending on weather conditions. For example, although icing conditions are not common on St. George’s shore, they can result in generation outages for multiple days. Such scenarios often lead to the complete outage of one or multiple types of generation resources. Having diesel fuel backup is necessary to ensure that the system has sufficient energy reserves when such contingencies arise.

6.5. Sensitivity to Uncertainties

6.5.1. Cost of Technologies

The cost of installing new technology in remote communities is highly uncertain. In the team’s review, a significantly wide range of costs (see Appendix B-2) was found for past microgrid projects for remote communities. This variation is due to several factors, including the microgrid location, the selected technology’s cost, technology maturity, and other cost overrun scenarios.

While the base cost parameters considered in previous sections already account for the adjustment factor for the Pribilof Island regions in Alaska, these estimates are likely optimistic for the actual costs of building projects in remote locations like St. George. To understand the impact of technology prices on technology selection and overall optimization goals, we conducted sensitivity analyses to account for potential variations in capital and operations costs. This was achieved by adjusting the CAF, which applies the same scaling factor to both capital and O&M costs of each new component in the microgrid.

As depicted in Figure 17, increasing the CAF shifts the minimum cost point to a lower diesel use reduction percentage. Nevertheless, for both CAF=1.5 and 2, the minimum cost point still achieves a reduction in diesel use exceeding 60%, indicating a promising role for local generation in the system. As expected, pursuing the energy independence goal becomes increasingly costly with higher CAF values. Figure 18 illustrates that as CAF values rise, the amount of generation curtailed decreases. However, this reduction can be attributed to a smaller fraction of generation supported by new technologies, resulting in lower generation curtailment, though it is at the expense of greater diesel use.

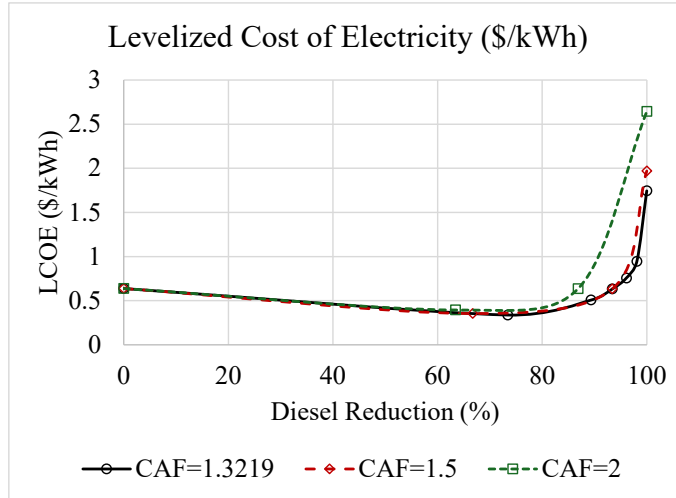


Figure 17. Comparing LCOE sensitivity to diesel use reduction for various cost adjustment factors.

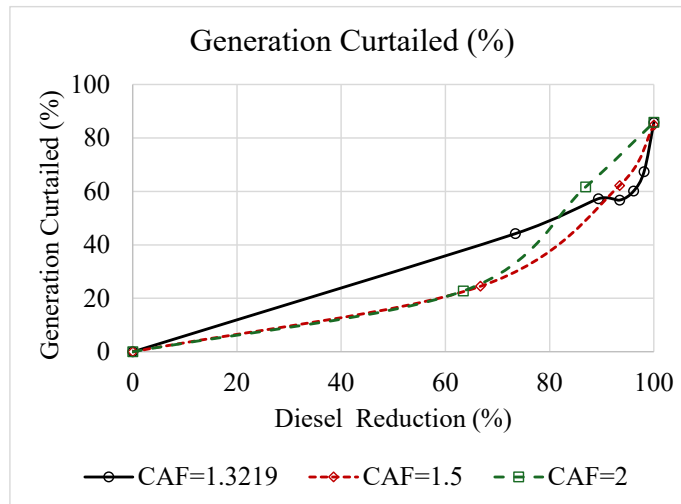


Figure 18. Comparing sensitivity of generation curtailment to diesel use reduction for various cost adjustment factors.

6.5.2. Wave Energy Converter Technology Maturation

WECs are at a lower technology readiness level compared to wind and solar technologies. While WECs are not cost-competitive with wind and solar currently, they can become cost-competitive as technology matures. Although the previous results already considered a moderate future cost projection for WECs in the base assumption, the O&M costs are nine times higher compared to similarly sized solar and wind resources. While it is expected that offshore systems like WECs will have higher maintenance costs (Chang et al. 2018), these selected O&M cost parameters resulted in the exclusion of WECs from most of the optimization scenarios. Considering the expected improvements in O&M costs for WECs, the team built two additional scenarios in addition to the moderate scenario, namely aggressive and advanced, which assume significant improvements in O&M costs as the technology matures. The advanced scenario has O&M costs similar to those of offshore wind today.

Although the O&M costs are reduced in the Aggressive and Advanced cases, they are still more expensive than wind and solar. Therefore, the cost minimization objective driven by the motivation to reduce costs see no changes in results in aggressive and advanced cases as compared to the moderate case

(Figure 19). Similarly, the energy independence scenario, which required a specific combination of resources to effectively achieve the goal, did not see any major differences due to the reduced O&M costs of WECs. Similar observations were made with all three CAF values (1.3219, 1.5, and 2).

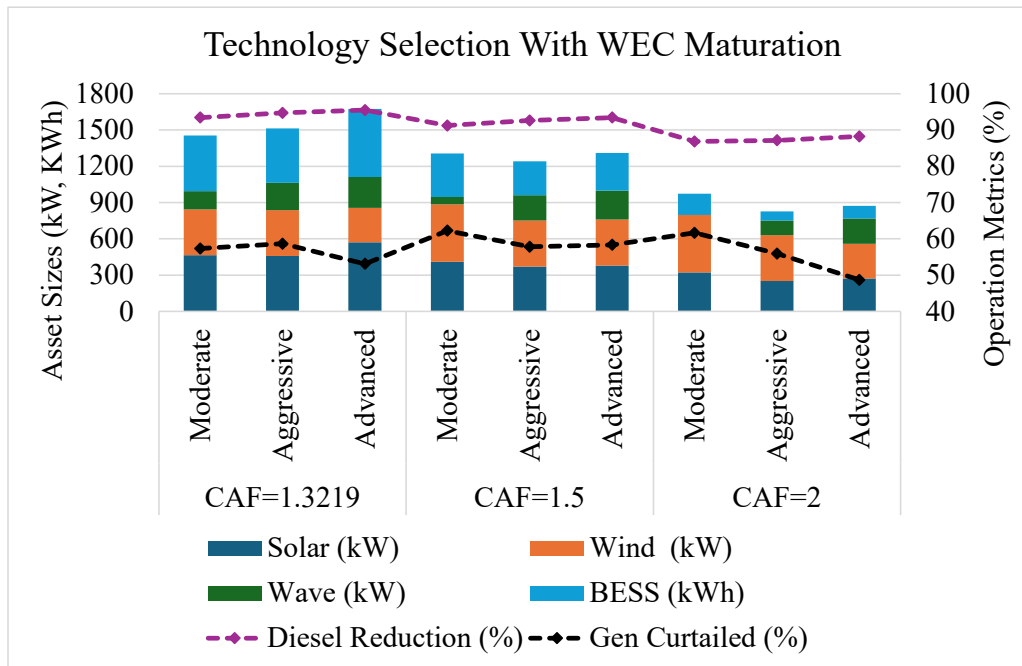


Figure 19. Sensitivity of asset selection and sizing and generation curtailment with respect to local generation adoption target (PCF=1).

The difference is mainly observed in the local generation adoption case (PCF=1), which are intermediate scenarios between the cost minimization and energy independence objectives. In all three CAF cases, the share of WECs in the mix increases as the O&M costs move from moderate to advanced. The diesel use reduction increases marginally, but the most significant improvement is in the generation curtailment. With the inclusion of more WECs in the mix, the percentage of available generation curtailment reduces, indicating better hybridization of resources.

6.6. Integrating Community Perspective

6.6.1. Future Growth

In this analysis, the team considers the expected growth in future electricity demand due to the construction of a new harbor and a fish processing plant, each with a 100-kW peak. These new changes nearly double the use of diesel fuels for electricity in the microgrid, as shown in Table 4.

Table 4. Future scenario with demand growth supported by diesel-based electricity (electricity-only case).

Quantity	Value
Diesel Fuel (gal)	124,140
Annualized Cost (k\$/y)	1,090.8
Operation Cost (k\$/y)	1,075
LCOE(\$/kWh)	0.629

The annualized and O&M costs also increase by a similar ratio compared to the current scenario, while the LCOE remains nearly the same. No new generation capacity would be necessary to support the

demand growth because the system already has the necessary diesel generation capacity to support the increased load.

The system is optimized with future loading, considering cost, local generation adoption and energy independence objectives. The results are provided in Table 5. With increased demand, the new generation capacity for each optimized case is much larger than cases based on the current loading conditions in Table 4.

Table 5. Results for electricity-only scenario for different objectives considering future.

	Cases	Cost Minimize	Adopting Local Generation (PCF=1)	Total Energy Independence
Technology Sizes	New Generation (kW)	PV: 301, Wind: 475	PV:1070, Wind: 760, WEC: 315	PV: 812, Wind: 2950 WEC:225
	BESS (kWh)	—	779	4,940
Financial Metrics	CAPEX (k\$)	4,330	12,703	31,758
	OPEX (k\$/y)	312	275	305
	Annual Cost (k\$/y)	559.1	1,096.3	2,969
	LCOE (\$/kWh)	0.3224	0.6255	1.69
Operation Metrics	Gen Curtailed (%)	41.77	59.11	85.15
	Diesel (gal)	32,015	6,444	0

Other financial and operational metrics do not see any major differences. The LCOE for the cost minimization and energy independence objectives are \$0.3224 and \$1.69 /kWh, which represent 1.52% and 5% reductions compared to the results for the current loading condition. Marginal improvements are observed in the percentage of generation curtailed and percentage of diesel use reduction.

6.6.2. Without Wind

During the team’s community visit, many members showed skepticism about wind energy. This is because of the failed attempts to install wind turbines, despite excellent wind potential at the site. Therefore, this section investigates the operation and economics of the system without including wind energy. The results for cost, local generation adoption, and energy independence objectives are provided in Table 6.

Table 6. Results for electricity-only scenario for different objectives excluding wind.

	Cases	Cost Minimize	Adopting Local Generation (PCF=1)	Total Energy Independence
Technology Sizes	New Generation (kW)	PV: 302	PV:298, WEC:240	PV:3550, WEC:630
	BESS (kWh)	—	1.96	4,180
Financial Metrics	CAPEX (k\$)	1,133	3,023	24,004
	OPEX (k\$/y)	449	395	440
	Annual Cost (k\$/y)	513	567.7	23,717

	LCOE (\$/kWh)	0.58	0.64	2.55
Operation Metrics	Gen Curtail (%)	26.14	18.38	74.39
	Diesel (gal)	50,521.47	32,420.47	0

Figure 20 compares the LCOE and generation curtailment for the scenarios without wind and with wind. As shown, the results for cost minimization without wind show a higher LCOE compared to that with wind. While generation curtailment improves, the diesel use reduction is 20% less than the case with wind. This is due to the higher capital costs of wave energy and the relatively lower resource potential for wave and solar compared to wind at St. George. As expected, the energy independence case is much more expensive without wind. However, generation curtailment is lower, indicating better hybridization between wave and solar compared to the combination of wind, wave, and solar.

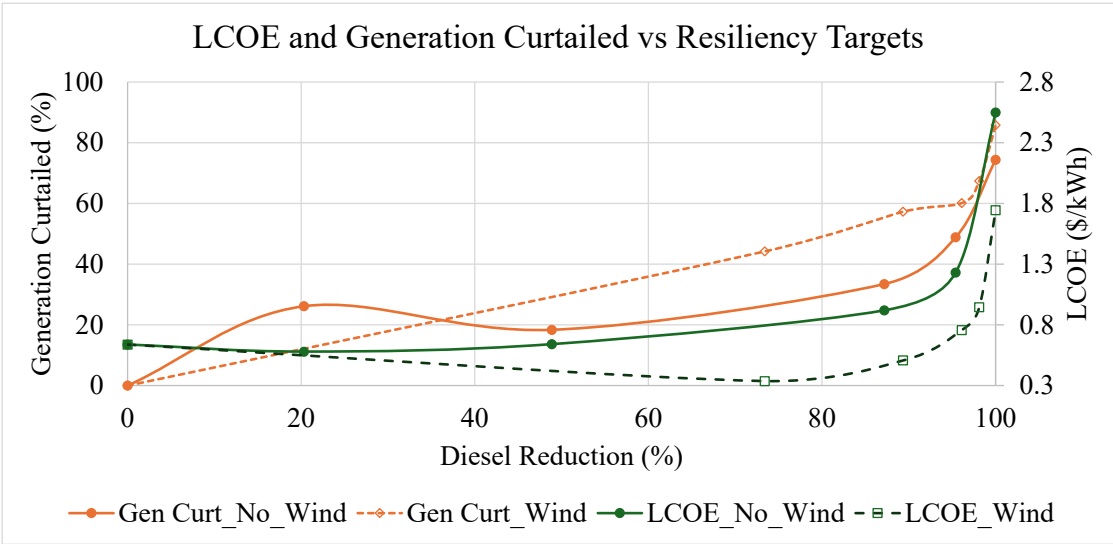


Figure 20. Comparing LCOE and generation curtailment for diesel use reduction targets.

6.7. Electrification of Heating Demand

Currently, 85% of heating demand is met with heat recovered from diesel generators operating in CHP mode. As a result, only a small quantity of diesel fuel is used to meet the remaining heating demand. However, with the introduction of local electrical generation resources and the reduction of diesel use for electricity, the heat recovered from the CHP process will also be reduced. Therefore, the heating demand will have to be met either by using diesel boilers, which doesn't support the energy independence goal, or by using electric heaters, which require additional electric generation capacity in the system.

This section analyzes the prospect of adopting local generation capacity for meeting both heat and electricity use. Table 7 shows financial and operational results for optimization cases considering cost, local generation adoption, and energy independence objectives. With the heating load included, the cost minimization objective results in a generation hosting similar to the electricity-only case, with electric heaters supporting nearly half of the heating peak load. The annual cost reduction is 38%, which is lower than the 47% observed when electricity demand was considered. The most significant improvement is in generation curtailment, which is reduced to 17% for electricity and heat compared to 44% for electricity-only, but the diesel use is not reduced as much. Achieving energy independence is 7.56 times more expensive than the diesel base case. This is considerably more expensive than the electricity-only scenario, which achieved energy independence at 2.77 times the annualized cost of the diesel base case.

Table 7. Prospect of using local generation resources to support both heat and electricity demand.

	Cases	Cost Minimize	Adopting Local Generation (PCF=1)	Total Energy Independence
Technology Sizes	New Generation (kW)	PV: 63.1, Wind: 285	PV:437, Wind: 760	PV: 426, Wind: 4,850
	BESS (kWh)	—	302	8,480
	Heater (kWth)	159	281	299
Financial Metrics	CAPEX (k\$)	2,210	7,286	46,501
	OPEX (k\$/y)	226	129	309
	Annual Cost (k\$/y)	366	593.2	4,466
Operation Metrics	Generation Curtailed (%)	17.37	58.09	91.24
	Diesel (gal)	24,328	8,461	0

Figure 21 shows the sensitivity of LCOE and generation curtailment with respect to diesel use reduction. The generation curtailment is initially lower for the electricity and heat case compared to the electricity-only case for similar levels of hosting local generation. However, it starts to overtake the electricity-only case for the final 20% of diesel use reduction.

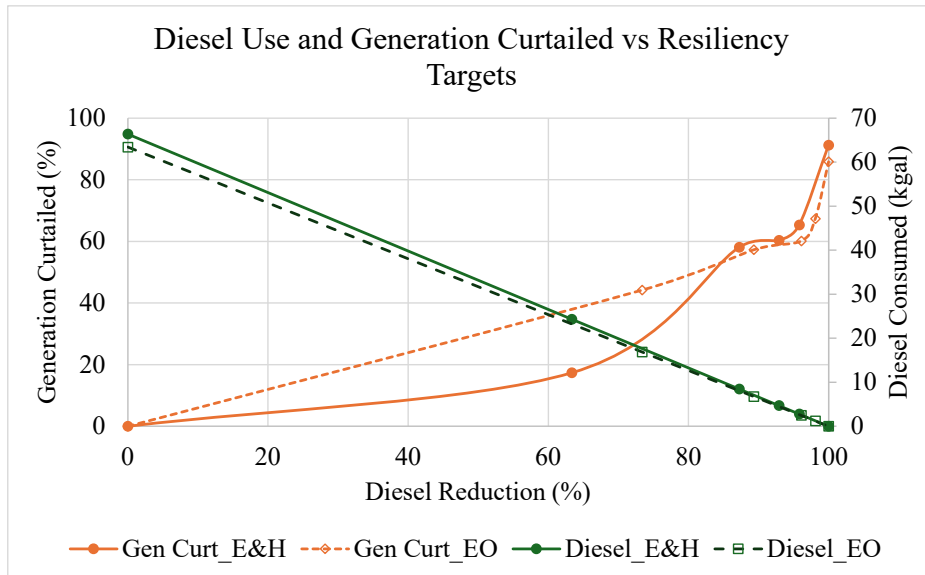


Figure 21. Comparing operational metrics for electricity and heat (E&H) cases with electricity only (EO) cases for diesel use reduction targets.

As shown in Table 7, WECs are not hosted for the three objective scenarios. The team analyzes asset selection for other intermediate local generation adoption cases to explore whether the optimizer ever hosts wave energy for heat and electricity. It is found that the WECs are hosted for intermediate adopting local generation cases when cost premiums are allowed (Figure 22). For cost minimization and adopting local generation cases with PCF=1, the optimizer found it less expensive to use cheaper solar and wind to achieve the objective. On the other hand, the total energy independence target is so extreme that it required significantly oversizing the assets, leading to the decision to host a larger wind plant and BESS without WECs.

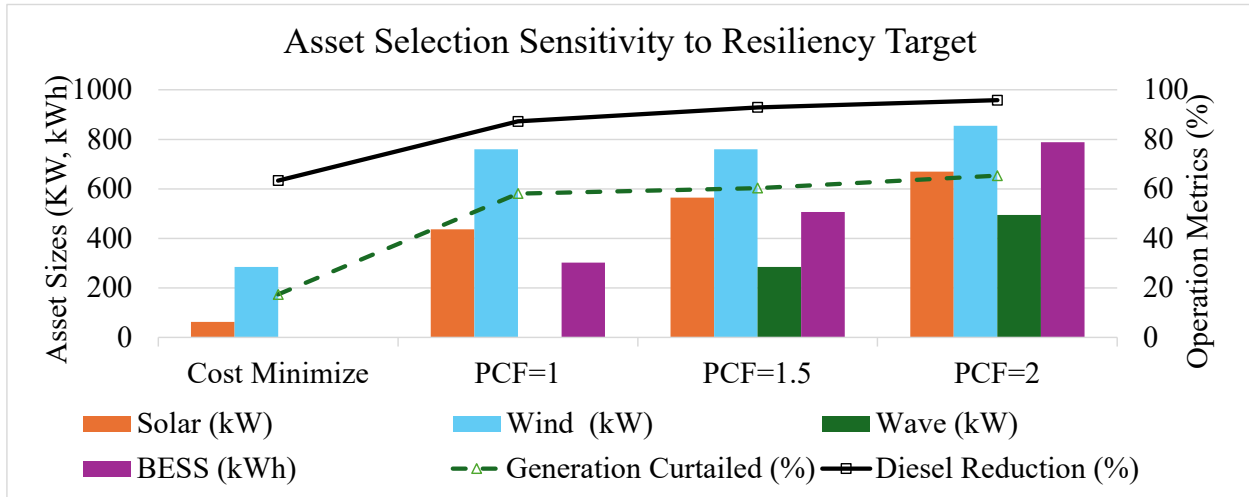


Figure 22. Sensitivity of technology selection and generation curtailment with respect to diesel import reduction targets.

6.8. Exploring the Role of Hydrogen

In all the cases analyzed, the introduction of new local generation resulted in lower costs compared to the diesel-only case. However, as more aggressive resiliency targets are set, the project becomes increasingly expensive and results in a highly inefficient use of generation resources. Including diesel generation is preferred not only from a cost and operational perspective but also to ensure the system has sufficient backup reserve to support emergency loads during extreme weather events, which can significantly constrain the power produced by local generation resources. While it is possible to replace most of the diesel generation, achieving complete energy independence is not financially feasible.

With the community still relying on diesel generation, it faces challenges due to diesel supply chain disruptions, necessitating significant diesel storage backup. Therefore, the team explores the prospect of onsite hydrogen fuel production through electrolysis to replace the last portion of diesel that is very difficult to eliminate to deliver absolute diesel independence. The assumption is that excess power from local energy technologies, which would otherwise be curtailed, can be used in the electrolysis process to produce hydrogen. The produced hydrogen can then be stored and used to produce electricity and heat when local generation is not available. This approach requires the microgrid to invest in the hydrogen ecosystem, including electrolyzers, hydrogen storage, hydrogen fuel cells, and hydrogen boilers.

Given the significant curtailment observed for the energy independence cases, such investment in hydrogen assets to use excess generation and produce local fuels replace imported diesel may prove more economical. Locally produced hydrogen means the system will not rely on diesel transportation to the community and will have a reliable fuel backup for emergencies. Additionally, onsite hydrogen production can be expanded to support local transportation.

Optimization is run for cases with and without wind. The results with hydrogen for the two cases are compared in Table 8. Although the system does not have an actual hydrogen demand, the entire hydrogen ecosystem is selected to support electricity and heating needs. This includes an electrolyzer that captures excess electricity to produce hydrogen, A hydrogen storage, a fuel cell generator to produce electricity and residual heat to meet part of the heating needs, and a hydrogen boiler to meet the rest of the heating demand. Electric heaters and battery energy storage are also selected.

Table 8. Prospect of using hydrogen in the mix to fully replace diesel use (total energy independence) for both electricity and heat.

	Cases	With Wind	Without Wind
Power Assets	New Generation (kW)	Wind: 1,140	PV: 1,101; Wave: 1,650
	BESS (kWh)	1.49	111
	Heater (kWth)	295	245
Hydrogen Assets	Electrolyzer (kg/h)	7	7
	Hydrogen Storage (kg)	989	1,718
	Fuel Cell (kW)	200	200
	Hydrogen Boiler (KWt)	183	163
Financial and Operation Metrics	CAPEX (k\$)	10,206	19,267
	OPEX (k\$/y)	291	1063
	Annualized Cost (k\$/y)	968.2	2,213.2
	Gen Curtailed (%)	48.81	23.81

With wind, the optimizer selects only wind and excludes both PV and wave due to the superior wind resource availability at St. George. Only 1.49 kWh of battery energy storage is selected, as most of its function is provided by the hydrogen storage. Compared to the energy independence case without hydrogen (see Table 7), the size of generation resources and the respective curtailment significantly reduce, as shown in Table 8. The annual cost also decreases significantly.

Similar results were obtained for the case without wind. The sizes of PV and wave are significantly reduced, along with a smaller size of battery energy storage. Energy curtailment also reduces to 23.81%. The capital expenditure (CAPEX), OPEX, and annualized cost are reduced sharply compared to the case without hydrogen, following a similar trend as the case with wind, but remains almost twice as expensive.

In both cases, the optimizer selects 7 kg/h (or 388.5 kW) electrolyzer. The size of H₂ storage is nearly twice the case with wind as compared to the case without wind, as shown in Table 8. The same size of a fuel cell generator is selected for both cases, but a slightly larger boiler and electrical heater are chosen for the wind case.

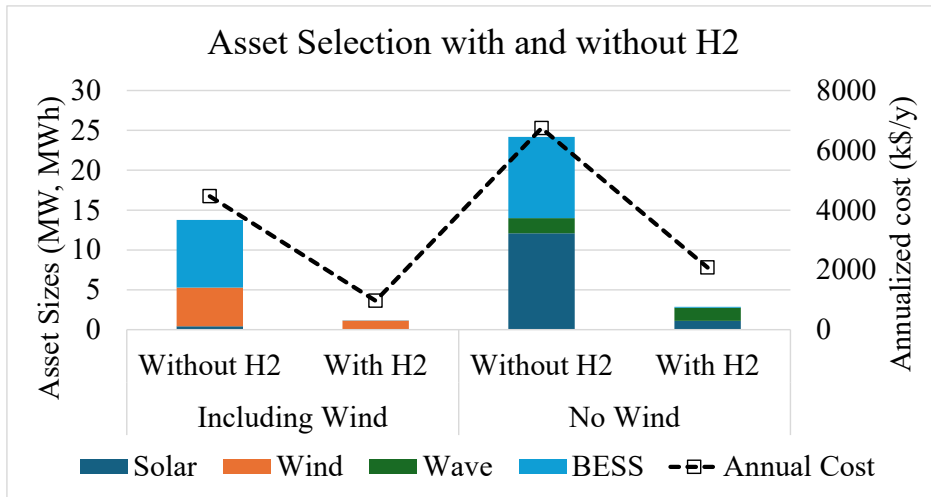


Figure 23. Comparing asset selection and annual cost for energy independence cases with and without hydrogen.

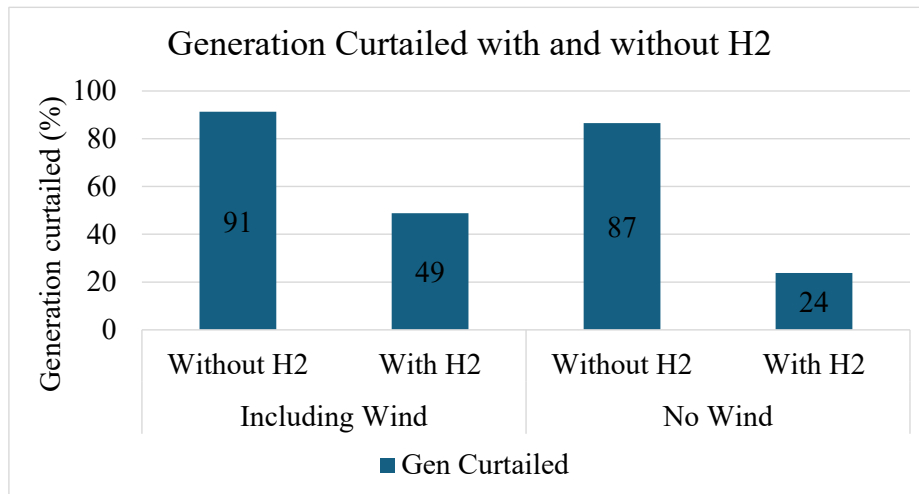


Figure 24. Comparing generation curtailment for energy independence cases with and without hydrogen.

Due to technical challenges, primarily related to transportation and storage, switching to 100% hydrogen may not be viable yet. Hydrogen can be blended with other local fuels (e.g., biogas) to produce synthetic fuels, which reduces the net-emission factor and improves the performance while making hydrogen useful with existing infrastructure. This blended approach could serve as a transitional strategy toward achieving energy independence by gradually replacing diesel usage. In locations where other fuels

are not available locally, hydrogen can be converted into a more flexible fuel, such as ammonia. Ammonia is easier to store and can be effectively used in remote communities.

7. INFRASTRUCTURE EVALUATION

The infrastructure evaluation involves simulating the St. George power network with new microgrid assets. This task evaluates the static and dynamic performance of the islanded system using steady-state and transient simulations. The infrastructure evaluation is conducted in two steps: quasi-dynamic power flow and operations evaluations. In quasi-dynamic power flow analysis, the hourly dispatch solutions generated by Xendee for different optimization scenarios are fed into the network model to examine power flow results, including steady-state voltage, transmission line limit violations, and system losses. The operations evaluation examines the dynamic operation of the system under normal and disruptive scenarios to analyze system frequency, voltage, and current dynamics through EMT and RMS simulations.

7.1. Network Power Flow

The voltages and currents in the network are analyzed using quasi-dynamic simulation models to investigate violations across different nodes and transmission components, including transformers and distribution lines. The Xendee dispatch results discussed in Section 6 are obtained by assuming all generation and loads are lumped into a single node. In this study, the team implements Xendee dispatch results with generation assets and load demand distributed throughout the network. This introduces transmission losses in the network, which are not accounted for in the Xendee dispatch results. The team selects several feasible cases from the techno-economic evaluation to examine the power flow in the network, including the base case diesel, optimized cases with and without wind, and optimized heat and electricity cases.

To simplify the power flow evaluation, the team considers the operating diesel generator as the slack bus providing power mismatch, thus supplying the excess power needed for transmission losses in addition to the power already estimated through the dispatch optimization problem, while other generation technologies dispatch only based on the Xendee optimization. There were numerous dispatch scenarios where a large amount of generation was curtailed, which could have been used to cover network losses. However, to maintain grid stability, the diesel generator remains online, and its minimum power output rating mostly covers the transmission losses observed in power flow studies, with a few exceptions. Therefore, the assumption of the diesel generator acting as a slack bus to cover network losses is valid.

7.1.1. Base Case Diesel

In the base case, the entire load demand is met by existing diesel generators. Heat demand is supplied using recovered waste heat from the operating diesel unit for community facilities and diesel boilers in each household. Therefore, the heat demand does not directly influence the power flow of the network. Figure 25 provides the summary results for the time-series power flow on the network. The overall load demand is distributed across different nodes in the St. George Residential and Zapadni Bay areas. Compared to the Xendee optimization results presented in Section 6.2, the network losses can get as high as 11.14 kW, coinciding with the annual peak demand in winter.

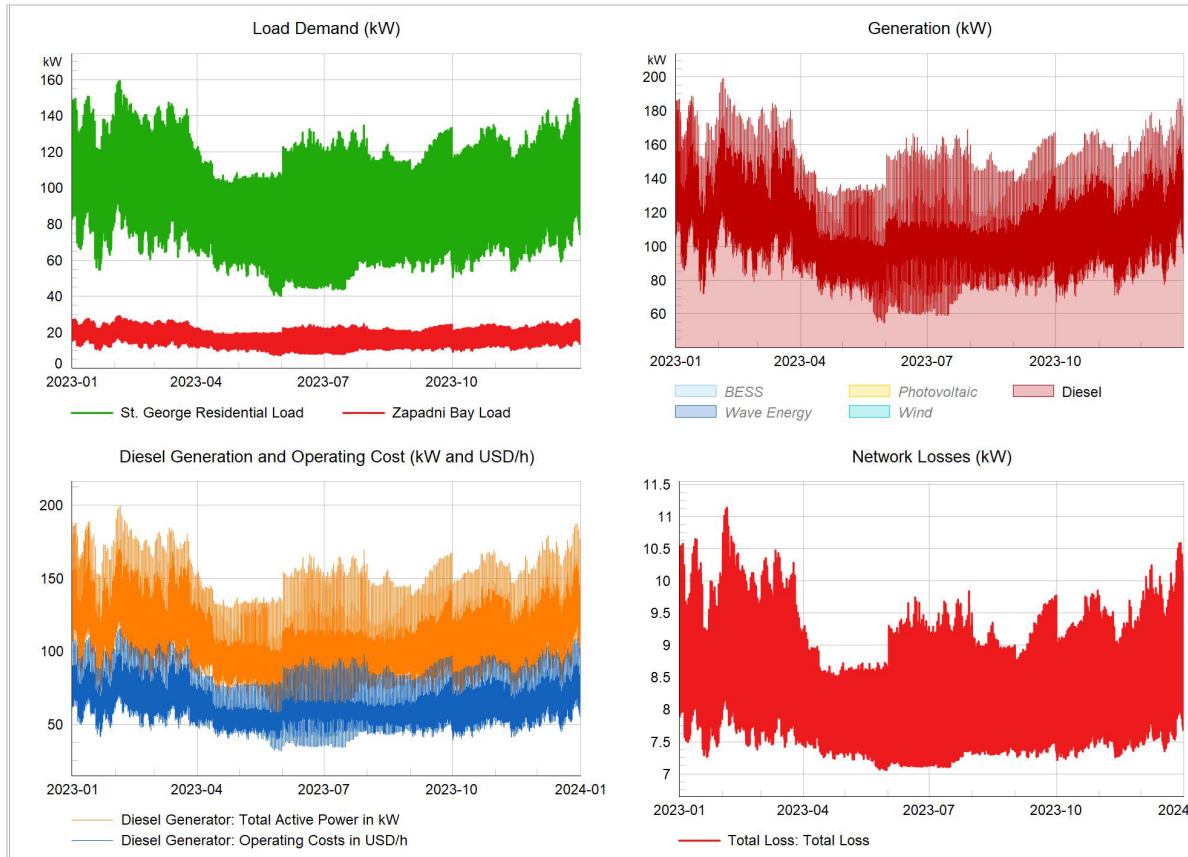


Figure 25. Power flow results for base case diesel scenario.

To account for the transmission losses in the system, the total power production and operating cost of the diesel plant increased to 956,654 kWh and \$553,903 (compared to 885,899 kWh and \$513,622 from Xendee without losses). Figure 26 shows a contour map of the St. George network, using color coding to highlight areas of voltage violations and overload conditions. A detailed analysis of the power flow results indicates that all nodes maintain a voltage between 0.95 and 1.05 p.u., indicating no voltage violations. However, the transformer supplying power from the diesel generators to the St. George residential area is overloaded. This is due to the transformers being rated at 150 kVA, which is inadequate for the peak load of 188 kW (based on 2013 demand data).

There are two possible explanations for this misalignment of the transformer size. First, the time-series profile was created using a standard residential load profile from Xendee, which estimates the peak load based on energy consumption, potentially leading to an inaccurate assessment of the residential area's peak demand. Second, the load data used in this analysis, which is from 2013, reflects a higher demand than what was observed by the team during their visit to the community in 2023. It should be noted that all network parameters, including transformer ratings used in the analysis, are based on what the team recorded in 2023.

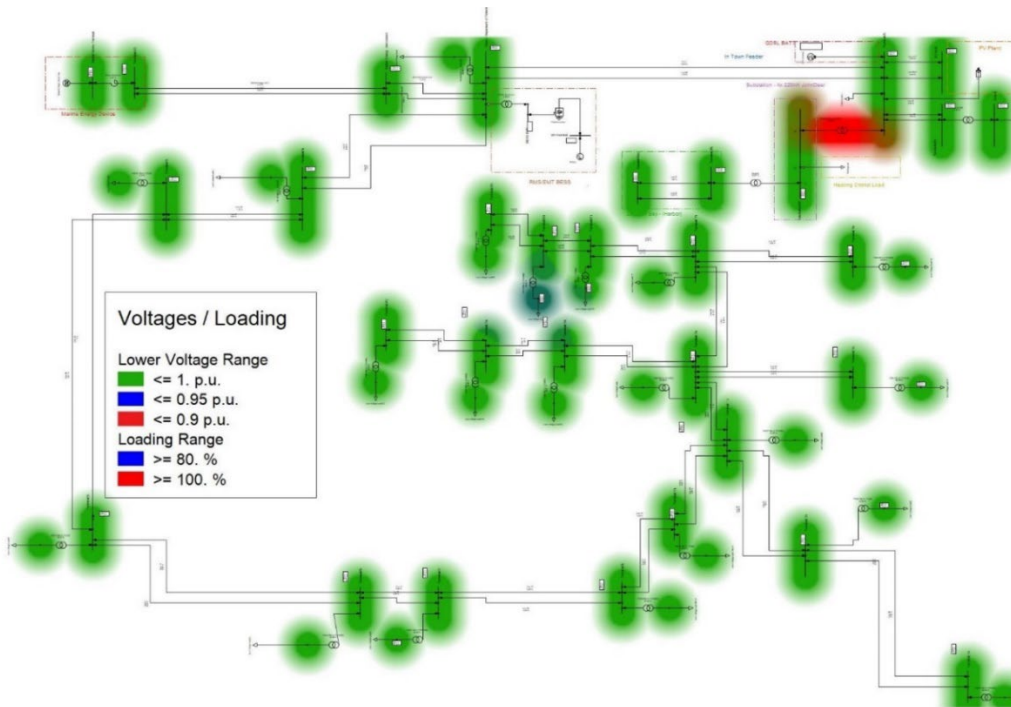


Figure 26. Voltage and transmission line loadings in the town facility for base case scenario. The only overload seen is in the transformer connecting diesel generator substation to the St. George residential area.

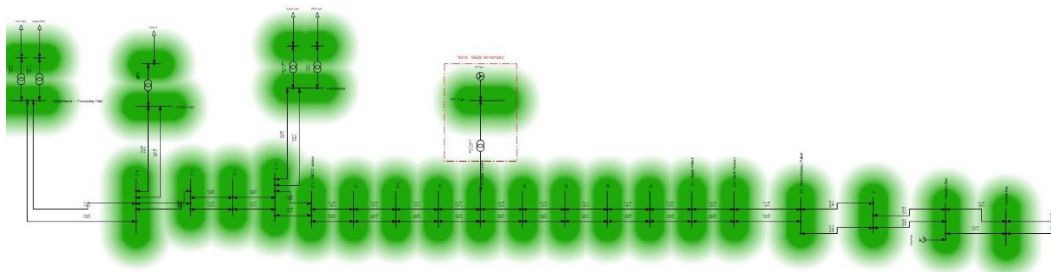


Figure 27. Voltage and transmission line loadings in Zapadni Bay feeder for base case scenario. No overload or voltage violation seen for diesel base case.

Optimized Electricity with Wind

When wind generators are considered, the system hosts wind and solar for the cost minimization objective, as discussed in Section 6.3. The wind plant is connected to a node in Zapadni Bay feeder, where Windmatic 17s wind turbines were previously installed. The PV is sited in the St. George residential area, either roof-mounted or ground-mounted. For simplicity, the team considers a centralized PV plant located near the St. George residential area and connected to the same network bus as the diesel generator. The power flow analysis is conducted to investigate voltage and current violations in the system for the technology sizing and dispatch optimized by Xendee.

It is found that network losses increase when more energy is produced by wind turbines. In the cost minimization scenario, which hosts 67.5 kW of PV and 285 kW of wind generation, the peak transmission loss can reach up to 26 kW during peak wind generation. The annual energy loss due to network power flow increases to 101,373 kWh, which is a 43.3% increase from the diesel base case. For the cost optimization case, the transformer connecting the St. George residential area to Zapadni Bay gets above 80% loading, which is because wind turbines produce most of the power to support the St. George grid.

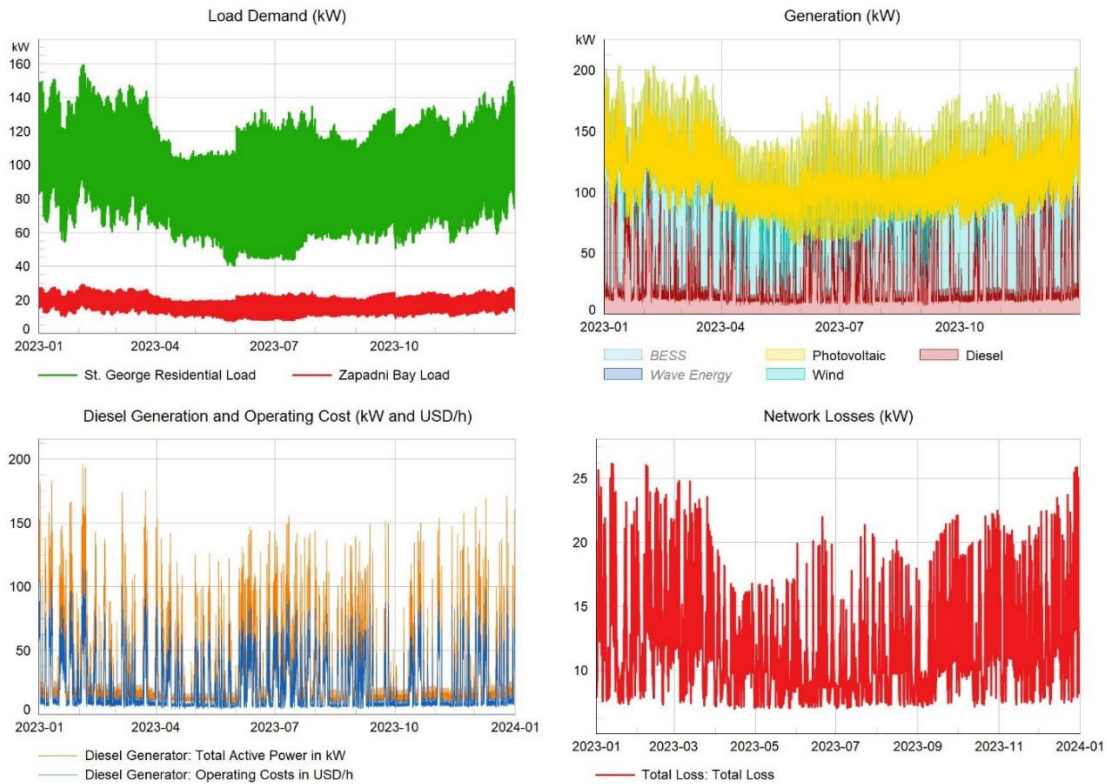


Figure 28. Power flow results for the case with wind for local generation adoption objective (PCF=1).

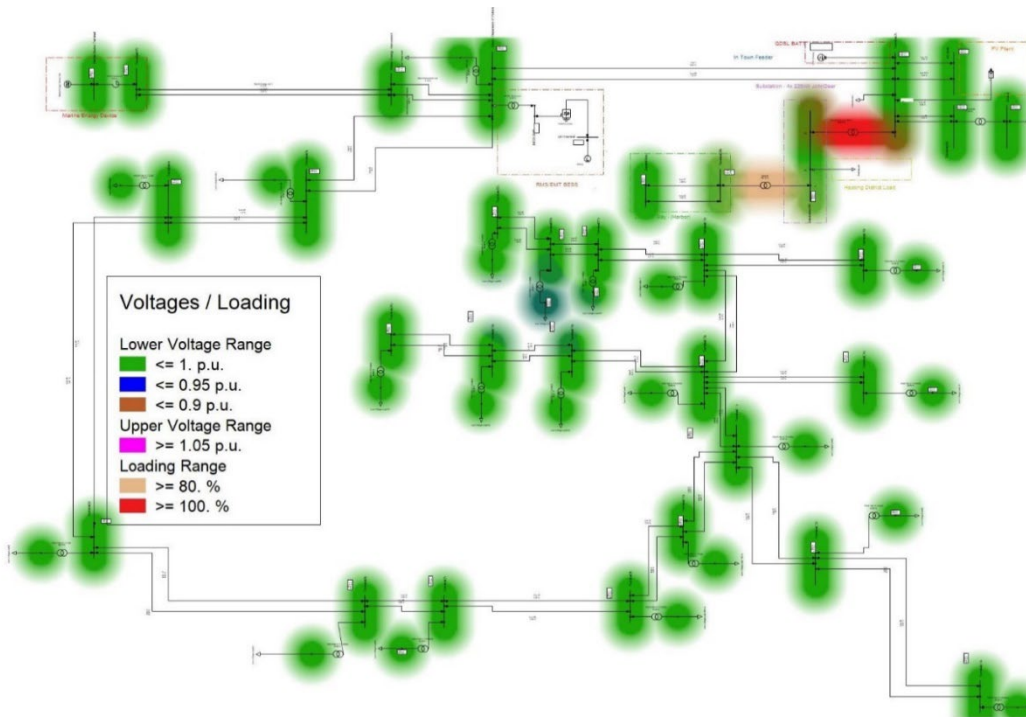


Figure 29. Voltages and transmission line loadings in the town facility for cost minimization with wind. Both the transformers connecting the central substation to the St. George residential area and Zapadni Bay feeder are overloaded. Network losses increase when aggressive resiliency targets are set, leading to larger

wind turbines. The adopting local generation case shows a significant increase in peak network loss and annual energy losses through power flow in the network. The system hosts BESS alongside wind and PV. The BESS is hosted in the St. George residential area. The BESS stores excess energy from wind and PV to release when generation is low. The interconnection point for the PV plant is closer to the BESS and, therefore, does not lead to large transmission losses. However, this is not the case for wind turbines, which are located far from the BESS in the Zapadni Bay area. Due to this, the power produced by wind during peak generation times must be transmitted through the network to support load demand in the town as well as to store excess energy in the BESS. The power produced by wind turbines can reach as high as 289 kW when the load demand is 118 kW, and the BESS charges at 185 kW, leading to a peak network loss of 53.77 kW.

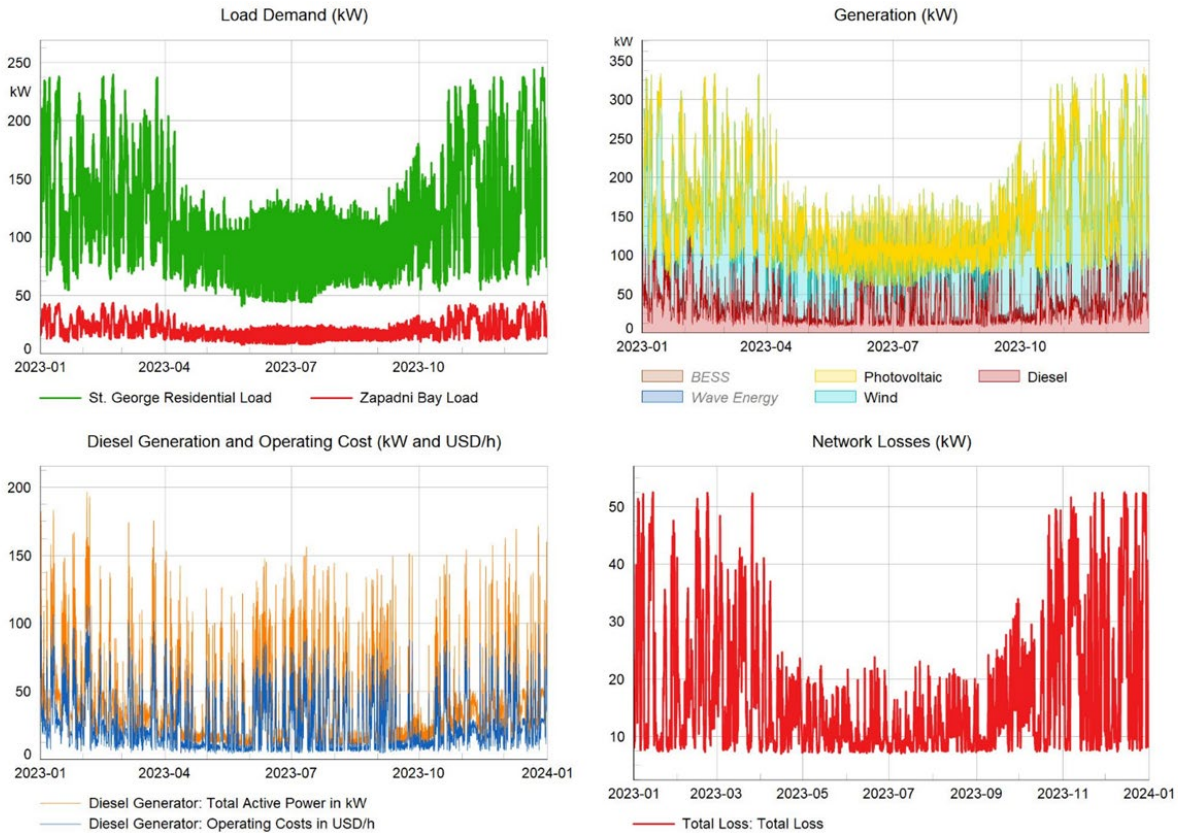


Figure 30. Power flow results for the case with wind for local generation adoption objective. Network losses increase when more power comes from wind turbines.

The technoeconomic analysis revealed that the energy independence scenario is highly uneconomical with different operational challenges. In this case, wind turbines, PV, BESS, and WEC are hosted. Similar to PV, the wave energy device is connected at a distribution bus in town in proximity to the BESS and the residential load. Like before, as wind turbines generate more power, the transmission losses increase. According to the dispatch optimization results from the technoeconomic analysis, during peak wind generation, the wind turbines generate 752 kW and the WEC generates 42 kW. With a load demand of 130 kW, the surplus power is allocated to energy storage. However, with large wind generation, the transmission loss for this scenario can reach 261 kW. Similarly, nearly every node in the network face overvoltage issues, with node voltages exceeding 1.05 p.u. during peak wind penetration (Figure 31).

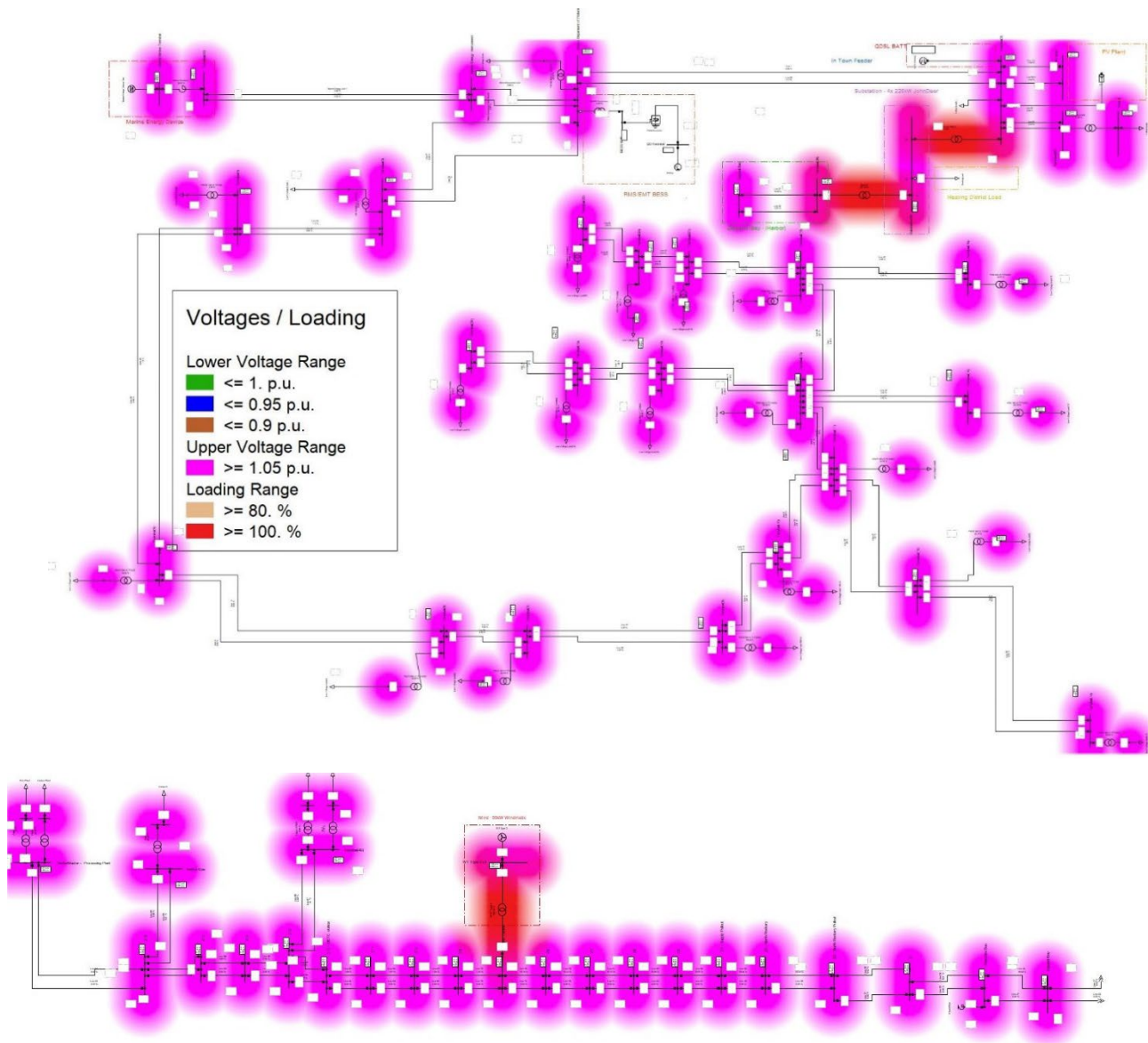


Figure 31. Voltages and distribution line loadings for the energy independence case with wind. The entire network face overvoltage issue during peak wind generation. As can be observed from the comparison of network losses in Figure 32, both the peak network loss and total annual network losses increase with a more aggressive resiliency target. This is mainly due to wind turbines being sited in Zapadni Bay instead of the in-town residential area where other assets are located. This transmission loss due to wind generation can be reduced by distributing part of the energy storage capacity closer to the wind turbines instead of centralizing it closer to the residential area. However, there are other generation assets also producing power and storing excess generation in energy storage. Alternatively, generation resources could be deployed in hybrid with energy storage instead of optimizing separately. The optimal siting and distribution of energy storage is a complex problem that would need to be solved separately.

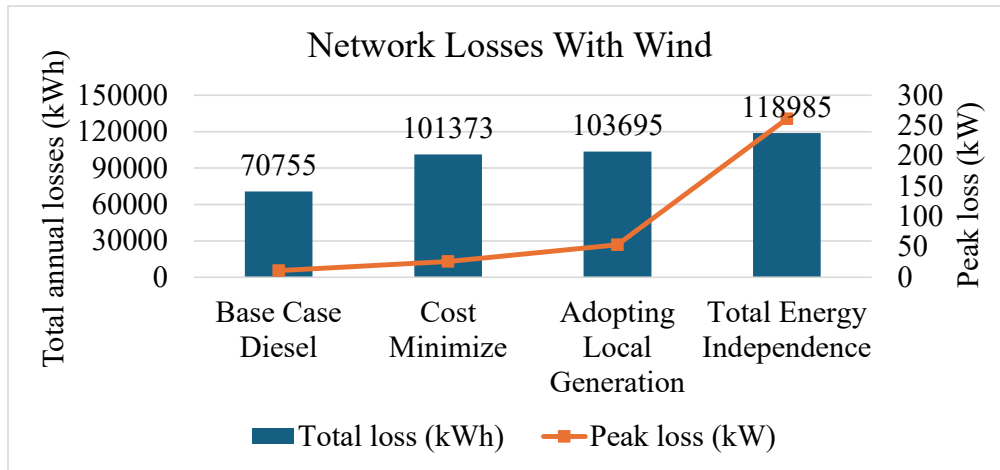


Figure 32. Transmission losses compared for optimized scenarios, including wind with different objectives.

7.1.3. Optimized Electricity Without Wind

With PV, WEC, and BESS sited in proximity to each other and connected to the St. George residential area, where most of the electricity demand exists, the transmission loss issue is significantly reduced when no wind is considered. Transmission losses for various objective scenarios are compared in Figure 33. In the cost minimization scenario, the peak transmission loss remains the same as that for the base diesel case, but the total energy loss due to network power flow is reduced by 2.39%. No additional voltage and transmission violations are seen compared to the diesel base case.

As can be observed from the comparison of network losses in Figure 34, the network losses decrease as a more aggressive resiliency target is set. In the local generation adoption scenario, the total annual network losses decrease by 6.4% compared to the base case diesel, whereas the peak loss also has a slight decrease compared to the base case diesel. In the energy independence case, the transmission loss further improves with a 9.4% increase in total energy loss, as well as the peak transmission loss decreasing to 8.56 kW, a 23.1% decrease from the diesel base case. In the energy independence case, the transformer overload issue is also resolved as the power from WEC and PV is directly supplied to the demand side of the residential loop transformer.

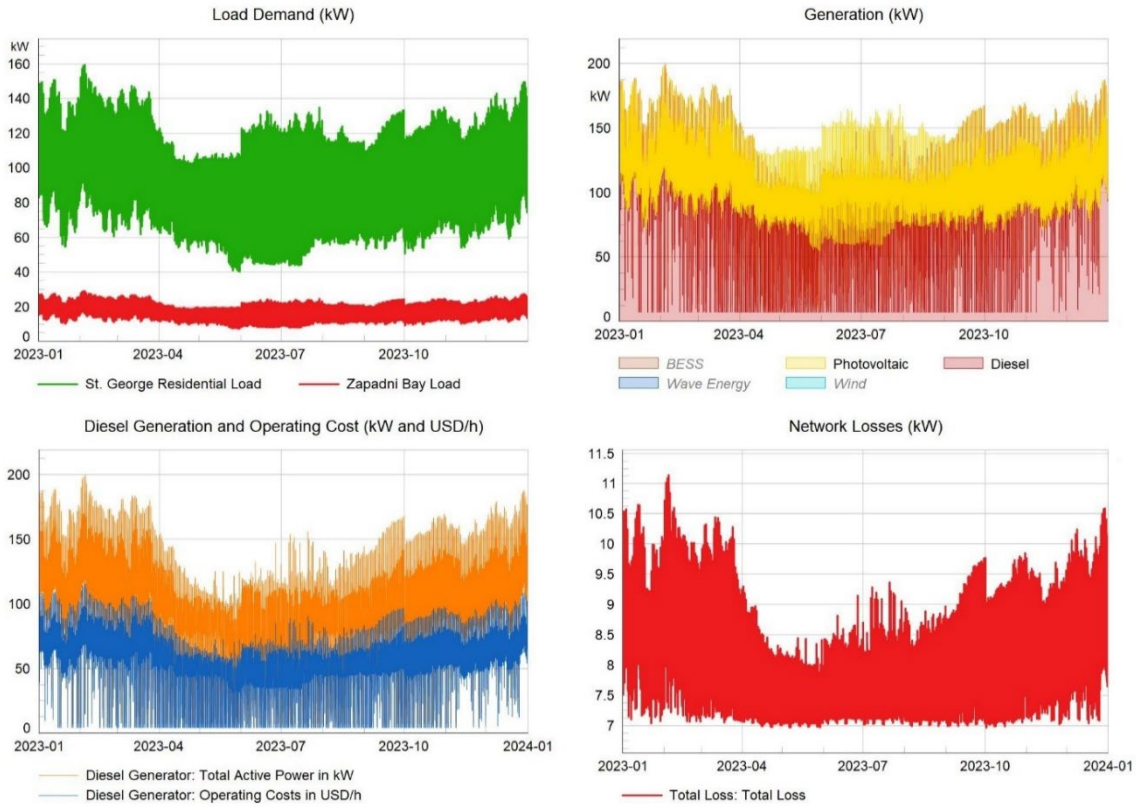


Figure 33. Power flow results for local generation adoption objective without wind. Network losses show a decreasing trend with new generation resources.

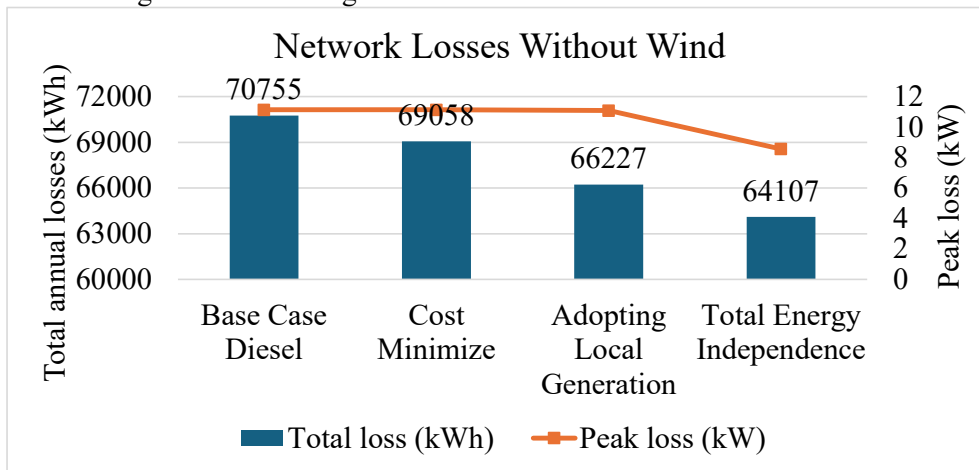


Figure 34. Transmission losses compared for optimized scenarios without wind with different objectives.

7.1.4. Optimized Heat and Electricity

Next, the team investigates the power flow of the heat and electricity optimization cases described in Section 6.7. As described in the optimization results in Section 6.7, the heating demand is gradually electrified with cost minimization and local generation adoption cases with heating demand fully electrified in the energy independence case. In power flow analysis, the electrified portion of the heating demand is distributed across the microgrid in a similar proportion to how electrical demand is distributed. The addition of heating demand increases the total connected load at each load center. As a result, numerous transformers across the St. George residential area were found to be overloaded during high demand periods of the simulated year, as shown in Figure 35. Voltage measurements from some of the load buses also dropped below 0.95 p.u., but none of the buses were below 0.9 p.u. This indicates that the capacity of transformers across the network needs to be upgraded if the heating demand is electrified.

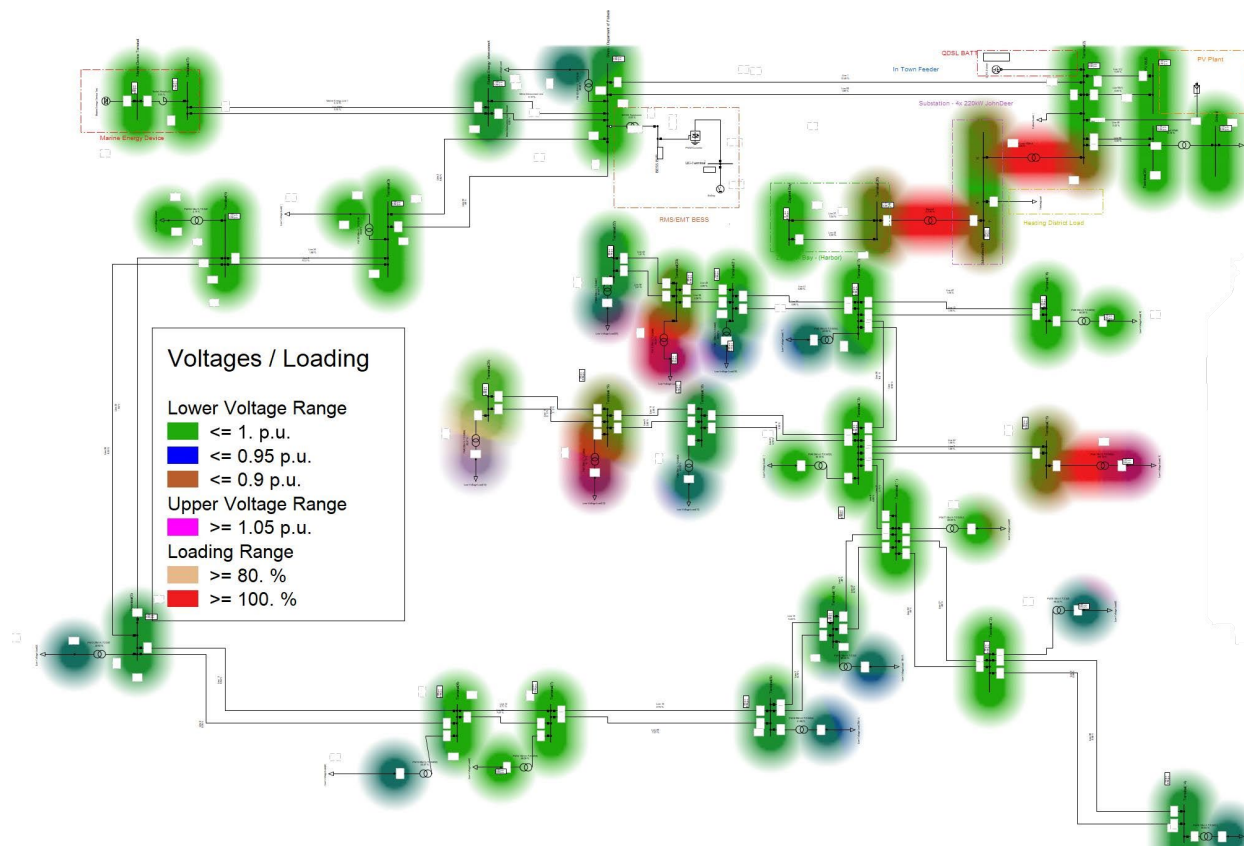


Figure 35. Voltages and transmission line loadings for heat and electricity optimization with cost minimization objective, including wind. Numerous load transformers across the network are overloaded due to the increase in demand from electrical heating. Similar to electricity-only cases, considering wind will result in significant transmission losses. For the cost minimization objective, the transmission loss can reach as high as 52.5 kW during peak wind generation, and the total energy loss increases by 109.3% compared to the diesel base case. In this scenario, a total of 270,900 kWh of heat is met using wind generation, which is 39.5% of the total heating demand.

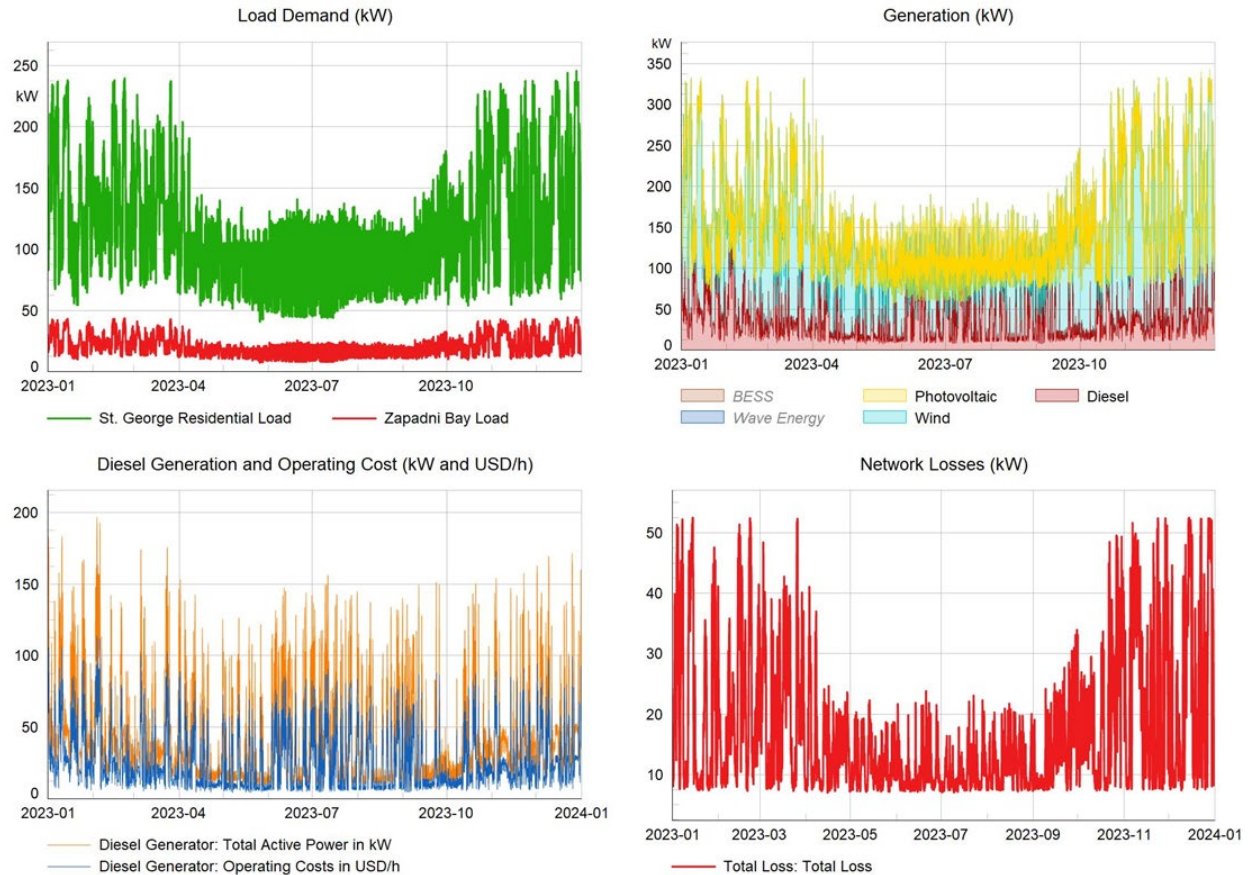


Figure 36. Power flow results for heat and electricity optimization with cost minimization objective with wind. Network losses increase more when heating loads are electrified. Without wind considered in the solution, the system relies solely on solar PVs for electrical generation along with electric heaters. No additional transmission overload or voltage violations were observed, and the total transmission loss is lower than that of the diesel base case. The peak transmission loss is similar to that of the diesel base case scenario; however, the total transmission loss decreases slightly, as shown in Figure 37. This was somewhat counterintuitive, as the electrification of heating demand would typically increase the total load and, therefore, result in losses in the network. Upon closer inspection of the results, it was found that only 33,150 kWh of the heating demand is met using electricity, which represents just 4.8% of the total heating demand. The remainder of the heating demand is met using diesel boilers, as in the diesel base case scenario.

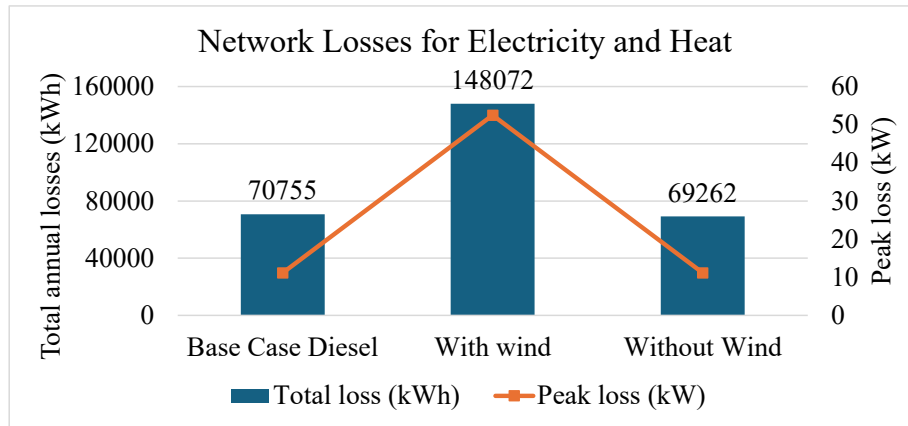


Figure 37. Transmission losses compared for heat and electricity optimization with and without wind for cost minimization objective.

Clearly, due to superior resource potential for wind, more wind turbines are selected whenever possible. However, due to their siting in Zapadni Bay instead of the residential area in town, various power flow issues were encountered, including large transmission losses and voltage and capacity limit violations. The scenarios without wind did not have similar power flow issues, which is due to the assumption that PV, BESS, and WEC could be sited close to the residential load. However, the scenarios without wind are economically less viable than the scenarios with wind, as shown by the technoeconomic results in Section 6. If wind turbines could be hosted closer to the residential area or if the power lines connecting Zapadni Bay to the residential area were upgraded, the power flow performance of scenarios with wind would be significantly improved.

7.2. Operations Evaluation

For operations evaluation, the team selects local generation adoption (PCF=1) scenario with wind for electricity-only case, as this scenario hosts all four resources, wind, PV, wave, and BESS, in the microgrid. The objective is to analyze how the infrastructure behaves with new technologies when exposed to abnormal operating conditions rather than focusing on the internal dynamics of each generation-technology type.

The RMS and EMT models developed in the PowerFactory tool are used for this analysis. The RMS simulation analyzes the response in terms of the phasor of 3-phase sinusoidal variables, assuming the entire system is synchronized to the same frequency. The EMT simulation, on the other hand, analyzes the system based on time-varying sinusoidal waves, considering electromagnetic interactions and higher-order harmonics.

In both RMS and EMT simulations, diesel generators and BESS are considered resources capable of supporting the system's dynamic response to recover from voltage and frequency transients. In all scenarios, diesel generators remain connected with a droop setting of 0.05, forming the microgrid and generating power based on dispatch, as well as meeting transmission losses. Whenever activated, the BESS also provides dynamic responses to assist the diesel generator in maintaining voltage and frequency stability. BESS operates in a grid-following mode with droop control characteristics. The BESS frequency control model is configured with a deadband of 0.0025 p.u. (0.15 Hz) and a droop setting of 0.004. This means that the BESS frequency response will not be activated unless the frequency deviation exceeds 60.15 Hz or drops below 59.85 Hz. The droop of 0.004 indicates that the BESS power output will change by 100% if the frequency changes by 0.004 p.u. or 0.24 Hz.

7.2.1. Root Mean Square Simulation

For the RMS simulation, the team selects specific dispatch instances from the quasi-dynamic analysis to impose disturbances on the system. Table 8 shows the hours considered for the RMS simulation, during which either load or generation technologies were operating close to their limits, making the entire system vulnerable to extreme disruption if disturbances were to occur. Two sets of results are included in Table 9. The first set shows dispatch values obtained directly from the Xendee simulation, which do not include network losses. The second set of results are obtained from PowerFactory simulations, which provide the total network losses and the updated diesel generation (dispatches from new assets remain the same). The power flow results from PowerFactory represent the initial point for all RMS simulations analyzed in this section.

Table 9. Operational instances analyzed for RMS simulation. The Xendee dispatch results optimize generation from hosted resources without considering network losses. The PowerFactory results show correct diesel output considering network losses.

Scenarios	Time	Xendee Dispatch Results						PowerFactory Results	
		Load (kW)	Diesel (kW)	PV (kW)	Wind (kW)	WEC (kW)	BESS (kW)	Loss (kW)	Diesel (kW)
Peak Load	Feb 4, HH 19	188.31	116.41	0	61.56	10.34	0	12.63	129.04
Peak Diesel	Feb 5, HH 19	182.19	182.19	0	0	0	0	10.84	193.03
Peak PV	Sept 4, HH 13	68.65	0.01	317.01	6	0	-254.4	7.01	7.02
Peak Wind	Dec 27, HH 6	117.92	0	0	289.56	12.81	-184.45	53.77	53.77
Peak Wave	Dec 4, HH 14	91.29	0	3.58	19.38	78.42	-10.09	7.34	7.34
Peak BESS	Jan 1, HH 21	170.87	0	0	11.02	12.55	147.3	8.2	8.2

7.2.1.1. Peak Load Condition

First, the team considers operation during peak load condition, which occurs on HH19 on February 4 of the time-series dispatch simulation. The electrical load is at its peak at 188.31 kW. Diesel, wind, and wave generation are available during this interval, with most of the demand met by the diesel generator. Diesel also provides transmission losses during this interval, which are not accounted for in dispatch values shown in Table 9.

At $t=20$ s, the system operation is disrupted by switching off the transformer connecting St. George residential area to Zapadni Bay. Initially, the system response is analyzed, considering just diesel as providing the frequency response. Clearly, with diesel alone providing dynamic frequency support, system frequency drops below 59.3 Hz at the nadir point, as seen in Figure 38. As the diesel governor responds to the frequency drop by injecting more fuel, the mechanical power output increases, and the frequency starts to recover. Due to the droop setting, the system frequency settles at 59.58 Hz. During the same transient event, the voltage across various network nodes fluctuates within a $\pm 5\%$ range. With the wind turbine generating 61.6 kW, which exceeds the load on the Zapadni Bay feeder, the loss of this feeder creates a 26-kW power deficit. This deficit is compensated by increasing the diesel generator's output. Simultaneously, the disconnection causes an excess of reactive power in the system, which is balanced by reducing the diesel generator's reactive power output from 40.17 kVAr before the disturbance to 6.79 kVAr after the disturbance.

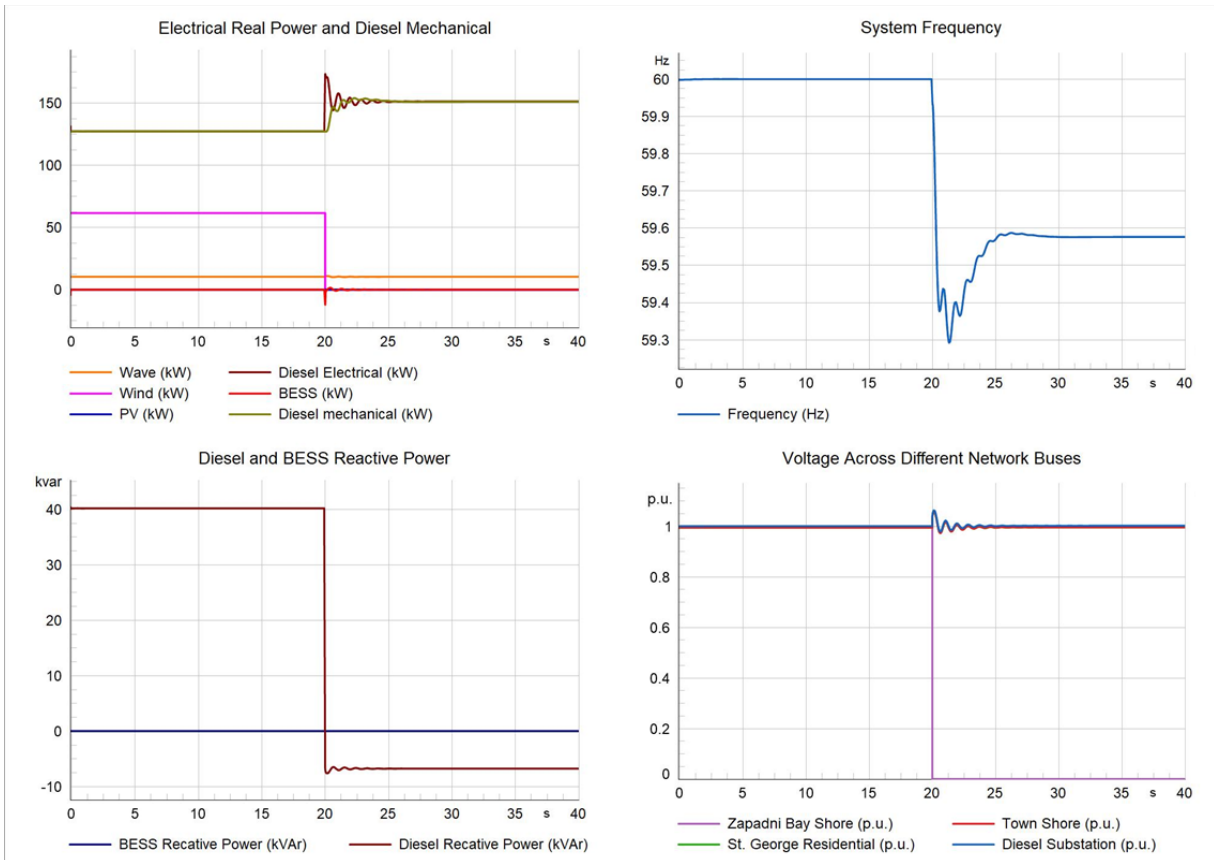


Figure 38. Dynamic performance of the system for the peak load scenario based on RMS simulation. BESS frequency control is deactivated, and only the diesel generator provides dynamic response. Next, the BESS is activated to provide both frequency and voltage support. With the inclusion of BESS, the frequency response significantly improves, as shown in Figure 39. Both the net deficit in real power and the net excess in reactive power are shared by the BESS and the diesel generator. The BESS only begins to adjust its power once the frequency drops below 59.85 Hz threshold. After the disturbance, the system recovers with a settling frequency of 59.84 Hz, with both the diesel generator and BESS sharing the power deficit according to their droop settings. This demonstrates that activating BESS control based on frequency feedback significantly enhances the system's dynamic performance and aids in recovering from large disturbances. Figure 40 illustrates the difference in system frequency dynamics for the same disturbance, comparing scenarios with and without BESS frequency control.

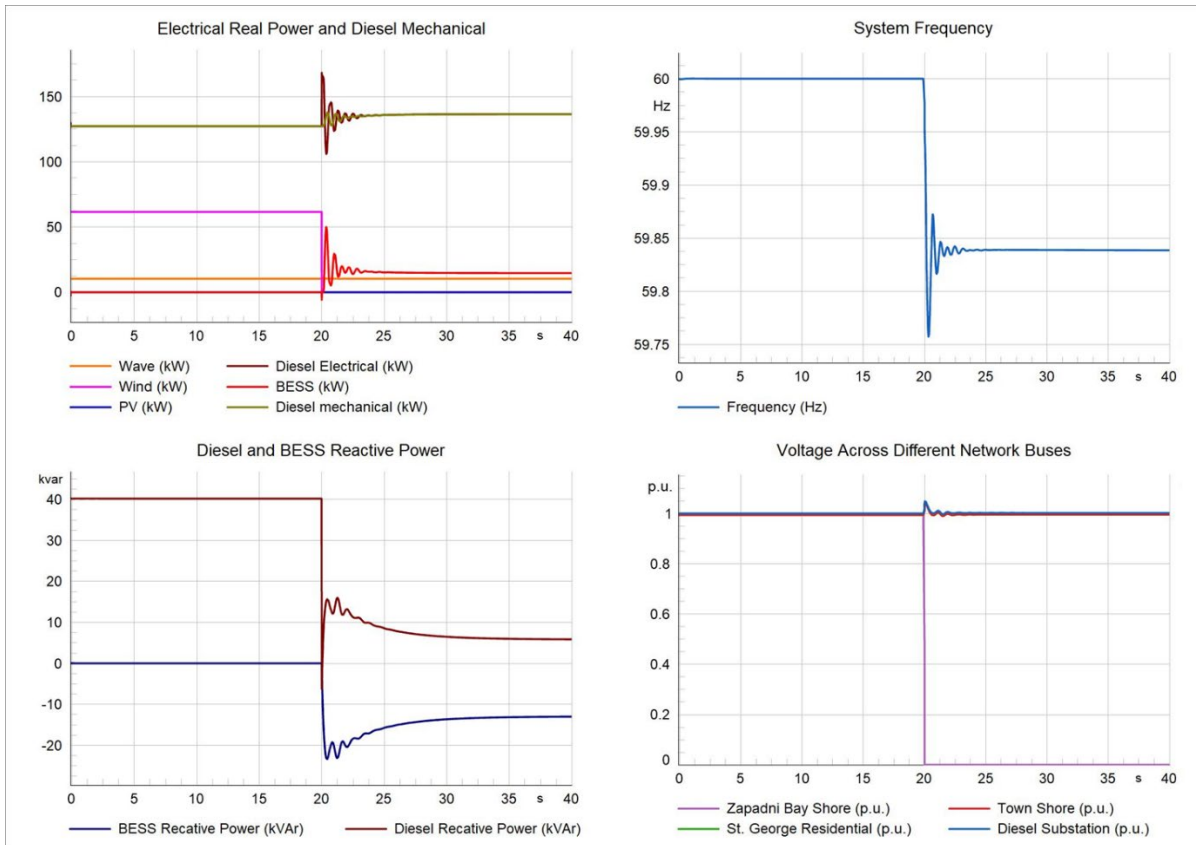
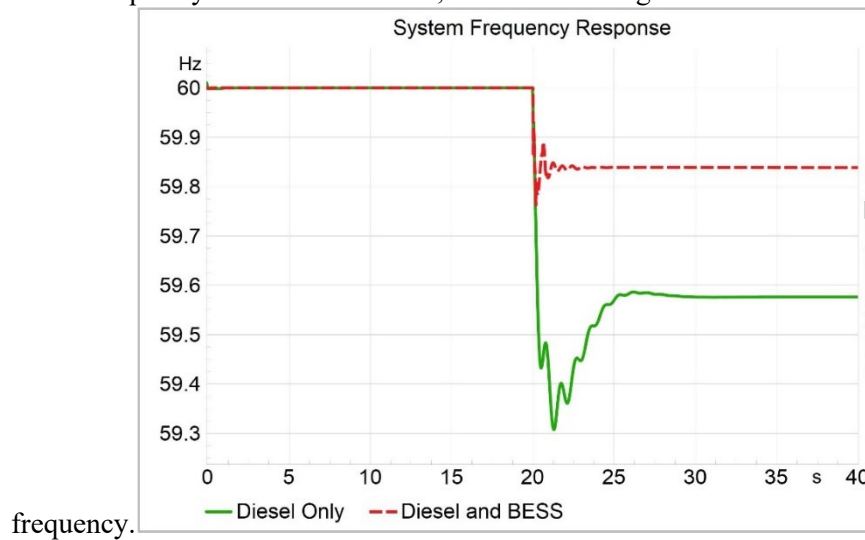


Figure 39. Dynamic performance of the system for the peak load scenario based on RMS simulation. BESS frequency control is activated, and both diesel generator and BESS contribute to stabilizing system



frequency.

Figure 40. Comparing frequency responses for cases when only diesel provides frequency response vs. both diesel and BESS provide frequency response.

7.2.1.2. Maximum Diesel Generation

In the second scenario, the team examines the interval when the diesel generator is operating at its peak capacity. Similar to the previous scenario, the transformer connecting the Zapadni Bay feeder is abruptly tripped off at $t=20$ s. However, unlike the previous scenario, the wind turbine is not generating any power, leading to a net excess of power in the network due to the loss of the Zapadni Bay feeder. Both the BESS and the diesel generator reduce their output to balance this surplus power, causing the frequency to overshoot. The maximum frequency deviation reaches a peak of 60.23 Hz, with the system eventually stabilizing at 60.17 Hz (Figure 41). The voltage at the diesel generator bus overshoots to a high of 1.07 p.u. but then recovers to 1 p.u. when the system stabilizes. Following the event, the reactive power consumption by the BESS decreases, which leads to a reduction in the reactive power produced by the diesel generator.

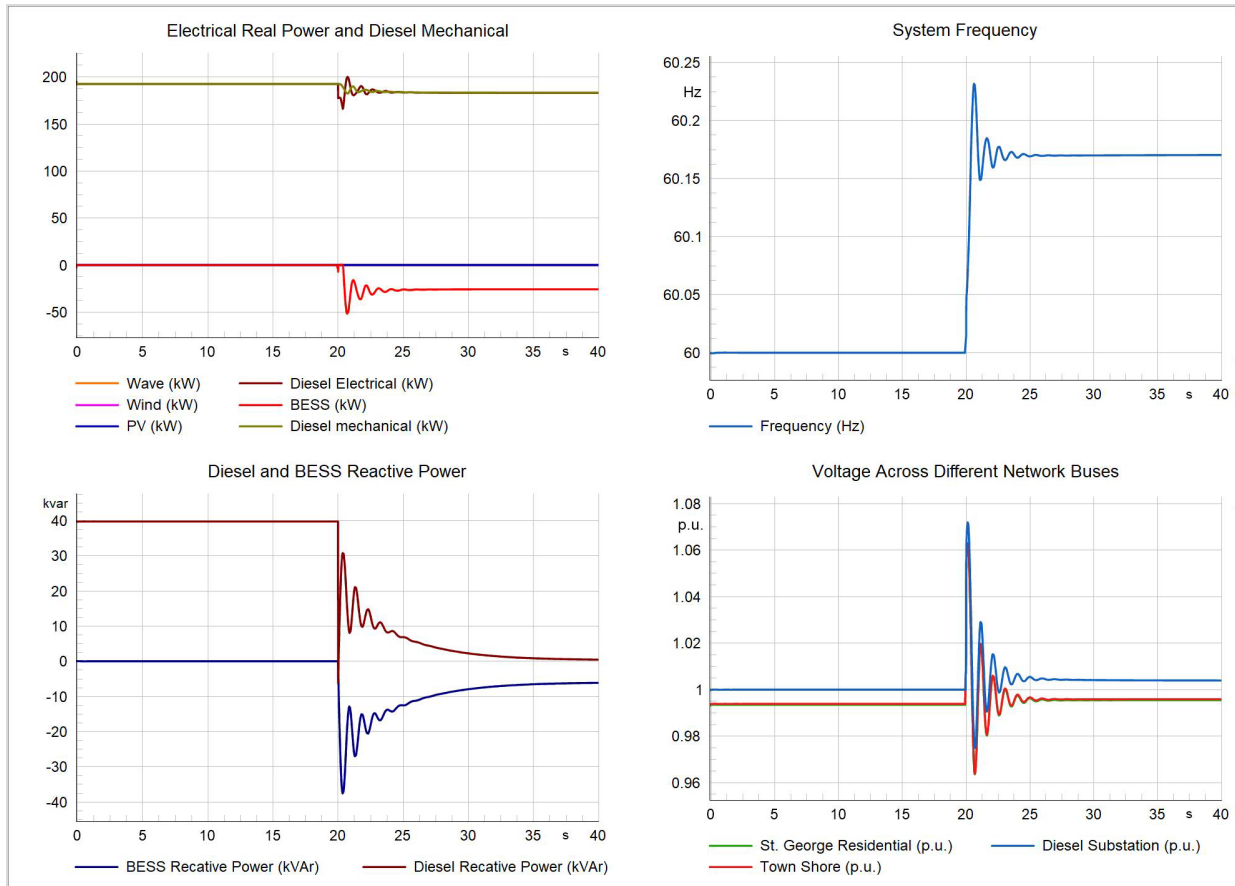


Figure 41. Dynamic performance of the system for the peak diesel generation scenario with both BESS and diesel providing frequency response.

7.2.1.3. Peak Solar Generation

The next scenario is the interval when solar generation is at its peak. During this hour, the PV plant generates 317.05 kW, which is 4.66 times the load of 68.65 kW. The excess solar generation is diverted to the collocated BESS charging at a rate of 254.41 kW. An abrupt tripping of the solar PV during this period would result in a significant generation-demand imbalance, the largest observed among the scenarios listed in Table 9. This imbalance cannot be managed by the diesel generator alone without support from the BESS.

Two different control options are considered for this scenario. In the first option, the BESS is tripped alongside the PV generation. Within 0.5 seconds of the PV tripping, the BESS also trips. Despite this, there remains a large mismatch as the PV was supporting the system's load demand. Following the disruption, the electrical power output of the diesel generator rises immediately, using the system's inertia, which results in a difference between electrical and mechanical power outputs. This leads to a significant frequency dip to 58.4 Hz at the nadir point, as shown in Figure 42. The governor responds to the frequency deviation by increasing the mechanical power of the diesel generator. Reactive power shows a small swing but settles at a value similar to what it was prior to the disruptive event. The frequency response shows a significant drop, with the nadir reaching 58.4 Hz. Following the event, the system frequency stabilizes at 58.94 Hz. Larger fluctuations are also observed in the system voltage, with the voltage nadir in one of the nodes where the PV was connected, reaching as low as 0.88 p.u.

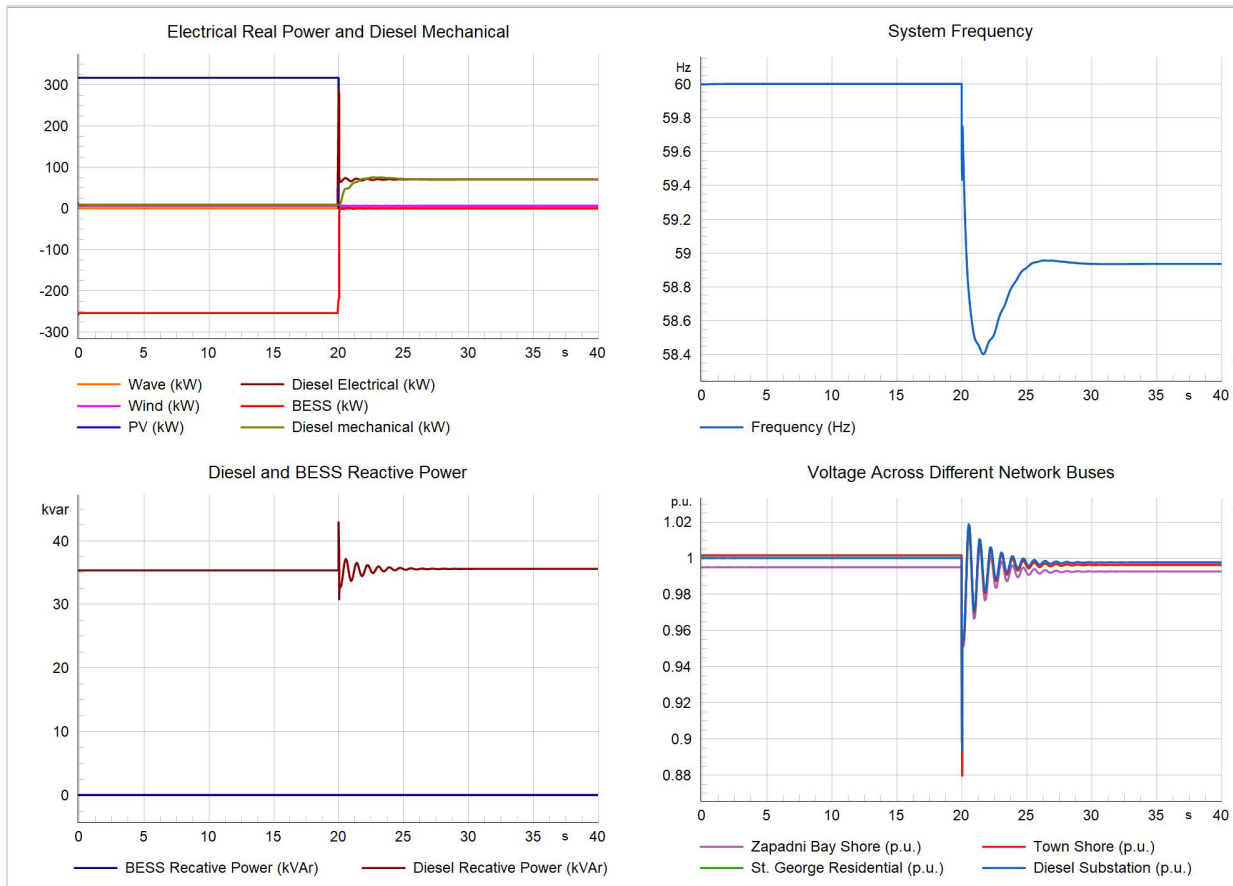


Figure 42. Dynamic performance of the system for the peak PV generation scenario with BESS tripped alongside PV. Only diesel generator provides the frequency response.

In the second control option, the BESS provides frequency response alongside the diesel generator. In this case, the BESS switches from charging at 254.4 kW to discharging at 42 kW to support the connected load. The remaining load demand and transmission losses are met by the diesel generator. Despite the large power change for the BESS, the frequency response still shows significant deviation, with the nadir point reaching as low as 58.79 Hz and the frequency settling at 59.6 Hz after the disturbance (Figure 43). Additionally, improvements are observed in the system voltage response due to the BESS contributing to reactive power support.

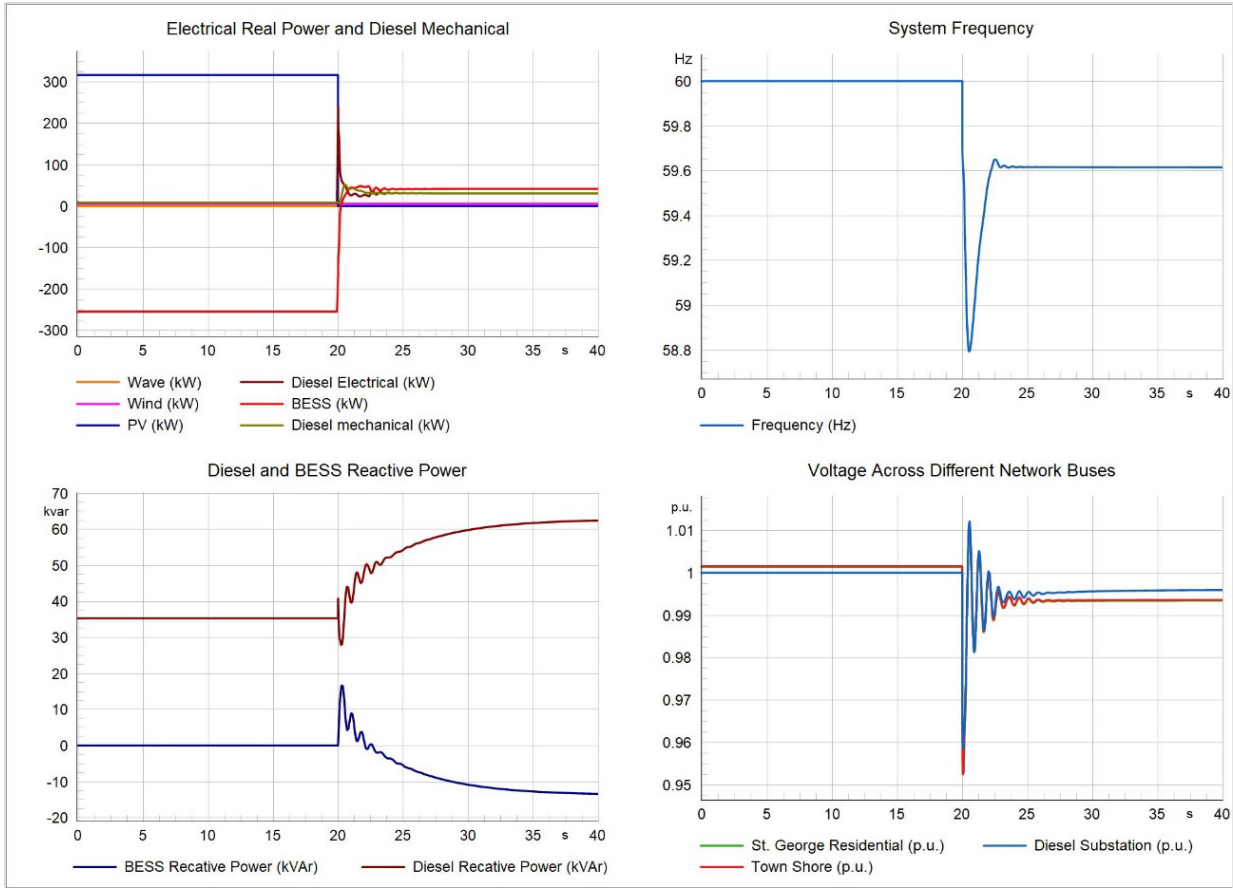


Figure 43. Dynamic performance of the system for the peak PV generation scenario with both BESS and diesel providing frequency response.

7.2.1.4. Peak Wind Generation

During the peak wind generation interval, the wind plant produces 289.56 kW, and the WEC produces 12.81 kW, while the BESS is charging at 184.45 kW. At $t=20$ s of simulation, the wind turbine is abruptly tripped off. Following this disruptive event, the BESS, participating in frequency response, switches to discharging mode with a new power setpoint of 68.5 kW based on the droop characteristics. The diesel generator's power output changes from 26.14 kW to 46.47 kW when the system stabilizes. This large swing in BESS power output results in a frequency nadir of 59.12 Hz, with the frequency settling at 59.65 Hz after the disturbance (Figure 44). Prior to the disturbance, the wind turbine provided most of the power, causing the voltage at Zapadni Bay to be slightly above the rated value at 1.01 p.u., which dropped to 0.99 p.u. following the disturbance. Some voltage disturbances were observed across different nodes in the system, but all remained within acceptable ranges. After the disturbance, the reactive power produced by the diesel generator and the reactive power consumed by the BESS increase by a similar magnitude.

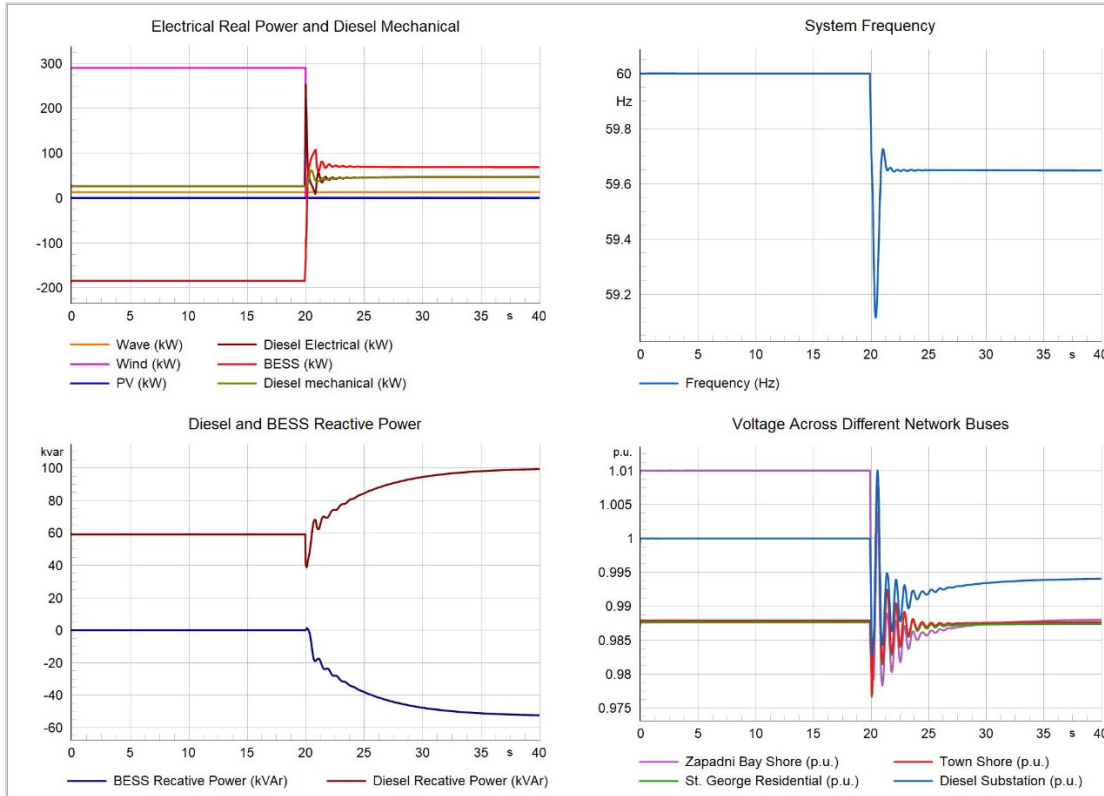


Figure 44. Dynamic performance of the system for the peak wind generation scenario with both BESS and diesel providing frequency response.

7.2.1.5. Peak Wave Generation

In this scenario, WEC provides most of the demand with small power coming from wind and PV. The BESS is charging at 10 kW, with a total load of 91.29 kW. The diesel generator also operates to remain active as well as meet the transmission losses that are not considered in the dispatch optimization problem. A disturbance is applied to the system at $t=20$ s by tripping off the WEC plant. Due to the loss of power produced by the WEC, there will be a net generation-load imbalance in the system. To respond to the resulting imbalance, both BESS and diesel generator ramp up their power output. BESS provides most of the generation deficit by ramping up to charging at 56.3 kW (66.38 kW net change). The diesel generator ramps up from 7.34 kW prior to disturbance to the 20.12 kW after the disturbance. The reactive power output of the diesel generator increases by 4.18 kVar, which is close to what BESS consumes (4.52 kVar) after the disturbance. The frequency and voltage show fluctuations, but all fluctuations remain within acceptable bounds and are lower than the disturbances for other scenarios.

In this scenario, the WEC provides most of the demand, with smaller contributions from wind and PV. The BESS is charging at 10 kW, and the total load is 91.29 kW. The diesel generator operates to stay active and meet the transmission losses. At $t=20$ s, a disturbance is applied by tripping off the WEC plant. This loss of power from the WEC creates a net-generation-load imbalance in the system. To address this imbalance, both the BESS and the diesel generator ramp up their power output. The BESS compensates for most of the generation deficit by increasing its output to 56.3 kW (a net change of 66.38 kW) as shown in Figure 45. The diesel generator ramps up from 7.34 kW before the disturbance to 20.12 kW after the disturbance. The reactive power output of the diesel generator increases by 4.18 kVar, which is close to the amount consumed by the BESS (4.52 kVar) after the disturbance. Although the frequency and voltage show fluctuations, they remain within acceptable bounds and are less severe than the disturbances observed in other scenarios.

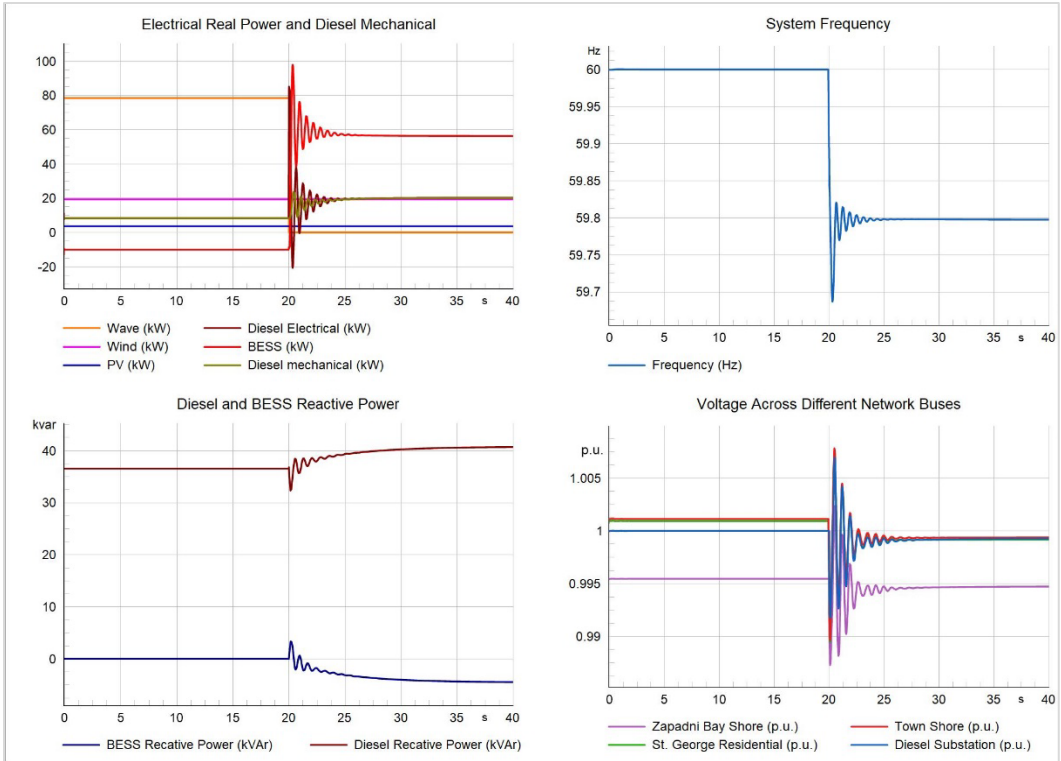


Figure 45. Dynamic performance of the system for the peak wave generation scenario with both BESS and diesel providing frequency response. WEC is tripped off at $t=20$ s. **Peak BESS Generation**

The final scenario analyzed involves the system operating at peak BESS output. During this period, the load is near its peak at 170 kW, and the BESS discharges to meet most of the demand, with wind and WEC providing marginal support, and the diesel generator remaining active to meet transmission losses. Losing the BESS at this critical instance results in a significant power imbalance in the microgrid and removes a crucial resource for dynamic system stability. Without the BESS, the diesel generator alone must ramp up to compensate for the generation deficit of 147.3 kW. Consequently, the system frequency drops to a nadir of 56.23 Hz and eventually settles at 57.28 Hz after the disturbance (Figure 46). Such a large frequency deviation is highly disruptive, even for islanded systems, and will likely cause diesel generators, other generation resources, and connected loads to trip. The system will likely require a black start following such disturbances. Similar fluctuations are observed in the voltage response across the network, with the voltage nadir dropping as low as 0.93 p.u. However, the voltages recover to acceptable levels within $\pm 5\%$ deviation.

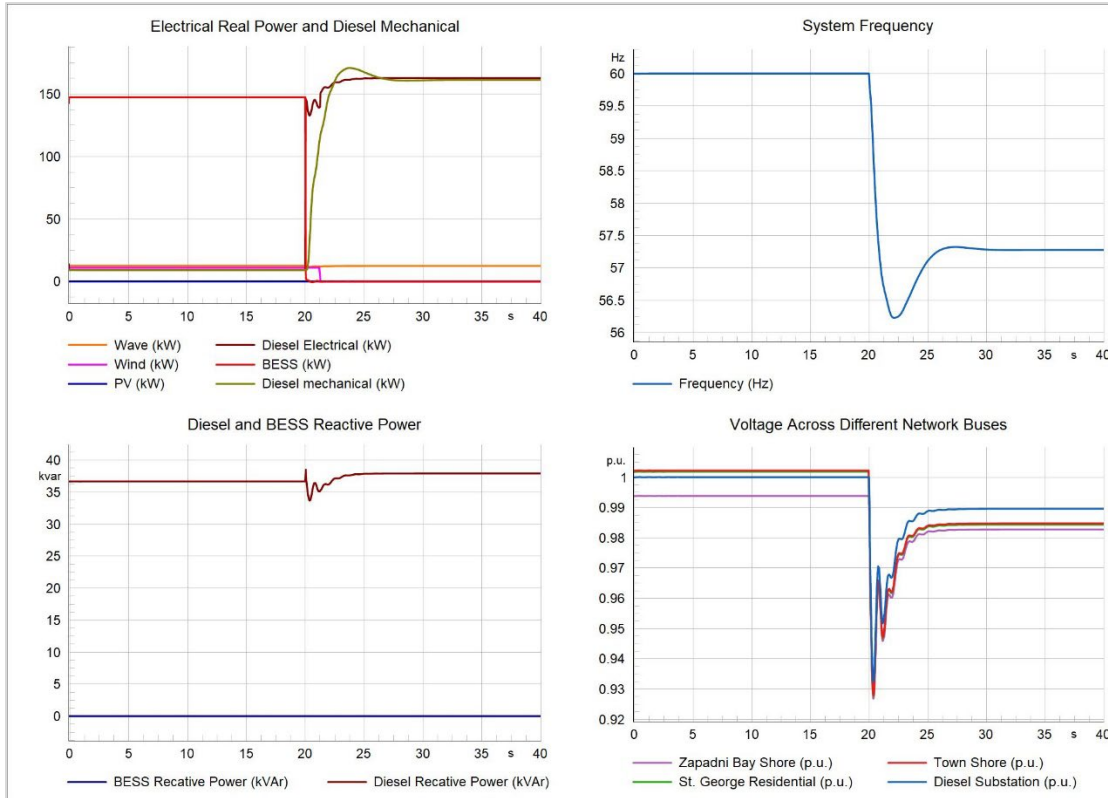


Figure 46. Dynamic performance of the system for the peak BESS generation scenario with BESS tripped off at $t=20$ s.

From the range of RMS simulations analyzed, it is evident that BESS plays a crucial role in maintaining system stability and enhancing dynamic performance under various disturbance scenarios. Despite the financial and environmental drawbacks, the diesel generator remains vital for keeping the system online. Coordinated control between the BESS and diesel generators is essential for managing power imbalances, frequency deviations, and voltage fluctuations effectively.

7.2.2. Electromagnetic Transients Simulation

The RMS simulations reveal that different operating instances are susceptible to various transients within the system. The responses ranged from significant frequency and voltage deviations, which could potentially trip connected devices and necessitate a black start to minor transients that would not substantially impact the system. While RMS simulation effectively captures the phasor dynamics of different system variables, it does not analyze harmonics within the system, particularly when dominated by inverter-based resources. Additionally, the system is highly unbalanced due to unequal power tapping from distribution lines by residential users, an issue not reflected in RMS simulations.

The goal is not to optimize the control of inverter-based resources during transient disturbances. Instead, the aim is to understand the impact of large disturbances on system operation and integrity and to identify limitations of existing infrastructure to host new technologies. For this purpose, the average value EMT models, as specified in Section 5.4, are sufficient.

7.2.2.1. Unbalanced Load Condition

The team conducted an EMT simulation for the operating instance from RMS simulation when WEC generation was at its peak. The network exhibited significant imbalance, as evidenced by flickers in power and frequency measurements recorded by the 3-phase sensors. Similar fluctuations were observed in the 3-phase active and reactive power supplied by the diesel generator.

At $t=5$ s, the Zapadni Bay feeder was abruptly tripped off, causing the wind turbine connected to the feeder and the associated loads to go offline. Although the system returned to a stable state after the disturbance, the flickers in frequency and power measurements persisted (Figure 47).

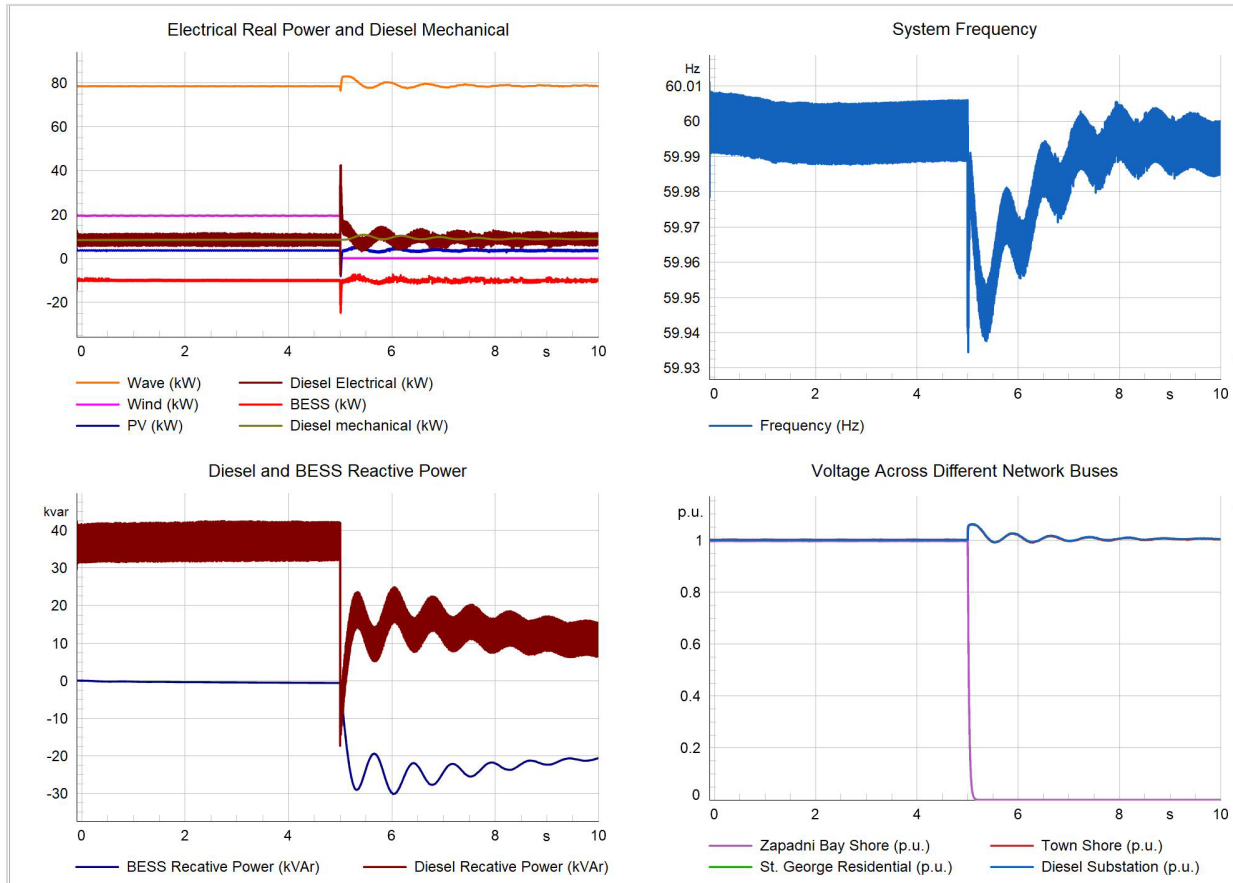


Figure 47. System measurements for the peak wave generation scenario with Zapadni Bay feeder tripped off at $t=5$ s (unbalanced case).

A closer examination of the 3-phase current output of the diesel generator reveals that the system is more heavily loaded on Phase A, both before and after the disturbance (Figure 48). This imbalance not only causes flickers in the system measurements but also presents a significant challenge for system control, as these power and frequency measurements are used to provide feedback for the control system. The BESS, in particular, relies on these voltage and frequency measurements to respond to system disturbances.

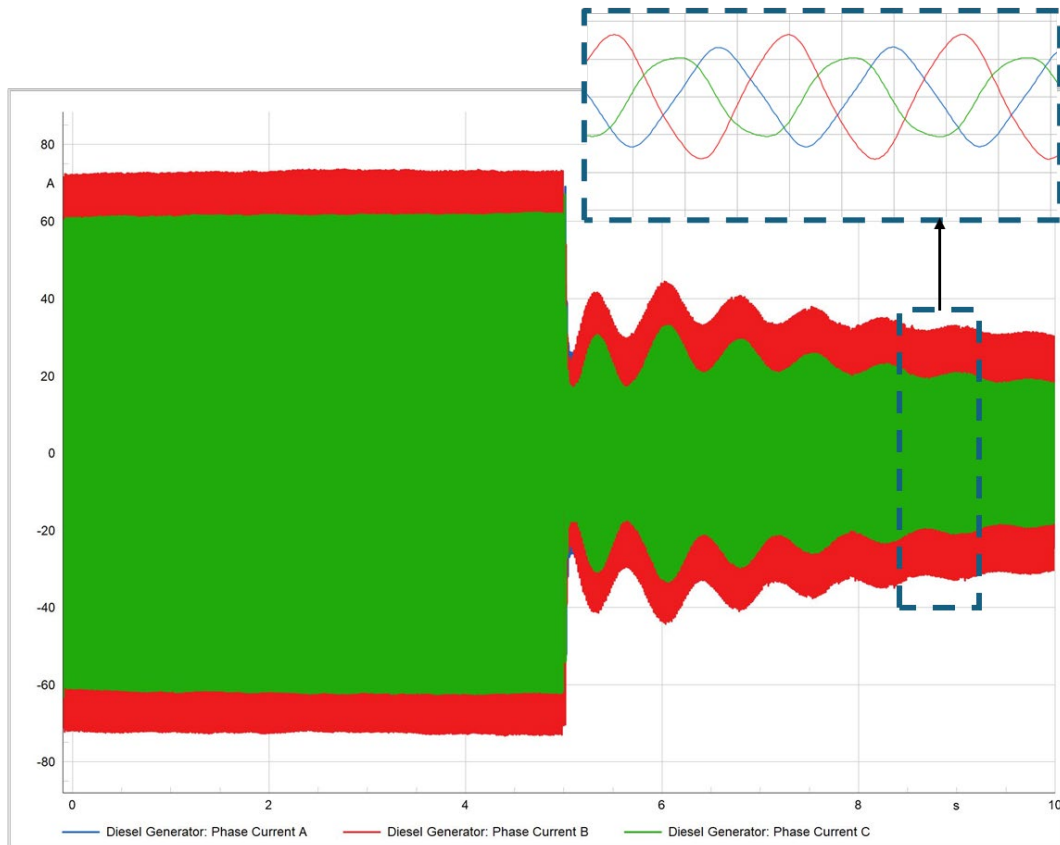


Figure 48. Current measurements in different phases of diesel generator output terminal (unbalanced case).

7.2.2.2. **Balanced Load Condition**

The team revisited the system network in the simulation tool and made efforts to balance the system as much as possible. After balancing, the plots for power, frequency, and current measurements showed significant improvement compared to the unbalanced case. However, some imbalance remained due to single-phase loads, causing Phase A to be more heavily loaded than the other phases (Figure 50).

Applying the same disturbance as in the unbalanced case, the team found that the system remained balanced both before and after the disturbance. Notably, the frequency nadir improved when the system was balanced compared to when it was unbalanced (Figure 49).

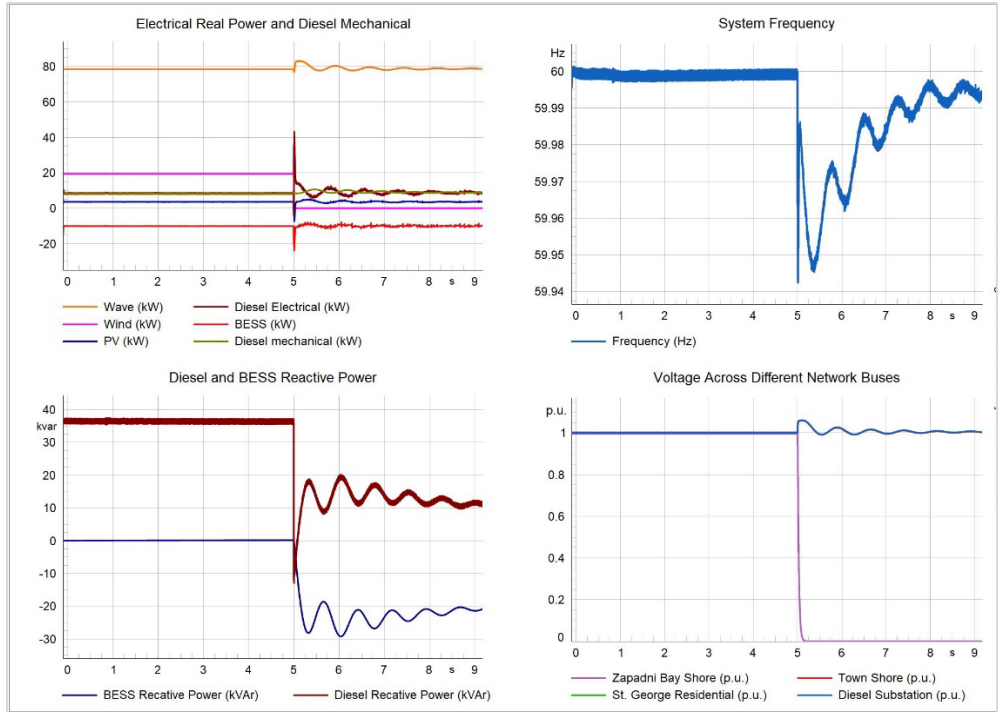


Figure 49. System measurements for the peak wave generation scenario with Zapadni Bay feeder tripped off at t=5 s (balanced case).

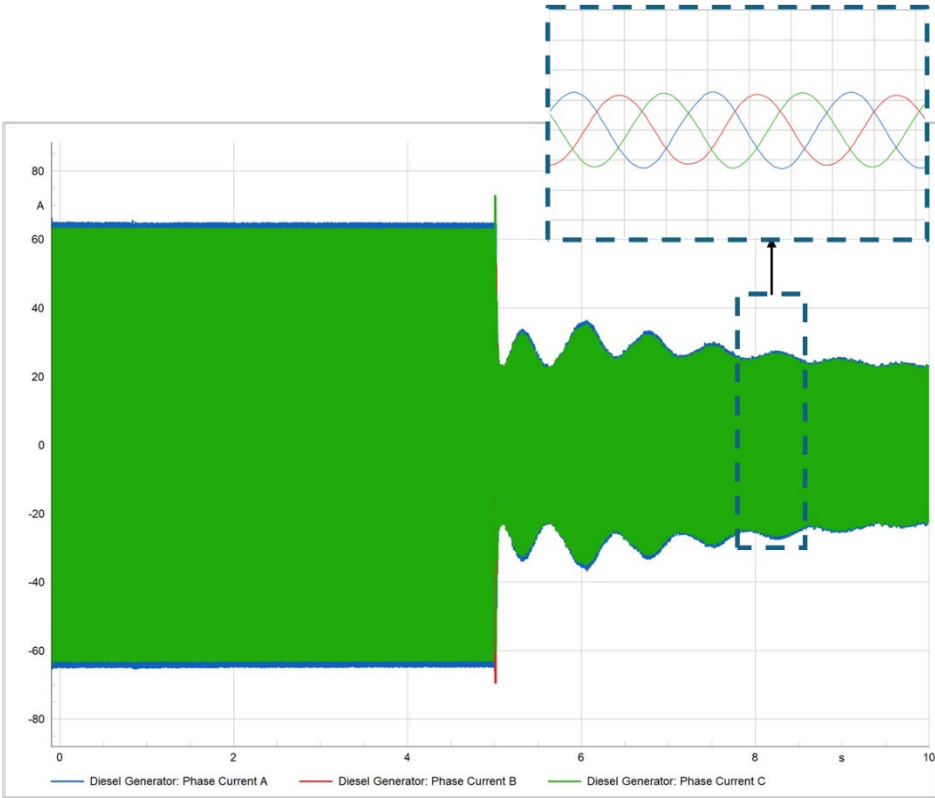


Figure 50. Current measurements in different phases of diesel generator output terminal (balanced case).

8. MARINE ENERGY MICROGRID TOOLKIT

The Marine Energy Microgrid Toolkit, as depicted in Figure 51, leverages the capabilities of Xendee and PowerFactory tools to implement the analysis framework developed in this project. Xendee's single-node optimization engine models and analyzes scenarios, generating sizing and dispatch solutions for quasi-dynamic analysis. PowerFactory then integrates these solutions into the microgrid's distribution network, distributing new technologies across the network and evaluating power flow to identify current and voltage violations. Additionally, Xendee's One-Line capability, powered by the OpenDSS engine, can import dispatch results to further analyze power flow and network violations. Following the power flow analysis, PowerFactory's RMS and EMT simulations assess the system's dynamic performance during both normal and abnormal scenarios. RMS simulations provide insights into the voltage and frequency dynamics during transient events, such as generation contingencies and faults. EMT simulations, on the other hand, predict detailed system dynamics, including harmonics. Together, these simulations offer valuable insights into control performance when multiple assets are combined to respond to transient events.

Optimizing the system as a single node excludes transmission losses from the analysis, often resulting in suboptimal sizing and dispatch or selection of solutions infeasible with existing infrastructure. This issue was evident in several scenarios analyzed in the use case of St. George. To address this, a tool capable of power distribution-constrained optimization is essential. Xendee's multi-node capability can optimize the system while considering network constraints, enabling both sizing and placement solutions. However, as the number of nodes and variables increases, the computational power required for optimization rises exponentially. Due to this high computational demand, Xendee's multi-node capability is currently limited to 20 nodes, and network-constrained sizing and dispatch solutions are conducted using day-type simulations instead of annual time-series simulations. Although this approach is not entirely accurate for dispatch, it provides reliable predictions of economic metrics.

The proposed framework and toolkit, which encompass a range of pre-deployment activities from community engagement to infrastructure operations evaluations, can be applied to other island and coastal communities, regardless of their grid access. Although specific problems, objectives, and scenarios will vary by community, the structured approach and standardized toolsets will provide comprehensive insights, facilitating successful microgrid deployments and enhancing resilience in vulnerable communities. In the future, this framework and toolkit will be used to offer technical assistance to interested communities, helping them implement and benefit from microgrid solutions.

The team aims to further enhance the proposed toolkit by incorporating new marine resources such as tidal and ocean current energy. Future developments will include dynamic and transient process models to emulate the internal dynamics of these technologies, as well as the development and testing of control algorithms for the unique operating conditions of community microgrids such as limited dispatchable resources or highly unbalanced networks. Additionally, the processes of Xendee and PowerFactory can be integrated and automated using the API capabilities of each software tool.

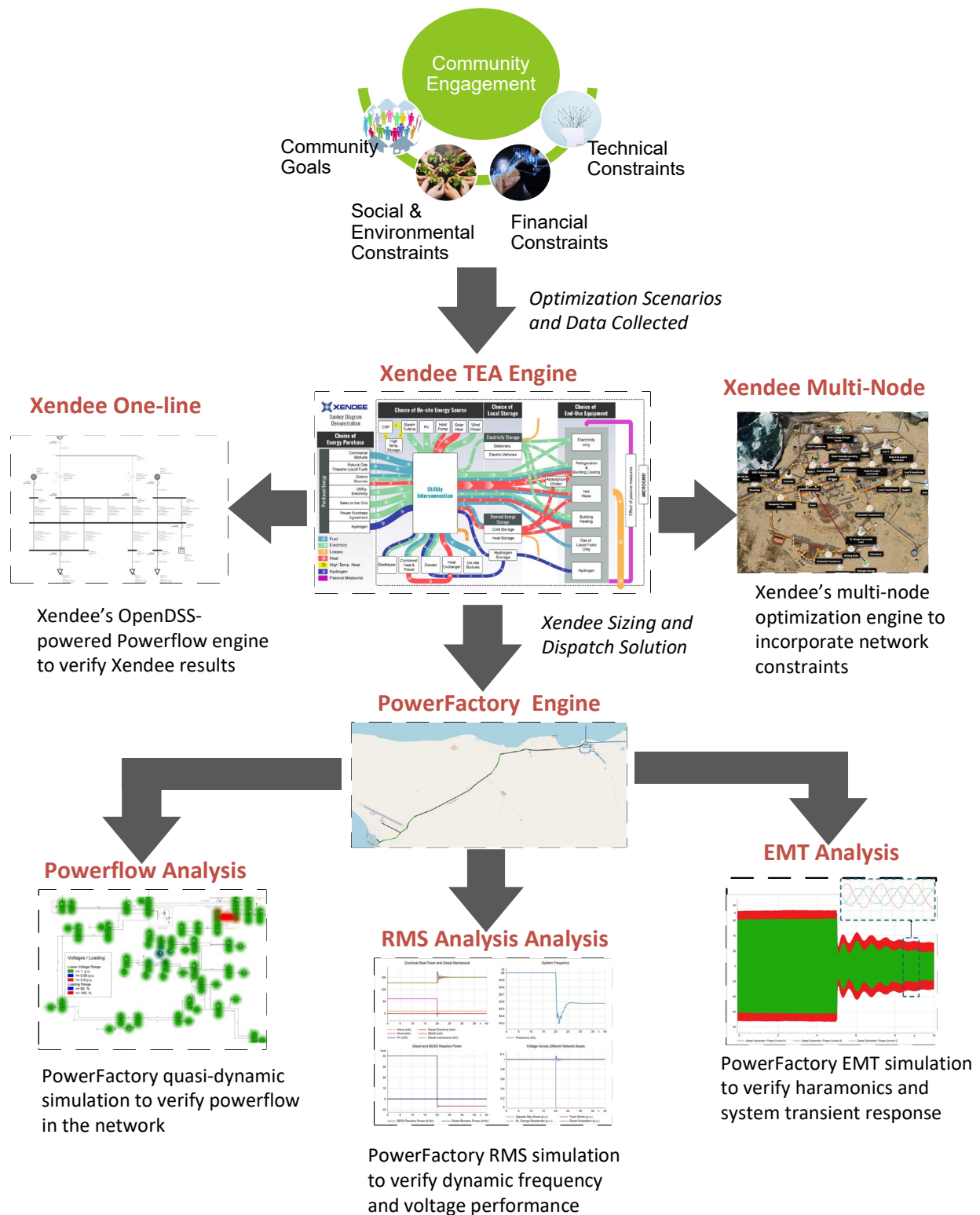


Figure 51. The proposed Marine Energy Microgrid Toolkit. The analysis kicks off with the community engagement followed by technoeconomic analysis and infrastructure evaluation using the capabilities of Xendee and PowerFactory capabilities. **CONCLUSIONS**

ME, when combined with other advanced generation technologies in microgrids, holds significant potential to deliver resilient energy systems for remote coastal and island communities. This report presents a community-centric model for microgrid planning that prioritizes community engagement as a crucial first stage of feasibility analysis. Through community engagement, various factors, such as community goals, perspectives, and social, technical, and economic constraints, were identified and translated into community development scenarios. These scenarios informed a technoeconomic optimization process aimed at determining the optimal generation portfolio, focusing on cost minimization, adoption of local generation, and resilience improvement objectives. The Xendee tool was used to model and optimize these scenarios, while the PowerFactory tool was used to investigate issues with existing infrastructure and new generation technologies within the microgrid.

St. George, a rural island community in Pribilof Island, Alaska, emerged as a top choice for the use case study due to its well-known wave energy potential, reliance on imported diesel fuels, availability of data, suitable population size, and involvement in commercial fishing. The technoeconomic analysis explored different optimization scenarios to provide cost-effective and resilient energy solutions, aiming to reduce reliance on externally imported fuels. Adopting local generation resulted in reduced energy costs, and diesel use. For the electricity-only scenario, the cost minimization objective resulted in a 47% reduction in LCOE and a 73.4% reduction in diesel use. When heat was considered, annualized costs were reduced by 38%, with diesel use reduced by 63.3%. However, more aggressive local generation adoption targets posed operational challenges such as increased generation curtailment and resource oversizing. Achieving energy independence was significantly costlier—2.78 times for electricity only and 7.5 times for combined heat and electricity—compared to the diesel baseline. The higher cost in the combined scenario was mainly due to the shift from diesel-based CHP to electrical heating, exacerbating operational issues.

Community concerns about wind energy led to a scenario excluding wind and incorporating a mix of PV and WEC with BESS. However, economic performance was inferior compared to wind scenarios, resulting in higher LCOE and lower diesel use reduction across all optimization cases, primarily due to weaker resource potential and high operational and maintenance costs for WECs. The study also considered uncertainties in technology costs, WEC technology maturation timelines, and future demand growth in remote communities. The optimization cases replacing 100% of imported diesel fuels with local energy resources incurred a significant cost premium, especially for the replacement of the last 10–20% of diesel. As a potential solution, integrating hydrogen into the energy mix was explored. This involved all hydrogen assets—electrolyzers, hydrogen storage tanks, fuel cells, and hydrogen boilers. This integration resolved operational issues in scenarios with and without wind, offering substantial savings in energy independence scenarios compared to those without hydrogen. While hydrogen's near-term feasibility remains uncertain, the analysis concludes that a locally produced fuel alongside advanced energy technologies is essential to fully replace imported fuels and achieve energy independence.

The infrastructure evaluation showed that while wind generation offers economic benefits, it introduces significant power flow challenges, such as increased transmission losses and voltage violations, due to the distant location of wind turbines from the load center in Zapadni Bay. Conversely, scenarios without wind experience fewer power flow issues and improved power flow performance, with reduced network losses, though they are less economically viable. To improve power flow performance in wind-inclusive scenarios, relocating wind turbines closer to the residential area, or upgrading the power lines connecting Zapadni Bay to the residential area is recommended.

The operations evaluation highlighted the critical role of BESS in supporting microgrid integration of new generation technologies and maintaining dynamic stability under various disruption scenarios. RMS simulations indicated that frequency support from BESS is essential for maintaining system stability. Developing control strategies to coordinate multiple flexible assets is important in microgrids dominated by highly volatile energy resources. EMT simulations revealed that load imbalances cause significant fluctuations in power and frequency measurements, posing challenges for system control. Balancing the load improved system stability, as evidenced by better frequency nadirs and current measurements. These findings underscore the need for coordinated control between BESS and diesel generators and highlight the importance of addressing load imbalances to ensure reliable microgrid operation.

Following this study, reengaging with the community is a pivotal next step. The team plans to present their findings, gather community feedback, and discuss potential pathways for microgrid deployment opportunities. This reengagement ensures that the community remains at the center of the decision-making process and that the analysis leads to fruitful outcomes. The insights gained from this reengagement will inform the development of the proposed framework and toolkit, making them more robust and adaptable for application in other island and coastal communities.

The developed framework and toolkit, encompassing a range of pre-deployment activities from community engagement to infrastructure operations evaluations, can be applied to other islands and coastal communities. In the future, this framework and toolkit will offer technical assistance to interested communities, helping them implement and benefit from microgrid solutions. Future work will also develop models to assess the technoeconomic feasibility of alternative generation resources, such as small nuclear reactors and alternative fuels like ammonia or biofuels, to effectively deliver resilient microgrids. Additionally, the team will enhance the toolkit by implementing dynamic and transient process models to emulate the internal dynamics of microgrid technologies, as well as developing and testing control algorithms for the unique operating conditions of marine coastal and island communities.

10. ACKNOWLEDGEMENTS

This work was funded by the U.S. Department of Energy’s Water Power Technologies Office (WPTO)’s Marine Energy Program under DOE Idaho Operations Office Contract DE-AC07-05ID14517. The authors sincerely appreciate the review and feedback provided by Dr. Jim McNally and Simon Gore from the Marine Energy Program. The authors are also grateful for the contributions of their interns, Mr. Haansol Lee and Dr. Jitendra Thapa, during their internships. Additionally, the authors extend their gratitude to Mr. Baxter Bond from the University of Alaska Fairbanks for his support during community engagement and the field trip. Finally, the authors deeply thank the Mayor of St. George, Alaska, as well as all the community members who provided valuable insights about the community during the field trip.

11. REFERENCES

- Alaska Energy Authority. 2012. “Concept Design Report and Construction Cost Estimate for Energy Infrastructure Projects in the Community of St. George.” Alaska Energy Authority. [https://www.akenergyauthority.org/Portals/0/Programs/Wind/Saint George Energy Projects CDR Final.pdf](https://www.akenergyauthority.org/Portals/0/Programs/Wind/Saint%20George%20Energy%20Projects%20CDR%20Final.pdf)
- Alzahrani, A., I. Petri, and Y. Rezugui. 2019. “Modelling and Implementing Smart Micro-Grids for Fish-Processing Industry.” 2019 IEEE International Conference on Engineering, Technology and Innovation (ICE/ITMC), June 17–19, 2019.
- Bhatnagar, D, V Chalishazar, S Bhattacharya, S Newman, DC Preziuso, J Lessick, S Hanif, et al. 2021. “Grid Value Proposition of Marine Energy: A Preliminary Analysis.” Pacific Northwest National Laboratory, Richland, Washington. https://www.pnnl.gov/main/publications/external/technical_reports/PNNL-31123.pdf.
- Black, Lydia T. 2004. “Russians in Alaska: 1732-1867.” Fairbanks: University of Alaska Press.

- Blavette, Anne, Dara L. O’Sullivan, Ray Alcorn, Tony W. Lewis, and Michael G. Egan. 2014. “Impact of a Medium-Size Wave Farm on Grids of Different Strength Levels.” *IEEE Transactions on Power Systems* 29(2): 917–923. <https://doi.org/10.1109/TPWRS.2013.2284513>.
- Chang, Grace, Craig A. Jones, Jesse D. Roberts, and Vincent S. Neary. 2018. “A Comprehensive Evaluation of Factors Affecting the Levelized Cost of Wave Energy Conversion Projects.” *Renewable Energy* 127: 344–354. <https://doi.org/https://doi.org/10.1016/j.renene.2018.04.071>.
- Contestabile, Pasquale, Enrico Di Lauro, Paolo Galli, Cesare Corselli, and Diego Vicinanza. 2017. “Offshore Wind and Wave Energy Assessment around Malè and Magoodhoo Island (Maldives).” *Sustainability* 9(4). <https://doi.org/10.3390/su9040613>.
- Corbett, H., and S. Swibold. 2000. “The Aleuts of the Pribilof Islands, Alaska.” In *Endangered Peoples of the Arctic: Struggle to Survive*, edited by M. M. R. Freeman, 1-15. Greenwood Press.
- Darrow, Ken, Rick Tidball, James Wang, and Anne Hampson. 2015. “Catalog of CHP Technologies: Section 6. Technology Characterization–Fuel Cells.” https://www.epa.gov/sites/default/files/2015-07/documents/catalog_of_chp_technologies_section_6_technology_characterization_-_fuel_cells.pdf.
- Department of Education and Early Development. 2023. “Instructions to Complete the Program Demand Cost Model for Alaskan Schools, 23 ed.” State of Alaska.
- Du, Yuhua, Yuxi Men, Xiaonan Lu, Jianzhe Liu, Feng Qiu, and Bo Chen. 2020. “Coastal Community Resiliency Enhancement Using Marine Hydrokinetic (MHK) Resources and Networked Microgrids.” <https://doi.org/10.2172/1767164>. <https://www.osti.gov/biblio/1767164>.
- Elliott, Shiloh N., Thomas M. Mosier, Jeremy VanderMeer, Michele Chamberlin, Phylcia Cicilio, Kelsey Fhay, Michael Stadler, et al. 2022. “Assessment Framework of Marine Hydrokinetic Technologies for Microgrid Applications.” <https://www.osti.gov/biblio/1868361>.
- Gilbert, Andrew, Michael Penev, Katelyn O’Dell, Campbell Howe, and Chris Wu. 2024. “Summary of Electrolyzer Cost Data Synthesized from Applications to the DOE Clean Hydrogen Hubs Program.” DOE Hydrogen Program Record No. 24002. <https://www.hydrogen.energy.gov/docs/hydrogenprogramlibraries/pdfs/24002-summary-electrolyzer-cost-data.pdf>.
- Guo, Chenglong, Wanan Sheng, Dakshina G. De Silva, and George Aggidis. 2023. “A Review of the Levelized Cost of Wave Energy Based on a Techno-Economic Model.” *Energies* 16(5). <https://doi.org/10.3390/en16052144>. <https://www.mdpi.com/1996-1073/16/5/2144>.
- Hagerman, George, and Brian Polagye. 2006. “EPRI North American Tidal In Stream Power Feasibility Demonstration Project.”
- Holst, Marius, Stefan Aschbrenner, Tom Smolinka, Christopher Voglstätter, and Gunter Grimm. 2021. “Cost Forecast for Low Temperature Electrolysis - Technology Driven Bottom-Up Prognosis for PEM and Alkaline Water Electrolysis Systems.” Fraunhofer ISE. <https://publica.fraunhofer.de/handle/publica/441376>.
- Hydrogen and Fuel Cells Technologies Office. 2024. “Hydrogen and Fuel Cell Technologies Office Multi-Year Program Plan: Fuel Cell Technologies.” <https://www.energy.gov/sites/default/files/2024-05/hfto-mypp-fuel-cell-technologies.pdf>.
- International Renewable Energy Agency. 2023. “Renewable Energy for Remote Communities: A Guidebook For Off-Grid Projects.”
- Jeanette, Wolak, and Erin Klauk. 2007. “Political Issues in the Pribilof Islands Resulting from Resource Development.”
- Jones, D. K. 1980. “A Century of Servitude: Pribilof Aleuts under U.S. Rule.” Lanham, MD: University Press of America.
- Keiner, Dominik, Orlando Salcedo-Puerto, Ekaterina Immonen, Wilfried G. J. H. M. van Sark, Yoosuf Nizam, Fathmath Shadiya, Justine Duval, et al. 2022. “Powering an Island Energy System By Offshore Floating Technologies Towards 100% Renewables: A Case for the Maldives.” *Applied Energy* 308: 118360-118360. <https://doi.org/https://doi.org/10.1016/j.apenergy.2021.118360>.

- Kohlhoff, Dean. 1995. "When the Wind was a River: Aleut Evacuation in World War II." Seattle: University of Washington Press.
- May-Varas, Nicholas; Robertson, Bryson 2020. "Wave Energy Converter Archetypes and Power Performance Representation." Oregon State University (Corvallis, OR, USA: Oregon State University). https://ir.library.oregonstate.edu/concern/technical_reports/p26772639.
- National Data Buoy Center. 2024. "Station 46073- Southeast Bering Sea - 205 NM WNW of Dutch Harbor, AK." National Oceanic and Atmospheric Administration, Accessed December 11, 2024. https://www.ndbc.noaa.gov/station_realtime.php?station=46073.
- National Renewable Energy Laboratory. 2023. "2023 Annual Technology Baseline." National Renewable Energy Laboratory, Golden, CO.
- . 2024a. "Marine Energy Atlas." Accessed December 12, 2024. <https://maps.nrel.gov/marine-energy-atlas>.
- . 2024b. "WEC-Sim (Wave Energy Converter SIMulator)." National Renewable Energy Laboratory. Accessed December 12, 2024. <https://wec-sim.github.io/WEC-Sim/main/index.html>.
- Papadias, D. D., and R. K. Ahluwalia. 2021. "Bulk Storage of Hydrogen." International Journal of Hydrogen Energy 46(70): 34527–34541. <https://doi.org/https://doi.org/10.1016/j.ijhydene.2021.08.028>.
- Sifakis, Nikolaos, Stefanos Konidakis, and Theocharis Tsoutsos. 2021. "Hybrid Renewable Energy System Optimum Design and Smart Dispatch for Nearly Zero Energy Ports." Journal of Cleaner Production 310: 127397. <https://doi.org/https://doi.org/10.1016/j.jclepro.2021.127397>.
- Stadler, Michael, and Adib Naslé. 2019. "Planning and Implementation of Bankable Microgrids." The Electricity Journal 32(5): 24–29. <https://doi.org/https://doi.org/10.1016/j.tej.2019.05.004>.
- Thresher, Robert. 2011. "A Commercialization Path and Challenges for Marine Hydrokinetic Renewable Energy." 2011 IEEE Power and Energy Society General Meeting.
- Trapani, Davide, Paolo Marocco, Domenico Ferrero, Karen Byskov Lindberg, Kyrre Sundseth, and Massimo Santarelli. 2024. "The Potential of Hydrogen-Battery Storage Systems for a Sustainable Renewable-Based Electrification of Remote Islands in Norway." Journal of Energy Storage 75: 109482. <https://doi.org/https://doi.org/10.1016/j.est.2023.109482>.
- U. S. Census Bureau. 2020. "2020 Census St. George City, Alaska."
- Uddin, Moslem, Huadong Mo, Daoyi Dong, Sondoss Elsayah, Jianguo Zhu, and Josep M. Guerrero. 2023. "Microgrids: A Review, Outstanding Issues and Future Trends." Energy Strategy Reviews 49: 101127-101127. <https://doi.org/https://doi.org/10.1016/j.esr.2023.101127>.

Appendix A

Community Engagement and Data Collection

A-1. Community Selection

The communities within Aleutian and Pribilof Islands of Alaska were considered for the community selection for this study. The team considered eight candidate communities: Adak, Atka, Akutan, King Cove, False Pass, St. George, St. Paul, and Nikolski (see Figure A-1). The key criteria for selection included population size, commercial activities, primary energy sources (e.g., diesel and hydro), identified energy resources (e.g., wave, tidal, hydro, wind, geothermal), connectivity, infrastructure upgrade needs and plans, potential stakeholders, and exposure to extreme events.

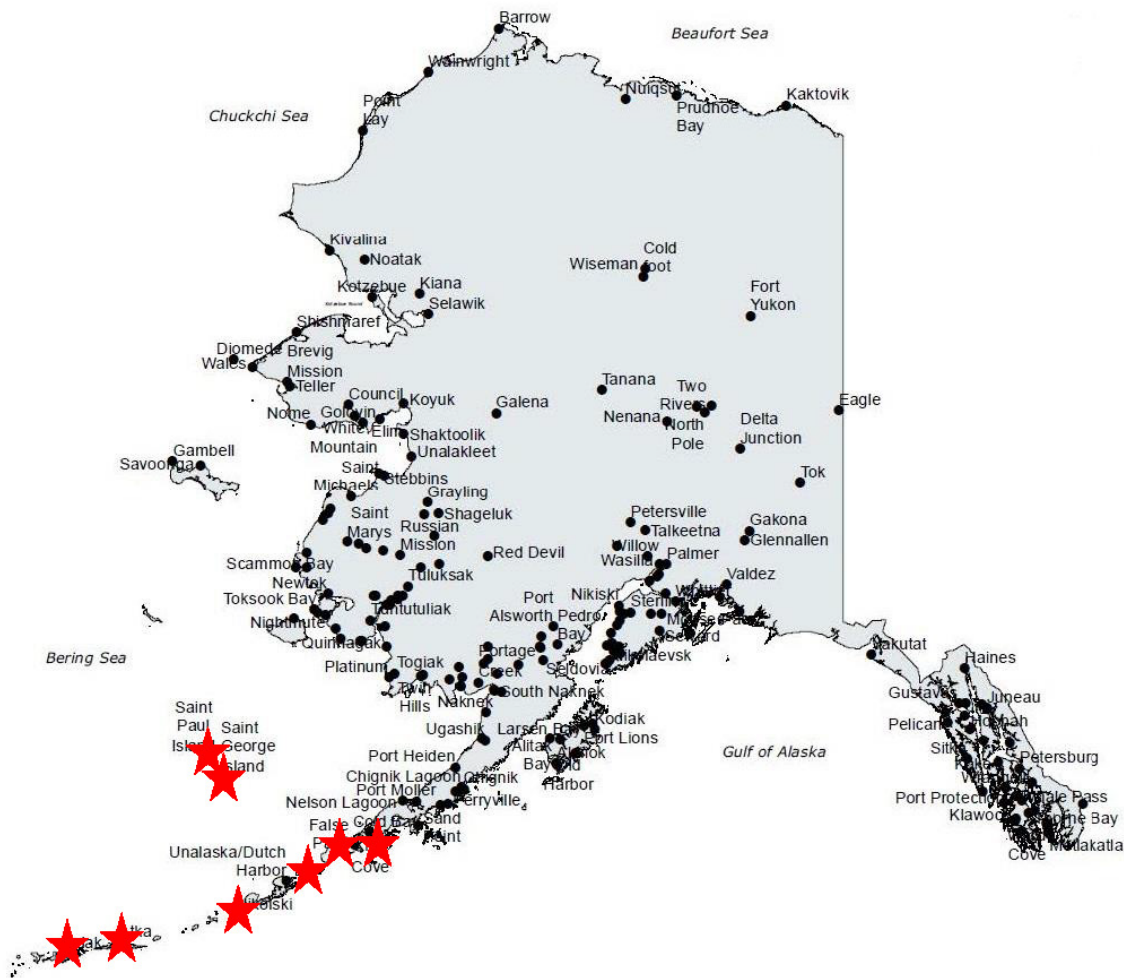


Figure A-1. Eight communities considered from Aleutian and Pribilof Islands

Table A-1 provides the summary of the communities and the ranking for selection for this study. The highest-ranked community, False Pass, already had an ongoing RivGen tidal project with Ocean Renewable Power Company (ORPC). Therefore, the team selected the second-ranked community, St. George, for this study. St. George was chosen due to its wave potential as well as the challenges the community faces in terms of diesel supply. The discussion below provides a summary of the eight communities that were under consideration.

Table A-1. Community profile summarized for eight selected communities during community selection process. False Pass had an existing, ongoing commercial project and, therefore, the second-ranked island, St. George, was selected for this study.

Community	Population	Commercial Activities	Primary Source	Identified Resources	Infrastructure Plans	Rank
Atka	100	Subsistence/ commercial fishing	Hydro, diesel	Hydro	—	5
Adak	150	Fueling, crew transfer, fishing, unexploded ordnance cleanup	Diesel	Hydro, Wind	Generation, distribution, water, landfill	4
False Pass	60	Subsistence/ commercial fishing	Diesel	Tidal	Generation, distribution	1
King Cove	800	Subsistence/ commercial fishing, harbor	Hydro, diesel	—	—	7
Akutan	85	Subsistence/ commercial fishing	Hydro, diesel	Geothermal	District heating	3
St. George	102	Subsistence/ commercial fishing	Diesel	Wave	Generation	2
St. Paul	479	Subsistence/ commercial fishing	Diesel	—	Generation	6
Nikolski	18	Work outside community	Diesel	Wind	Generation	8

A-1.1 Community 1: Atka

Atka, with approximately 100 residents, who are predominantly Aleut, is reliant on subsistence and commercial fishing economy. The community is home to a small fish processing plant operated by Aleutian Pribilof Island Community Development Association for cod and halibut fishing, which is reliant on city power and operates seasonally. The community desires to expand the fish processing plant. The primary energy sources are diesel and a hydroelectric facility. Infrastructure improvements are needed for most utilities and facilities. Water is supplied by a stream and wooden reservoir dam northwest of the city. Water is treated and stored in a 130,000 gallons water tank before distribution. All homes are connected to the piped water and sewer system and are plumbed. Wastewater flows untreated through outfall lines into Nazan Bay.

A-1.2 Community 2: Adak

Adak has a population of around 150 and was a former naval base, which was closed in the 1990s, leaving many buildings empty and in disrepair. Half of the island is owned by the Aleut Corporation and the other half by the U.S. Fish and Wildlife Service. The economy is based on a fueling and crew transfer facility, an airport, sport hunting and fishing, and unexploded ordnance cleanup. The existing fish processing plant requires an overhaul to become operable. The power plant, owned by TDX Corporation since 2008, has seen over \$1 million in repairs and upgrades. Like Atka, Adak needs significant infrastructure improvements. The city operates water, sewer, and landfill services. Water is derived from Lake Bonnie Rose, Lake De Marie, and Nurses Creek, stored in any of the four water tanks throughout the community, and piped to facilities and housing units. The wastewater treatment system discharges through a marine outfall line to Kuluk Bay. The community has also experienced issues with aging infrastructure and contamination for drinking water. Adak Petroleum, owned by Aleut Corporation owns nine fuel storage tanks with the combined capacity of 22 million gallons.

A-1.3 Community 3: False Pass

False Pass, with about 60 residents (majority Aleut), has a subsistence and commercial fishing economy focused on salmon, halibut, and cod fishing. It has a seasonally operated fish processing plant (Silver Bay) and a relatively new small boat harbor. The community was studied for tidal power potential in 2014 and, reportedly, the community has a significant tidal potential. It is currently under consideration for energy development due to its existing infrastructure and energy resource potential. Water is derived from a nearby spring and reservoir and is treated and stored in a 60,000-gal tank. Most homes are connected to the piped water system.

A-1.4 Community 4: King Cove

King Cove is the largest community under consideration with around 800 residents, primarily Aleut. It has a subsistence and commercial fishing-based economy and hosts a large year-round fish processing plant (Peter Pan Seafoods), which has a separate power system from the city. The community features both small and large boat harbors and relies on diesel and hydroelectric power sources. Since initial construction in 1995, a hydroelectric facility on Delta Creek has provided most of the electricity to the community of King Cove, as have three backup diesel generators. The energy demand comes from fish processing, sewage treatment, shipping dock and an airport besides residential energy usage. Water in King Cove is sourced from Ram Creek, using a sheet pile dam that stores approximately 980,000 gallons of unfiltered water. The City of King Cove manages the water and sewage systems. A piped sewage collection system connects all homes and facilities to central septic tanks. Two lift stations and tanks provide primary (20,000 gallons) and secondary (84,000 gallons) treatment of waste, with discharge through an outfall line. All homes are connected to the piped water system, and fully plumbed.

A-1.5 Community 5: Akutan

Akutan has about 85 residents, mainly Aleut, and a subsistence and commercial fishing economy with a small local halibut fishery. It hosts a large fish processing plant (Trident Seafoods) that employs 800–1,000 migrant workers year-round, operating independently from the city’s utilities. Akutan has a new harbor and uses hydroelectric power and diesel generators. The community has been explored for geothermal potential as well. Water is supplied by a local stream and dam, originally constructed in 1927. It is treated and piped into all homes, while sewage is directed to a community septic tank with effluent discharge through an ocean outfall. Refuse is collected three times a week and taken to the landfill. The city also recycles aluminum. Natural hazards threatening the community include tsunamis, earthquakes, storm surges, coastal erosion, coastal flooding, riverine erosion, and volcanoes. According to the Aleutians East Borough Hazard Mitigation Plan, there is a high probability of an earthquake or volcanic event affecting the community, with moderate chances of tsunamis, severe weather, and erosion events occurring. As of 2010, erosion was threatening the impoundment pond carrying the community’s water supply.

A-1.6 Community 6: St. George

St. George with a population of 40 (majority Aleut), relies on subsistence and commercial fishing, is entirely powered by diesel, and is often facing significant fuel shortages. The community has a rich socioeconomic and sociocultural history and needs improved energy infrastructure to support its small population. The community is currently based on subsistence and commercial fishing but has a history of fur seal hunting. The community is known to have good wave and wind resource potential. A 500-kW wind power project was canceled in the past, but a 95 kW Windmatic wind turbine was installed twice by the Alaska Energy Authority (AEA). Both times, it failed due to lack of maintenance and high wind speed.

A-1.7 Community 7: St. Paul

St. Paul has 479 residents, mostly Aleut, and an economy based on subsistence and commercial fishing, with a history in the fur seal industry. The Central Bering Sea Fishermen’s Association (CBSFA) operates a cooperative with Trident Seafoods and American Seafoods, making Trident Seafoods a top local employer. The community relies on diesel power, supplemented by a small wind turbine providing electricity and hot water to the airport. St. Paul’s water supply comes from an aquifer and wells.

A-1.8 Community 8: Nikolski

Nikolski, with 18 inhabitants (majority Aleut), has a subsistence and cash economy and is interested in developing a value-added fish processing plant. The community’s water supply comes from a community well and surface water, with all houses fully plumbed. Electricity is produced by a diesel generator. The wind power plant project in Nikolski faced challenges in the past in establishing a wind-diesel configuration without onsite technicians.

A-2. Wave Energy Converter Generation Profile

This section outlines the steps the team followed to synthesize the hourly generation profile for WECs. This method leverages data from authoritative sources such as the National Data Buoy Center (NOAA) National Data Buoy Center and the NREL Marine Energy Atlas. By adhering to these steps, researchers can create a detailed and dynamic profile of wave energy generation, which is essential for optimizing the deployment and performance of WECs in specific locations.

Step 1: Identify Location and Available Data

To begin the synthesis of the hourly WEC generation profile, it is essential to identify the location of interest and gather available data. The NOAA National Data Buoy Center provides critical information on significant wave height (meters) and dominant wave period (seconds) at various weather stations across the United States (Figure A-2). In this case, neither the St. George nor St. Paul stations report wave meteorological data. However, hourly wave meteorological data can be obtained from the Southeast Bering Sea Station 46073, as shown in Figure A-3 (National Data Buoy Center). It is important to note that the Southeast Bering Sea Station is located 136 miles away from St. George.

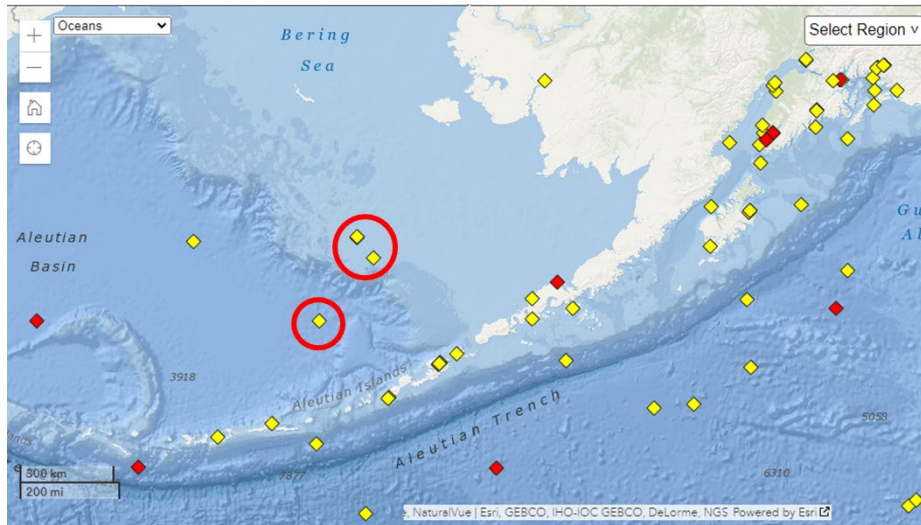


Figure A-2. NOAA meteorological stations in St. George, St. Paul, and Bering Sea. The St. George and St. Paul stations do not report wave meteorological data, whereas the Bering Sea station does.

#YY	MM	DD	hh	mm	WDIR	WSPD	GST	WVHT	DPD	APD	MWD	PRES	ATMP	WTMP	DEWP	VIS	PTDY	TIDE
#yr	mo	dy	hr	mn	degT	m/s	m/s	m	sec	sec	degT	hPa	degC	degC	degC	nmi	hPa	ft
2023	06	12	20	50	MM	MM	MM	1.1	7	5.1	41	1012.2	6.8	6.9	MM	MM	+2.2	MM
2023	06	12	19	50	MM	MM	MM	1.0	6	4.9	31	1011.5	6.7	6.8	MM	MM	+2.3	MM
2023	06	12	18	50	MM	MM	MM	1.1	6	4.8	36	1010.7	6.6	6.8	MM	MM	+2.2	MM
2023	06	12	17	50	MM	MM	MM	1.1	7	5.0	40	1010.0	6.6	6.9	MM	MM	+2.0	MM
2023	06	12	16	50	MM	MM	MM	1.2	7	5.1	51	1009.2	6.5	6.8	MM	MM	+1.5	MM

Figure A-3. A snapshot of wave meteorological data reported by the Bering Sea station. Significant wave height and dominant wave periods are extracted for this analysis. **Step 2: Explore Wave Energy Contour**

The next step involves exploring the wave energy contour to understand the energy potential at the location. The NREL Marine Energy Atlas provides annual and monthly average kW/m contours (National Renewable Energy Laboratory 2024a). These contours are instrumental in determining power scaling factors, which will be used to estimate the wave energy potential at the specified location. By analyzing the wave energy contour data, researchers can gain insights into the spatial and temporal distribution of wave energy, which is crucial for accurate energy generation predictions.

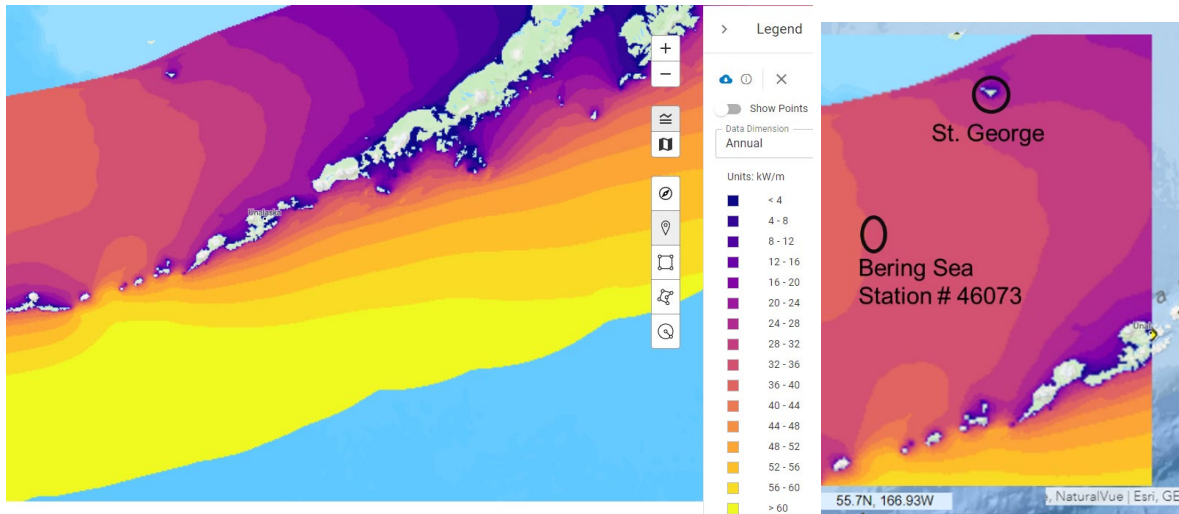


Figure A-4. Average wave energy contours from NREL's Marine Energy Atlas.

The data from the NOAA National Data Buoy Center map can be overlaid with the information from the NREL Marine Energy Atlas. This integrated approach allows for the calculation of the power at St. George relative to the power at the Southeast Bering Sea Station. The scaling factor that will be used later in an hourly profile generation can be calculated from the average monthly wave energy data according to Equation (A-1):

$$K = P_{BeringSea}[kW] / P_{St.George}[kW] \quad (A-1)$$

Table A-2. Monthly average wave energy reported by NREL Marine Energy Atlas at St. George and Bering Sea locations.

Month, m	St. George (kW/m)	Bering Sea (kW/m)	Scaling, K_m
January	23.78104296875	52.79078515625	2.219868
February	20.966021484375	50.3463046875	2.401328
March	15.1796435546875	42.985265625	2.83177
April	11.2972880859375	35.259359375	3.121046
May	6.4623369140625	17.179064453125	2.658336
June	3.77616552734375	9.9779228515625	2.642343
July	3.14216552734375	8.9069521484375	2.834654
August	5.2667724609375	13.61546875	2.585164
September	12.25277734375	26.374033203125	2.152494
October	19.808802734375	40.27388671875	2.033131
November	28.5619609375	66.3746953125	2.323884
December	28.636048828125	64.68787890625	2.258967

Step 3: Assess the Available Energy Period and Wave Heights

With the location and scaling factors determined, the next step is to assess the energy period and wave heights. The data from the Southeast Bering Sea Station #46073 is used to investigate the wave conditions over time. By analyzing the two distribution charts of wave periods and heights (Figure A-5 and Figure A-6), researchers can classify the wave energy potential and identify the most favorable periods for energy generation. This information is critical for selecting an appropriate WEC and optimizing its performance.

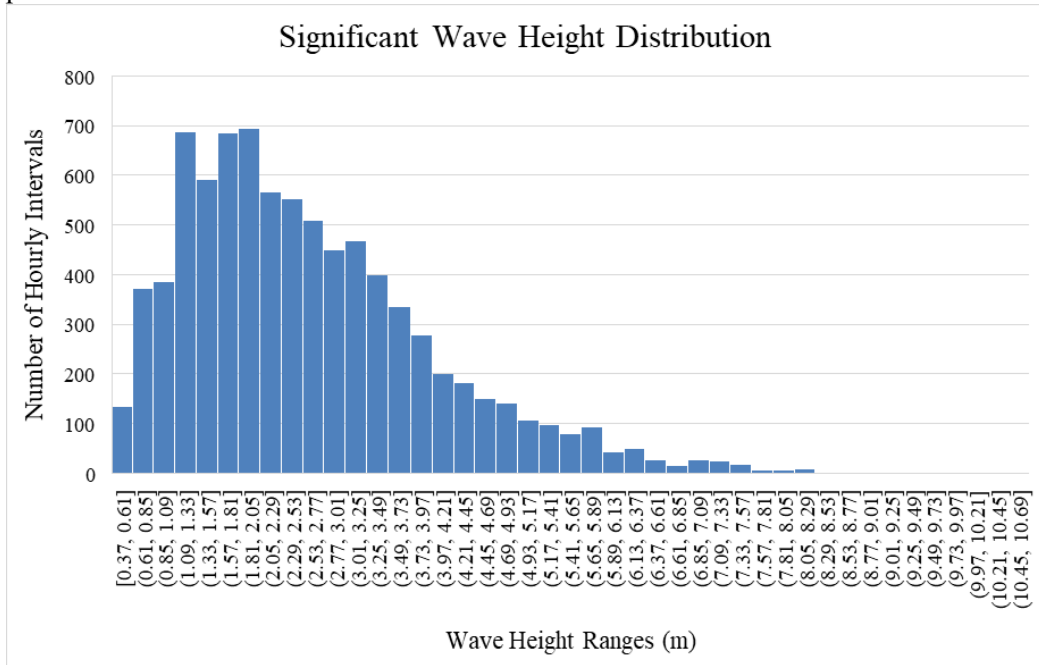


Figure A-5. Significant wave height distribution at Bering Sea station #46073.

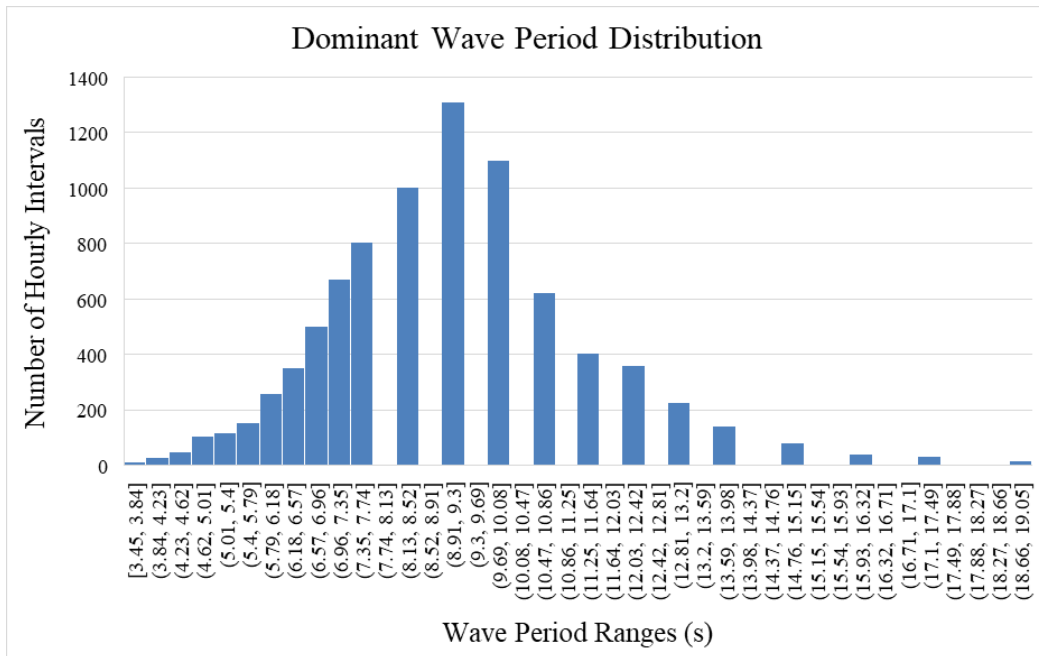


Figure A-6. Dominant wave period distribution at Bering Sea station #46073.

Step 4: Select WEC with Appropriate Power Performance Matrix

Selecting the WEC technology requires a thorough understanding of its power performance characteristics. The report, “Wave Energy Converter Archetypes and Power Performance Representation,” offers valuable insights into various WEC types, excluding the two-body floating point absorber (May-Varas 2020). For the two-body floating point absorber, the power performance matrix is available on page 125 of the report titled, “Grid Value Proposition of Marine Energy: A Preliminary Analysis” (Bhatnagar et al. 2021). The performance matrix is essential for understanding how different WECs respond to varying wave conditions and for selecting the most suitable converter for the location.

P [kW]		Wave Energy Period (s)												
		3.43	4.29	5.14	6	6.86	7.71	8.57	9.43	10.28	11.14	12	12.86	13.71
Significant Wave Height (m)	1	5	9	9	10	7	6	5	4	3	3	2	2	1
	1.5	12	19	22	20	15	13	10	8	6	6	4	3	3
	2	13	32	38	32	25	23	17	13	11	9	7	7	5
	2.5		48	54	47	41	33	26	20	17	14	10	9	8
	3		65	75	68	56	46	36	26	23	18	15	10	10
	3.5			97	86	71	62	46	33	29	23	20	15	13
	4			119	121	97	69	58	47	38	31	27	21	16
	4.5			147	146	107	93	74	61	48	37	33	26	21
	5			156	174	139	116	83	63	59	45	38	25	22
	5.5				201	164	133	89	79	66	54	41	35	28
	6				216	197	153	127	88	79	65	46	40	33
	6.5				244	209	175	151	113	95	76	55	44	39
	7				260	209	183	157	114	103	82	62	51	42

Figure A-7. A sample wave performance matrix for a WEC device.

Step 5: Apply Bilinear Interpolation to Create Hourly Generation

To synthesize the hourly generation profile, bilinear interpolation is applied. This mathematical technique interpolates the power output based on two variables: the dominant wave period (seconds) and the significant wave height (meters) using Equation (A-2):

$$f(x, y) = \frac{1}{(x_2 - x_1)(y_2 - y_1)} [x_2 - x] [y - y_1] \begin{bmatrix} f(Q_{11}) & f(Q_{12}) \\ f(Q_{21}) & f(Q_{22}) \end{bmatrix} \begin{bmatrix} y_2 - y \\ y - y_1 \end{bmatrix} \quad (\text{A-2})$$

The resulting power output (watts) is then calculated for each hour. By applying this method, researchers can generate a continuous and accurate hourly power output profile, which reflects the dynamic nature of wave energy.

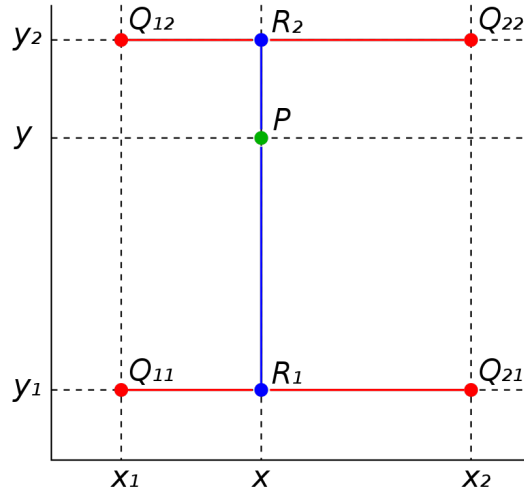


Figure A-8. Bilinear interpolation of wave height and energy period to calculate maximum wave generation for each interval.

Step 6: Calculate Wave Power Time Series Using Selected Performance Matrix

The final step is to calculate the wave power time series using the selected performance matrix. For each month, the power at the Southeast Bering Sea Station is calculated. This value is then adjusted to estimate the power at St. George Equation (A-3):

$$P_{St.George} kW = \frac{P_{BeringSea} kW}{K_m} \tag{A-3}$$

where

K_m = monthly scaling factor.

This calculation provides a time series of wave power, which can be used to predict the energy generation potential at St. George over time.

A-3. Resource and Demand Profiles

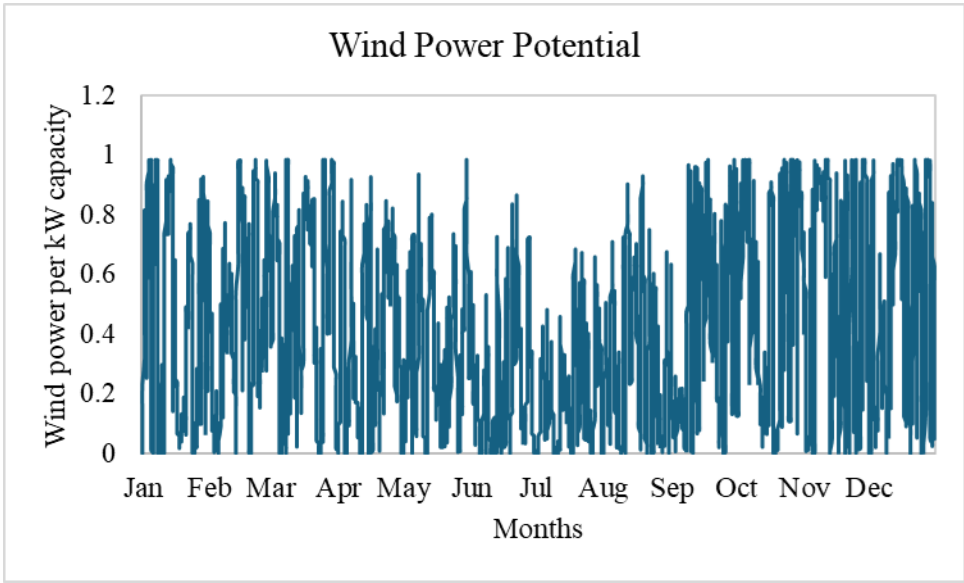


Figure A-9. Wind power potential for St. George Island, AK.

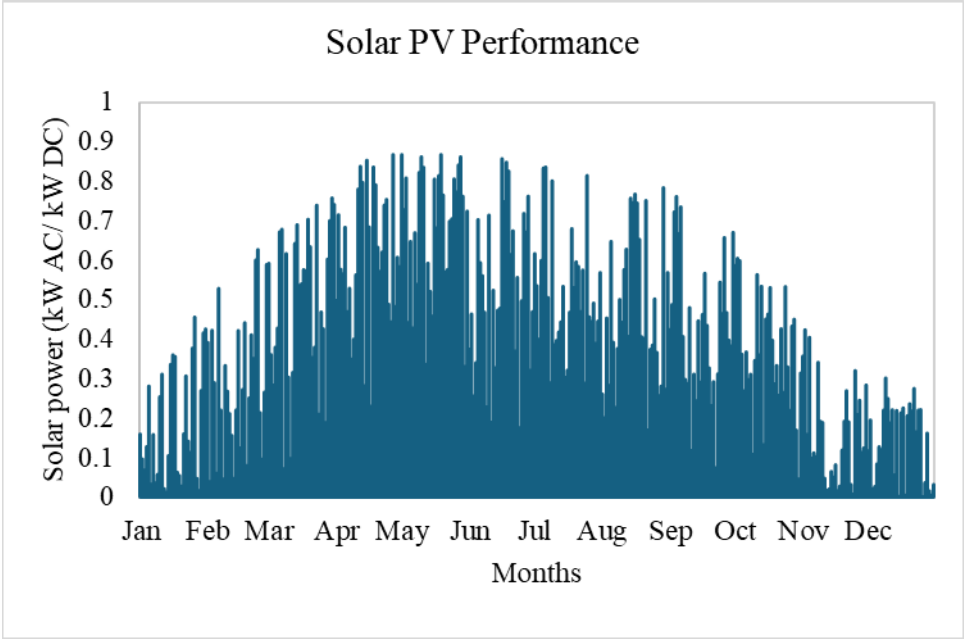


Figure A-10. Solar power potential for St. George Island, AK.

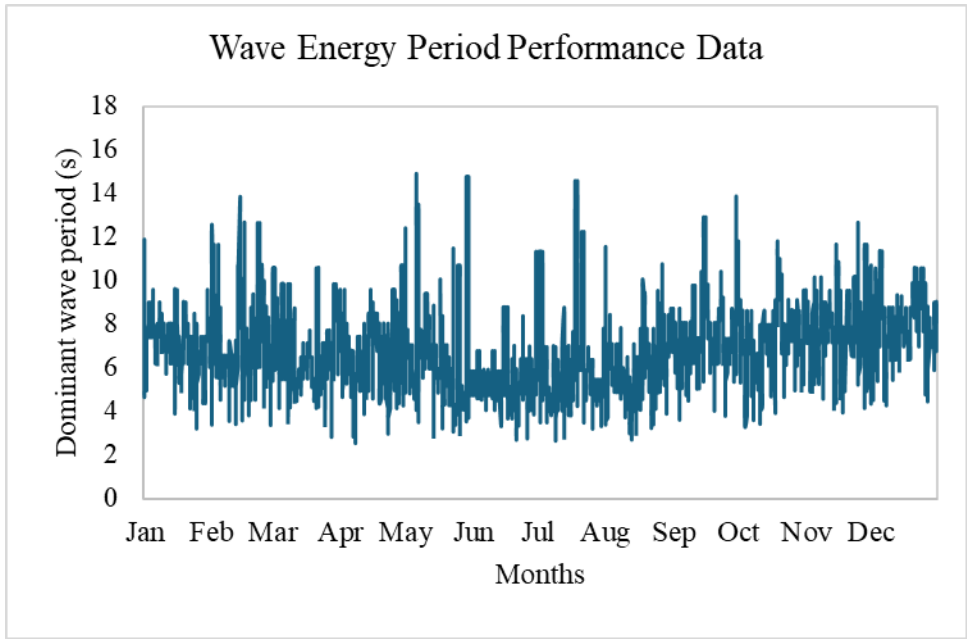


Figure A-11. Wave energy period performance data for St. George, AK.

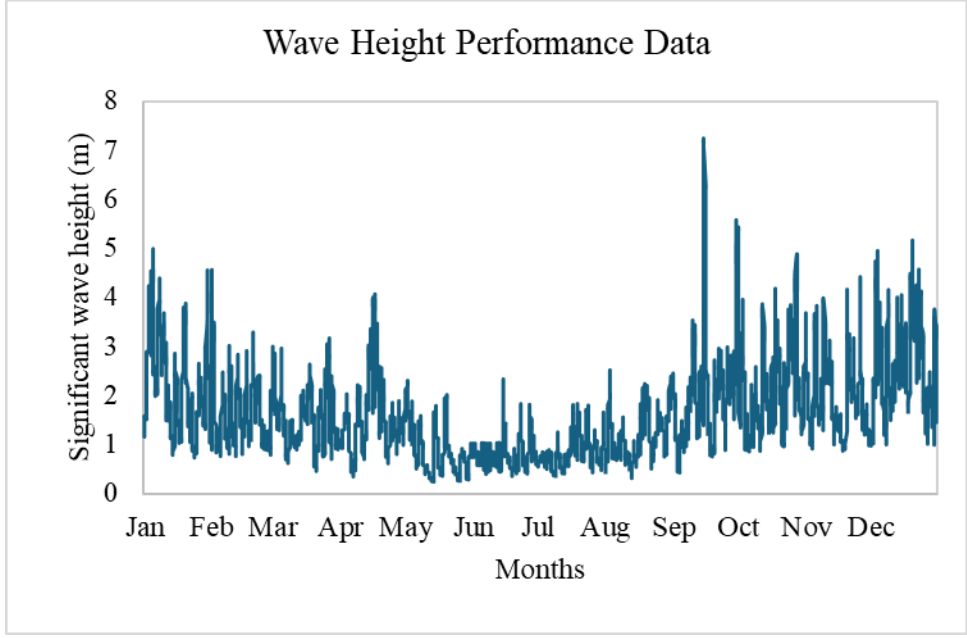


Figure A-12. Wave height performance data for St. George, AK.

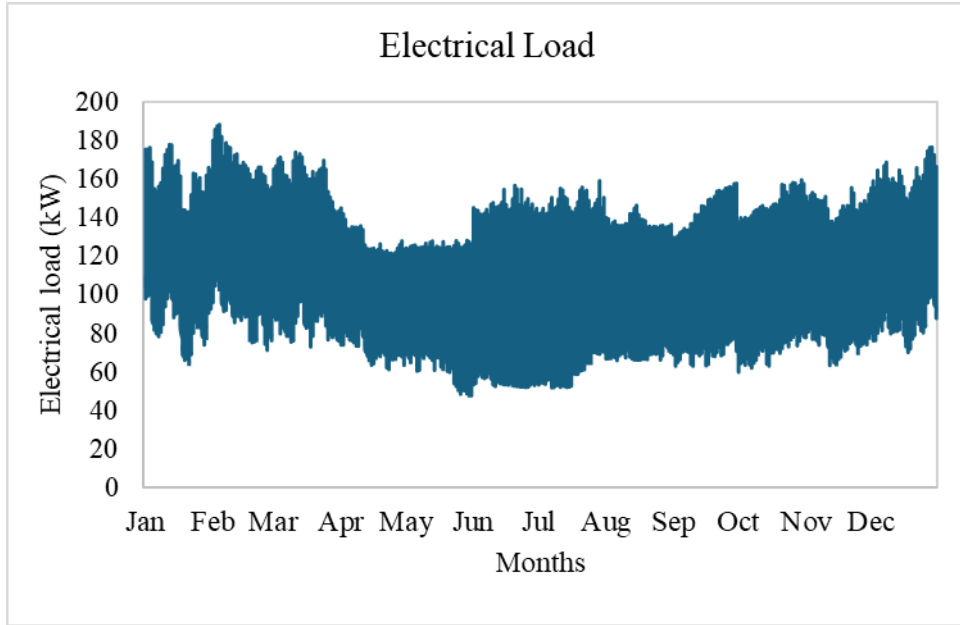


Figure A-13. Electricity demand for St. George Island, AK.

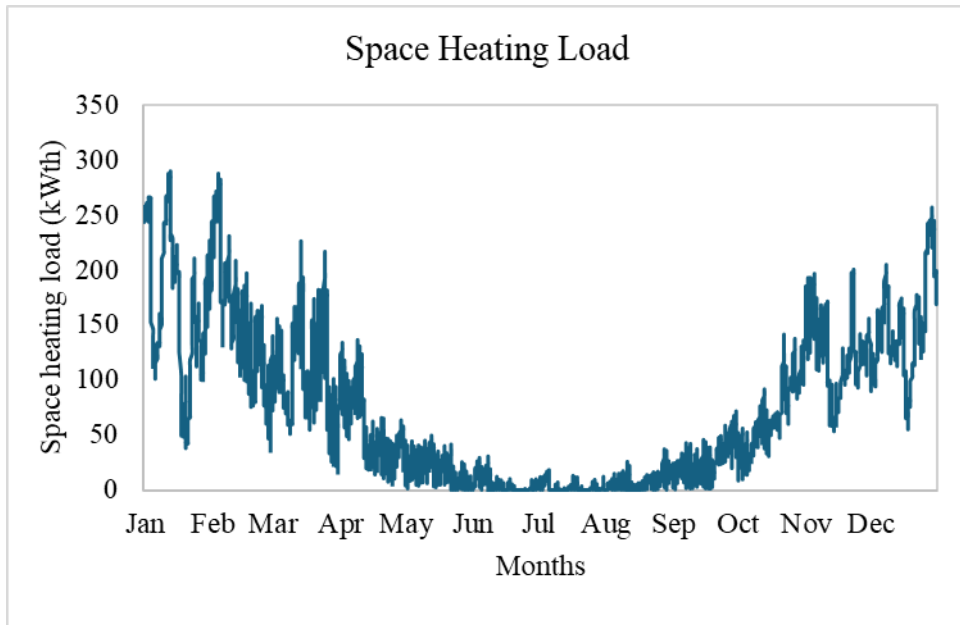


Figure A-14. Space heating demand for St. George Island, AK.

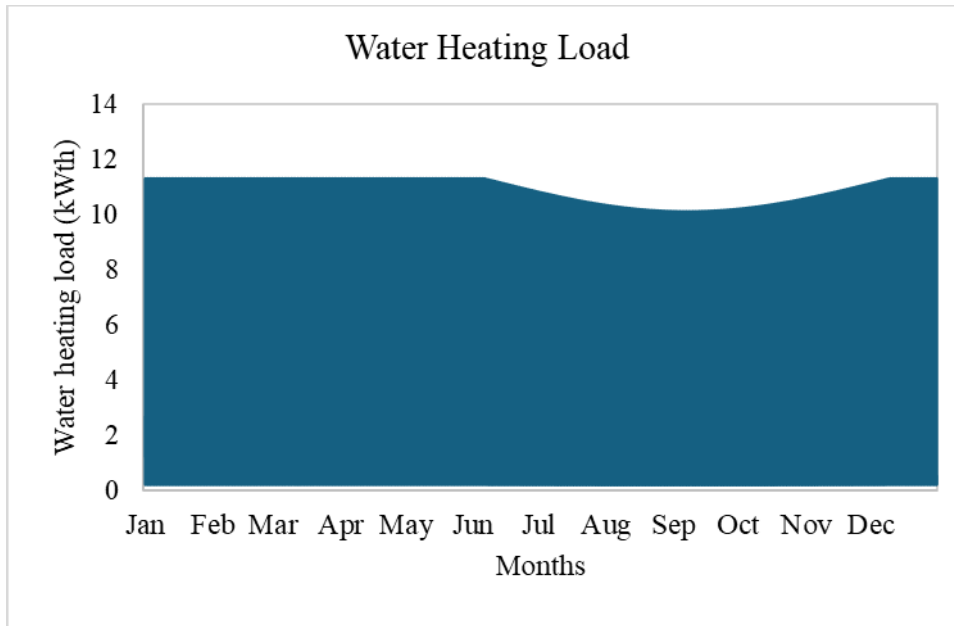


Figure A-15. Water heating demand for St. George Island, AK.

A-4. Future Demand Projection

The community perspective on potential energy growth in St. George revolves around the proposed development of a new harbor, which is expected to increase electrical and heating loads. Currently, annual residential power consumption is declining due to a population decrease from 2000 to 2011. However, the establishment of a new fish processing plant, although not in use yet, could increase peak demand by 100 kW if operational. Furthermore, the design of a new deep-water harbor would add another 100 kW to peak demand. If both projects proceed, peak loads could reach 350–400 kW, based on 2011 data. On the contrary, without these developments, peak load is expected to decrease and remain below 200 kW (Alaska Energy Authority 2012) and decrease significantly as the population in St. George declines. However, the team has not included such a scenario in future analysis.

Comparative examples include Heraklion Port in Crete, Greece, which had an average annual demand of 2,676,907 kWh and a peak load demand of 553.14 kW in August, based on data from 2010–2019 (Sifakis, Konidakis, and Tsoutsos 2021). Another example is Milford Haven Port in Wales, where the total power consumption in 2012 was 1,600 MWh. Packway building on the site, which has a fish processing plant in Milford Haven, consumed approximately 60,000 kWh annually (Alzahrani, Petri, and Rezgui 2019).

For their analysis, the team considers 100 kW peak load each for both fish processing plant and the new harbor. Because of the unavailability of the actual load profile, the team considers two separate representative commercial facility load profile models for these additional load projections, as shown in Figures. The added load profiles have higher daily peaks in winter compared to summer months; however, they fluctuate significantly on a daily basis, as seen in typical commercial facilities.

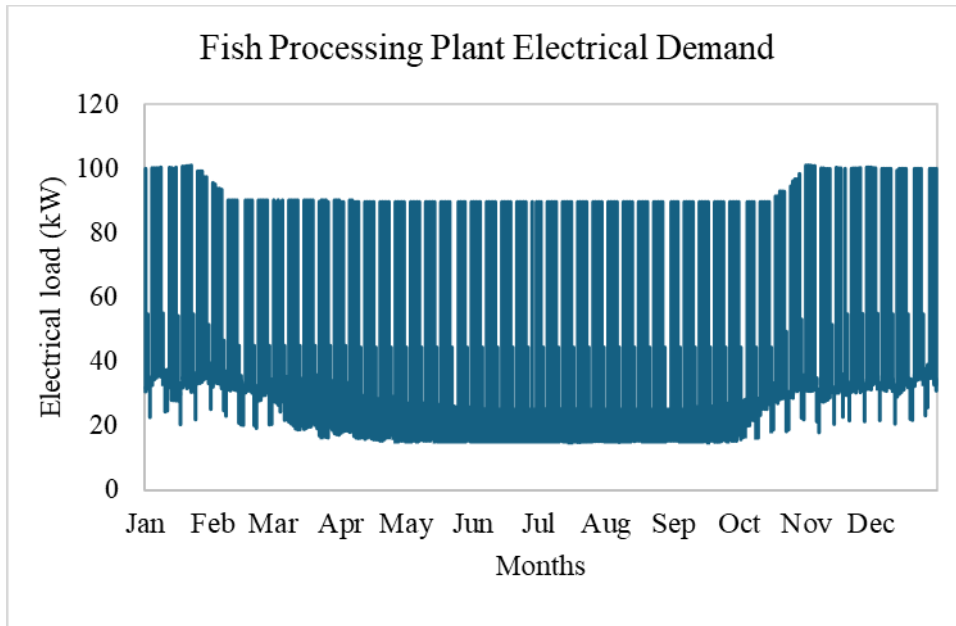


Figure A-16. Load demand profile considered for the proposed fish processing plant.

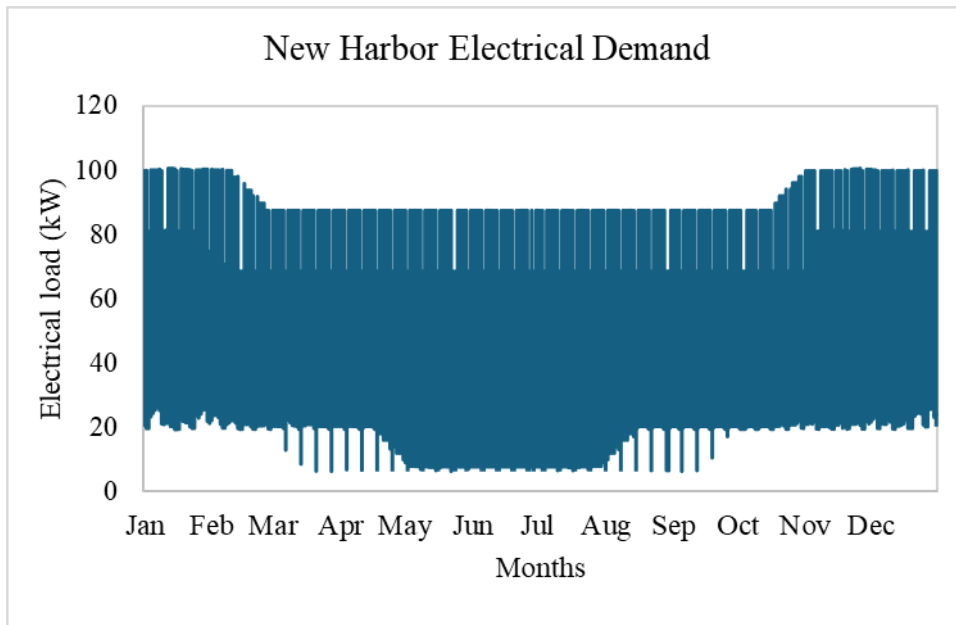


Figure A-17. Load demand profile considered for the proposed new harbor.

Appendix B

Cost and Modeling Parameters

B-1. Modeling Parameters Used for this Study

Table B-1. Modeling parameters and considerations for existing primary, reserve diesel generator (Alaska Energy Authority 2012).

Modeling Parameters	Modeling Considerations	Source
Total Numbers	3	(Alaska Energy Authority 2012)
Power Rating (kW)	200	
Installation Cost (\$/kW)	639.78,* 609**	
Variable O&M Cost	0.04	
Existing Age (years)	10	
Modeled Lifetime (years)	20	
Efficiency (%)	34.7	
Fuel Cost (\$/gallon)	0.201182	

Note: *Primary diesel genset, **Backup spinning and reserve diesel genset

Table B-2. Modeling parameters for WEC (before cost adjustment).

WEC 1		
Modeling Parameters	Modeling Considerations	Source
Model Type	BREF-HB	(Chang et al. 2018)
Rated Capacity (kW)	15	
Capital Cost (\$/kW)	5,478.18	
Cable Length (m)	1000	—
Cable Cost (\$/m)	133.5	(Guo et al. 2023)
Fixed Maintenance Cost (\$/kW)	325.318	(Chang et al. 2018)
Lifetime (years)	20	—
WEC 2		
Modeling Parameters	Modeling Considerations	Source
Model Type	BREF-SHB	(Chang et al. 2018)
Rated Capacity (kW)	260	
Capital Cost (\$/kW)	5,639.87	
Cable Length (m)	1,000	—
Cable Cost (\$/m)	133.5	(Guo et al. 2023)
Fixed Maintenance Cost (\$/kW)	333.879	(Chang et al. 2018)
Lifetime (years)	20	—

Table B-3. Modeling parameters for solar photovoltaic (before cost adjustment).

Modeling Parameters	Modeling Considerations	Source
Installation Cost (\$/kW)	2,842	(National Renewable Energy Laboratory 2023)
Fixed Maintenance Cost (\$/kW/mo)	2.51	
Lifetime (years)	20	—

Table B-4. Modeling parameters for BESS (before cost adjustment).

Modeling Parameters	Modeling Considerations	Source
Installation Cost (\$/kW)	1,082	(National Renewable Energy Laboratory 2023)
Lifetime (years)	5	—
Max C-Rating	1C	—
Round Trip Efficiency (%)	90	—

Table B-5. Modeling parameters for wind (before cost adjustment).

Modeling Parameters	Modeling Considerations	Source
Wind Turbine Rated Capacity (kW)	95	(Alaska Energy Authority 2012)
Capital Cost (\$/unit)	484,228	(National Renewable Energy Laboratory 2023)
Fixed O&M Cost (\$/mo/unit)	286.62	
Hub Height (feet)	98	(Alaska Energy Authority 2012)
Lifetime (years)	20	

Table B-6. Modeling parameters and considerations for electric heaters.

Modeling Parameters	Modeling Considerations	Source
Installation Cost (\$/kW)	250	Xendee default inputs
Conversion Efficiency (%)	100	
Lifetime (years)	20	

Table B-7. Modeling parameters for electrolyzer (before cost adjustment).

Modeling Parameters	Modeling Considerations	Source
Installation Cost (\$/kW)	2,100	(Gilbert et al. 2024)
Fixed O&M (\$/kW/y)	196	(Holst et al. 2021)
Efficiency (%)	60.5	(Holst et al. 2021)
Lifetime (years)	15	—

Table B-8. Modeling parameters for hydrogen storage (before cost adjustment).

Modeling Parameters	Modeling Considerations	Source
Installation Cost (\$/kg)	560	(Papadias and Ahluwalia 2021)
Fixed O&M (\$/kg/mo)	10	
Efficiency (%)	90	Default Inputs
Minimum Filling and Emptying Rate	0.5	
Lifetime (years)	25	

Table B-9. Modeling parameters for fuel cells (before cost adjustment).

Modeling Parameters	Modeling Parameters	Source
Installation Cost (\$/kW)	2,000	(Hydrogen and Fuel Cells Technologies Office 2024)
Fixed O&M Cost (\$/kW)	55	
Efficiency (%)	50	
Heat-to-Power Ratio	0.7	(Darrow et al. 2015)
Lifetime (years)	15	(Hydrogen and Fuel Cells Technologies Office 2024)

Table B-10. Modeling parameters for hydrogen boiler (before cost adjustment).

Modeling Parameters	Modeling Considerations	Source
Installation Cost (\$/kW)	250	Default Inputs
Efficiency (%)	85	
Lifetime (years)	20	

B-2. Capital and O&M Cost Review

There are significant number of past energy projects (Table B-11), such as wind and solar projects, in St. George and neighboring islands. For example, the False Pass Wind Energy Project, Nelson Lagoon Wind Energy Project, and Nikolski Wind Integration construction were closed after their completion. Similarly, the St. George Wind Farm project, which involved the installation of a remanufactured Windmatic 17s (95 kW) turbine, and the St. Paul Wind-Diesel Project, which included the setup of a 225-kW Vestas V27 wind turbine and two 150-kW Volvo diesel engine generators, have been completed. Other projects, such as the Sand Point Wind Project and the City of Unalaska Wind Power Feasibility, were also closed after the funds were fully spent.

Table B-11. AEA past wind and solar projects in Aleutian and Pribilof Islands.

SN	Projects	Energy Fund		Community Contribution		Notes
		Budget	Spent	Budget	Spent	
1	False Pass Wind Energy Project R4-Closed	\$68,652.75	\$68,652.75	\$5,000	\$5,000	—
2	Nelson Lagoon Wind Energy Project R4-Closed	\$75,756.47	\$75,756.47	\$7,260	\$7,260	—
3	Nikolski Wind Integration Construction – Closed	\$409,430	\$409,430	\$41,500	\$69,082.24	65kW Vesta V-15 Wind Turbine Generator System
4	St. George Wind Farm Construction-Closed	\$1,485,167.34	\$1,485,167.34	—	—	Windmatic 17s (95kW) turbine remanufactured
5	St. Paul Wind-Diesel Project R3-Closed	\$1,790,301.15	\$1,790,301.15	\$191,605.61	\$191,605.61	225-kW Vestas V27 wind turbine, two 150-kW Volvo diesel engine generators
4	Sand Point Wind-Closed	\$639,494.85	\$639,494.85	\$437,900	\$437,900	Two 500-kW Vestas V39 turbines
5	City of Unalaska Wind Power Feasibility	\$139,000	\$24,444.18	\$13,900	—	—

Regarding energy technology options and associated costs, various scenarios were considered. The expected capital and operational expenditures for energy projects were analyzed, including investments in wind power plants, solar-battery systems, and wind-battery hybrids. Table B-12 shows the expected capital and O&M for technologies and possible uncertainty range for the sensitivity analysis.

Table B-12. Expected capital and O&M costs for energy projects in remote communities and off-grid locations.

	Li-Ion Battery	Wind Power Plant	Solar-Battery	Solar-Battery + Diesel	Wind-Battery	Diesel
Range of Investment Cost \$/kW	550 €/kW (Trapani et al. 2024)	1,175 €/kW (Trapani et al. 2024)	4,000–7,000 (International Renewable Energy Agency 2023)	3,000–6,000 (International Renewable Energy Agency 2023)	4,500–13,000 (International Renewable Energy Agency 2023)	420 €/kW (Trapani et al. 2024) 300-800 (International Renewable Energy Agency 2023)
Pure O&M Cost (20% Life without Depreciation) as % of Investment	10 €/kW (Trapani et al. 2024)	3%/yr (Trapani et al. 2024)	10–15% (International Renewable Energy Agency 2023)	10–20% (International Renewable Energy Agency 2023)	5–15% (International Renewable Energy Agency 2023)	—
Range of Cost LCOE in U.S. Cent per kWh	—	—	30–100 (International Renewable Energy Agency 2023)	50–100 (International Renewable Energy Agency 2023)	30–100 (International Renewable Energy Agency 2023)	35–120 (International Renewable Energy Agency 2023)
Replacement Cost	550 €/kW (Trapani et al. 2024)	—	—	—	—	420 €/kW (Trapani et al. 2024)

Shipping medium-to-large items from Anchorage can be done via Alaska Central Express (ACE), a small freighter plane capable of transporting moderately large or heavy items, such as 4-wheelers. For items larger than this, shipping would need to be arranged by barge through a company called Bowhead. Bowhead only delivers to St. George if they have a specific load, and they typically make deliveries once a year to St. Paul. When shipping from the lower 48 states, large items are transported by barge from Seattle to Seward, then to Dutch Harbor, and finally to St. George. For accurate price estimates, direct contact with these shipping companies is necessary.

A single container load costs approximately \$10,000 when shipped from Seattle to Anchorage, with typical costs ranging from \$10,000 to \$18,000. For wind turbine transportation, ATS, a company based in St. Cloud, Minnesota, charges between \$30,000 and \$40,000 for short-haul shipments and over \$100,000 for long-haul shipments.

Shipping cost estimates can be further examined through the Alaska Department of Education’s Cost Model instructions, which include factors such as the Geographic Area Cost Factor, Size Adjustment Factor, and Escalation Index. For the Pribilof Islands, the adjustment cost factor is 32.19%, with Anchorage serving as the base point for calculations (Department of Education and Early Development 2023).

There are many factors that can impact the actual deployment cost of energy technologies in remote and island communities. There are far too many uncertainties to use specific cost for any technology based on historical data. Rigorous market analysis is necessary for each cost component and should be performed prior to getting a correct prediction for actual cost of deployment. Therefore, to simplify the cost assumptions as well as to ensure the considered technologies are compared on a common baseline, the team considers the reference cost of the energy generation technologies provided in the NREL's Annual Technology baseline (ATB) (National Renewable Energy Laboratory 2023). For technologies not reported in NREL's ATB, other reliable references are considered. The parameters used are provided in Table B-1 through Table B-10. These cost parameters are further scaled up using a locational cost adjustment factor for Pribilof Islands.

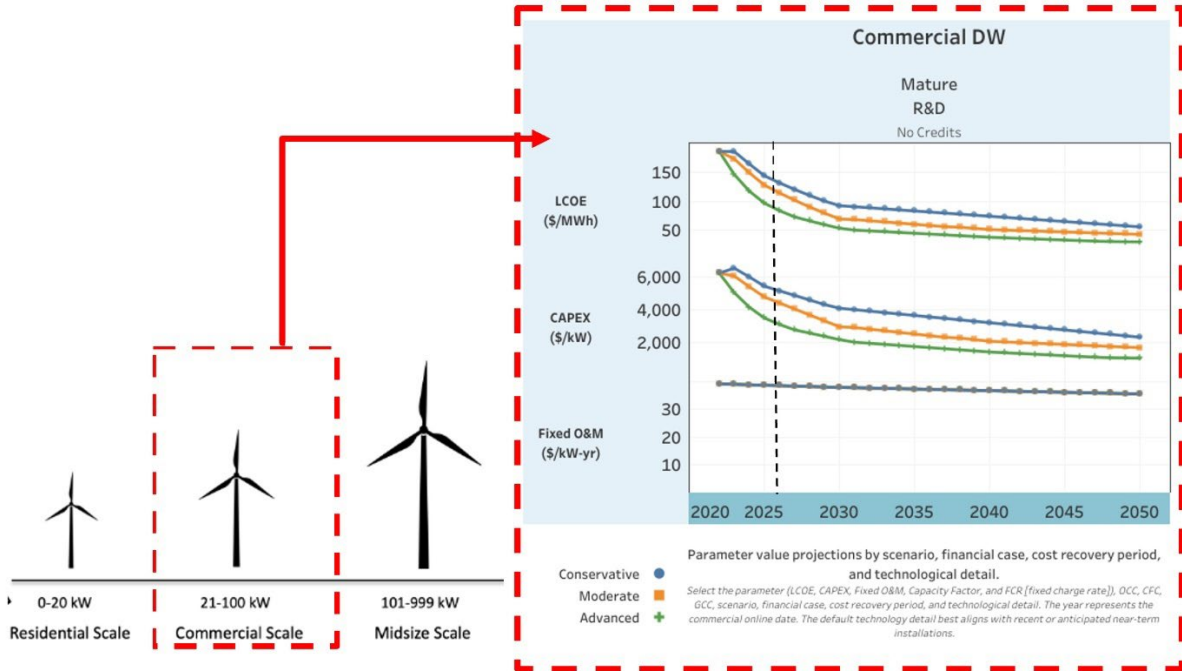


Figure B-1. NREL ATB estimates wind turbines for commercial-scale distributed wind turbines. (2023 Moderate estimates for CAPEX and fixed O&M are used for the analysis.)

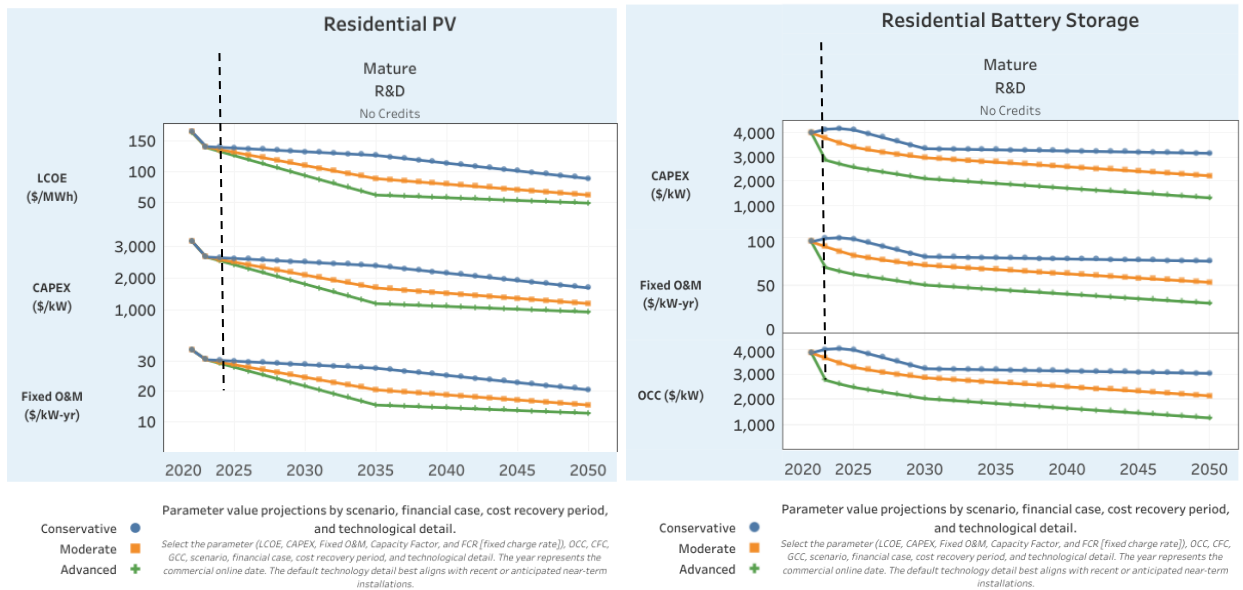


Figure B-2. NREL ATB estimates for residential-scale PV and battery energy storage considered for St. George. (2023 Moderate estimates for CAPEX and fixed O&M are used for the analysis.)